

# Integrated Ocean Drilling Program Expedition 342 Scientific Prospectus

## Paleogene Newfoundland Sediment Drifts

**Richard D. Norris**

Co-Chief Scientist  
Scripps Institution of Oceanography  
University of California, San Diego  
308 Vaughan Hall  
La Jolla CA 92093-0244  
USA

**Paul A. Wilson**

Co-Chief Scientist  
National Oceanography Centre  
University of Southampton  
European Way  
Southampton SO14 3ZH  
United Kingdom

**Peter Blum**

Expedition Project Manager/Staff Scientist  
Integrated Ocean Drilling Program  
Texas A&M University  
1000 Discovery Drive  
College Station TX 77845-9547  
USA



Published by  
Integrated Ocean Drilling Program Management International, Inc.,  
for the Integrated Ocean Drilling Program

## **Publisher's notes**

Material in this publication may be copied without restraint for library, abstract service, educational, or personal research purposes; however, this source should be appropriately acknowledged.

### **Citation:**

Norris, R.D., Wilson, P.A., and Blum, P., 2011. Paleogene Newfoundland sediment drifts. *IODP Sci. Prosp.*, 342. doi:10.2204/iodp.sp.342.2011

### **Distribution:**

Electronic copies of this series may be obtained from the Integrated Ocean Drilling Program (IODP) Scientific Publications homepage on the World Wide Web at [www.iodp.org/scientific-publications/](http://www.iodp.org/scientific-publications/).

This publication was prepared by the Integrated Ocean Drilling Program U.S. Implementing Organization (IODP-USIO): Consortium for Ocean Leadership, Lamont-Doherty Earth Observatory of Columbia University, and Texas A&M University, as an account of work performed under the international Integrated Ocean Drilling Program, which is managed by IODP Management International (IODP-MI), Inc. Funding for the program is provided by the following agencies:

National Science Foundation (NSF), United States

Ministry of Education, Culture, Sports, Science and Technology (MEXT), Japan

European Consortium for Ocean Research Drilling (ECORD)

Ministry of Science and Technology (MOST), People's Republic of China

Korea Institute of Geoscience and Mineral Resources (KIGAM)

Australian Research Council (ARC) and GNS Science (New Zealand), Australian/New Zealand Consortium

Ministry of Earth Sciences (MoES), India

## **Disclaimer**

Any opinions, findings, and conclusions or recommendations expressed in this publication are those of the author(s) and do not necessarily reflect the views of the participating agencies, IODP Management International, Inc., Consortium for Ocean Leadership, Lamont-Doherty Earth Observatory of Columbia University, Texas A&M University, or Texas A&M Research Foundation.

This IODP *Scientific Prospectus* is based on precruise Science Advisory Structure panel discussions and scientific input from the designated Co-Chief Scientists on behalf of the drilling proponents. During the course of the cruise, actual site operations may indicate to the Co-Chief Scientists, the Staff Scientist/Expedition Project Manager, and the Operations Superintendent that it would be scientifically or operationally advantageous to amend the plan detailed in this prospectus. It should be understood that any proposed changes to the science deliverables outlined in the plan presented here are contingent upon the approval of the IODP-USIO Science Services, TAMU, Director in consultation with IODP-MI.

## Abstract

The Newfoundland ridges are covered by large-scale sediment drift deposits that accumulated under the Deep Western Boundary Current during the Late Cretaceous and early Paleogene greenhouse. The area is famous because it is the resting place of RMS *Titanic*, which sank after colliding with an iceberg en route from Southampton, England, to New York City, USA, in April 1912. Integrated Ocean Drilling Program (IODP) Expedition 342 will drill a depth transect between ~2400 and 5000 m water depth into a sequence of rapidly accumulated sediment drifts of Paleogene age on J Anomaly Ridge and Southeast Newfoundland Ridge. Drilling this transect will allow us to study multiple extreme climate events at unprecedented temporal resolution from a high-latitude site during an interval of time when Earth was much warmer than today, featuring a genuinely green Greenland and estimated atmospheric carbon dioxide levels similar to those projected for the end of this century. The targeted sedimentary sequences accumulated directly under the flow path of the Deep Western Boundary Current. These sediments, therefore, will provide an archive of changes in chemistry, flow history, and depth structure of waters exiting the Nordic seas and Arctic Ocean during the transition from an ice-free peak Cenozoic warm interval in the early Eocene to the onset of Arctic sea ice formation and the growth of major ice sheets on Antarctica. Our drill sites are located in a region that climate modeling suggests should have a particularly high-amplitude climate response to orbital forcing, which, together with excellent age control from magnetostratigraphy seen in existing drill cores, should help extend the astronomical timescale through the Cenozoic.

Approximately two days of Expedition 342 ship time will be spent testing the Motion Decoupled Hydraulic Delivery System (MDHDS). The MDHDS is an IODP-funded engineering development and will serve as a foundation for future penetrometer and other downhole tool deployments. The tests will take place at Ocean Drilling Program Site 1073 (Leg 174A), offshore New Jersey, by deploying both the SET-P and T2P pore pressure penetrometers.

## Schedule for Expedition 342

Expedition 342 is based on Integrated Ocean Drilling Program (IODP) drilling Proposal 661-Full2 (available at [iodp.tamu.edu/scienceops/expeditions/newfoundland\\_sediment\\_drifts.html](http://iodp.tamu.edu/scienceops/expeditions/newfoundland_sediment_drifts.html)). Following ranking by the IODP Scientific Advisory Structure, the expedition was scheduled for the R/V *JOIDES Resolution*,

operating under contract with the U.S. Implementing Organization. At the time of publication of this Scientific Prospectus, the expedition is scheduled to start in St. George, Bermuda, on 18 June 2012 and to end in St. John's, Newfoundland, on 17 August 2012. A total of 60 days will be available for the drilling, coring, downhole measurements, and tool testing described in this report (for the current detailed schedule, see [iodp.tamu.edu/scienceops/](http://iodp.tamu.edu/scienceops/)). Further details about the facilities aboard the *JOIDES Resolution* and the United States Implementing Organization (USIO) can be found at [www.iodp-usio.org/](http://www.iodp-usio.org/). Supporting site survey data for Expedition 342 are archived at the [IODP Site Survey Data Bank](#).

## Introduction

On 15 April 1912, the RMS *Titanic*, en route westward from Southampton, England, to New York City, USA, hit an iceberg off the Grand Banks of Newfoundland and sank, killing more than 1500 people. The two halves of the wreck lie between the volcanic seamounts of the Southeast Newfoundland Ridge because there the southward-flowing surface waters of the cold Labrador Sea carry icebergs to their intersection with the warm tongue of the Gulf Stream. Today the *Titanic* is bathed by the Deep Western Boundary Current because these new abyssal waters pass at depth under the Gulf Stream on their circuit throughout the deep basins of the world oceans (Fig. F1). IODP Expedition 342 is designed to study the nature of this deep current system near its northern sources during the balmy climates of the Paleogene (65.5 to ~21.8 Ma).

During the early Paleogene, global temperatures were considerably warmer than today and supported forests rather than ice sheets in the high polar latitudes (Greenwood et al., 2010). The early Paleogene greenhouse world represents a radiative forcing state that we are rapidly re-approaching. At current and projected rates of fossil fuel consumption, atmospheric greenhouse gas concentrations are set to rise to Paleogene levels in the next 80 y (National Research Council, 2011). How did the climate and ecosystems of the Paleogene world work? What should we expect in the next century? Although the Eocene is not a perfect analogue to the near future (Haywood et al., 2011), understanding Eocene climate dynamics will provide information on what to expect from a warmer planet.

The primary objectives of our program are to obtain a depth transect of drill cores between ~5 and 2 km water depth. Because the ocean is layered, with different water masses formed in various parts of the planet arranged above one another, our depth

transect of drill sites will permit a detailed reconstruction of the chemistry, circulation, and history of Greenhouse Earth. Furthermore, because we will target sediment drifts that accumulate faster than typical deep-sea sediments, we should also be able to reconstruct the history of a warm Earth with unusual fidelity. These two things—detailed assessment of the structure and circulation of the warm-world ocean and unusually detailed climate history—will help us test models of Earth’s climate and ecosystem evolution that have been difficult or impossible to resolve with typical deep-sea or land-based records of the Eocene.

Our drilling target is J Anomaly Ridge and Southeast Newfoundland Ridge offshore Canada’s Grand Banks. The drill sites, not far from the *Titanic*’s resting place, are positioned to monitor the strength and chemistry of deepwater formation in the Atlantic as well as outflows from the Arctic basins through Baffin Bay and the Norwegian seaway (Fig. F2). Today, both the northward-flowing Gulf Stream and the southward-flowing Deep Western Boundary Current cross over the drilling area, leaving a record of their flow strength, chemistry, and biology in the sediment drifts beneath them (Fig. F1). The shape of the North Atlantic margin suggests that a similar current configuration occurred in the past, with any deep waters formed in the North Atlantic constrained to flow over the Newfoundland ridges. Therefore, Expedition 342 sites will be particularly useful to monitor the overturning history of the North Atlantic Ocean.

The Newfoundland ridges are mantled with some of the oldest sediment drifts known in the deep sea and range in age from the Late Cretaceous to Paleogene. Pliocene–Pleistocene drifts in the northeastern Atlantic commonly have sedimentation rates of 4–20 cm/k.y. and therefore can be used to study rates of abrupt climate change (Channell et al., 2010). Previous drilling of drifts on Blake Nose (off the southeastern United States) revealed sedimentation rates in the middle Eocene of ~5–6 cm/k.y., far higher than the ~1 cm/k.y. rates typical of previous Paleogene-focused drilling targets (Norris et al., 2001b). If, as expected, the Newfoundland sediment drifts also have high accumulation rates, we will obtain records of warm-period climates and evolution with unusual fidelity, and these will be particularly useful for assessing rates of change in the Earth system during both transient episodes of extreme warming (analogous to the near future) and transitions from warm climates into the glaciated world.

Expedition 342 is focused on the Paleogene record on the Newfoundland ridges. Although there is an extensive Cretaceous record of both drifts and fossil reefs in the seismic record, we do not have time to do justice to Cretaceous objectives without sac-

rificing our studies of the Paleogene system. Furthermore, although we will likely obtain a record from the majority of the Paleogene, our particular area of focus will be the middle Eocene to Oligocene interval where thick sediment drift deposits preserve unusually expanded records of the transition from the greenhouse world of the Eocene climatic optimum to the glaciated world of the Oligocene. Therefore, our expedition has four major objectives:

- First, we aim to reconstruct a detailed history of the carbonate saturation state of the North Atlantic through numerous episodes of abrupt global warming. An interval of particular focus will be the middle Eocene to early Oligocene record, where we expect to find expanded records of hyperthermal events and the middle Eocene climatic optimum. This history of the carbonate system, coupled with detailed geochemical studies, will allow us to test theories for the origin of “hyperthermals”—abrupt periods of greenhouse gas-fueled warming known to punctuate the Paleocene and Eocene (Galeotti et al., 2010; Quillévéré et al., 2008; Sexton et al., 2011). Natural experiments with global changes such as hyperthermals can enhance our understanding of the consequences of abrupt climate change for Earth’s ecosystems, climate, and chemistry. This record will be enhanced by our efforts to obtain the first depth transect that captures the truly deep ocean as well as the intermediate depths captured in previous drilling programs (Norris, Kroon, Klaus, et al., 1998; Bralower, Premoli Silva, Malone, et al., 2002; Lyle, Wilson, Janecek, et al., 2002; Erbacher, Mosher, Malone, et al., 2004; Zachos, Kroon, Blum, et al., 2004; Pälike, Lyle, Nishi, Raffi, Gamage, Klaus, and the Expedition 320/321 Scientists, 2010; Zachos et al., 2005).
- Second, we aim to obtain a very detailed record of the flow history of the Deep Western Boundary Current issuing from the North Atlantic. Today, deepwater formation draws warm water into the Nordic seas, keeping them warm. Our work will show how far back this pattern of overturning circulation extends and its influence on climates of the past greenhouse world.
- Third, we aim to obtain a detailed record of the Eocene–Oligocene transition (EOT; ~33.7 Ma) and the onset of major glaciation following the warm climates of the Eocene. Our drill cores through the EOT will not only provide a highly resolved record of the events leading up to and following the greenhouse-to-icehouse transition, but they are also well positioned to display how Greenland and the high northern latitudes responded to this event.
- Fourth, we aim to address major uncertainties in the development of the geologic timescale by obtaining records of the Eocene that can be used to link the astronom-

ical timescale developed for the last ~40 m.y. to the “floating” timescale of the early Paleogene developed over a series of IODP and earlier drilling expeditions.

This drilling proposal completes the North Atlantic objectives laid out in a 1997 Marine Aspects of Earth System History (MESH) workshop on warm period dynamics and the Ocean Drilling Program (ODP) “Extreme Climates” program planning group (PPG) (see [www.odplegacy.org/program\\_admin/sas/ppg.html](http://www.odplegacy.org/program_admin/sas/ppg.html)). This proposal also addresses initiatives of the IODP Initial Science Plan in the areas of extreme climates and rapid climate change. Finally, our expedition takes up proposals of the recent National Research Council report *Understanding Earth’s Deep Past: Lessons for Our Climate Future* (National Research Council, 2011), which advocates focused efforts to resolve the timescale and use mechanisms of past hyperthermal events as possible analogues for future global change.

## Background

### Structure and stratigraphy of J Anomaly Ridge and Southeast Newfoundland Ridge

The J Anomaly and Southeast Newfoundland Ridges (Fig. F1) formed along the axis of the mid-Cretaceous Mid-Atlantic Ridge in a fashion analogous to the modern Reykjanes Ridge and Iceland (Tucholke and Ludwig, 1982). The tops of both ridges were above sea level in the Aptian and subsequently subsided to abyssal depths by the Late Cretaceous (Tucholke and Vogt, 1979). Aptian rudist platform carbonates were drilled at Deep Sea Drilling Project (DSDP) Site 384 (now at 3900 m) (Tucholke, Vogt, et al., 1979), and buried reeflike seismic features are present on the flank of J Anomaly and Southeast Newfoundland Ridges. Pelagic carbonates began to blanket the tops of the ridges by ~75–80 Ma (Tucholke, Vogt, et al., 1979) and accumulated to a total thickness of nearly 1.5 km by the late Neogene.

There are five principal sedimentary sequences on the Newfoundland ridges, bounded by reflection Horizons A–D (Fig. F3). The uppermost sequence of Pleistocene age displays well-defined internal reflections and mantles the northern side of Southeast Newfoundland Ridge. Nearly all piston cores collected from the Newfoundland ridges (Figs. F4, F5) are of Pleistocene age, including “long piston” Core MD95-2027. The presence of thick Pleistocene sections on the north side of the Newfoundland ridges may reflect the accumulation of iceberg-transported sediment derived from the Hudson Bay and Greenland. To the south, on Southeast Newfoundland and J Anom-

aly Ridges, the Pleistocene cover is nearly absent and is represented by only a thin (3–5 m thick) layer of Pleistocene foraminifer sand mixed with glacially transported sediments. This thin Pleistocene cover over our target sediments likely reflects the barrier imposed by the warm Gulf Stream to icebergs drifting southward along the Newfoundland margin. Pleistocene glacial sand protects the Paleogene sediment drifts from extensive erosion and preserves them in unconsolidated condition, as seen in piston Cores KNR179-1-13PC and KNR179-1-15PC from Southeast Newfoundland Ridge.

The second sequence, bounded by reflection Horizons A and B, displays poorly defined, discontinuous reflections (Fig. F3) and is probably of Oligocene and Neogene age on the basis of its similar acoustic character to other drifts in the North Atlantic (Davies et al., 2001). In some areas, the discontinuous reflections can be resolved as fields of sediment waves, suggesting that much of the unit was deposited under strong, directional bottom currents. Large parts of the southern flank of Southeast Newfoundland Ridge and the northern end of J Anomaly Ridge are covered by this sequence, which has thicknesses of >700 m. We have no cores that firmly date this sequence because of failure of the hydraulic winch during our site survey cruise.

The third sequence, bounded by reflection Horizons B and C, is seismically transparent and has a poorly defined contact with the overlying sequence of discontinuous reflections (Fig. F3). The absence of a strong reflector between these seismic units suggests that seismic Unit 3 has a conformable relationship with overlying Unit 2. Piston cores and seismic ties to DSDP Site 384 show that this sequence is of early Eocene age (nannofossil Zones NP14 and NP15) and younger. Its great thickness (up to 800 m; Fig. F6) suggests an unusually expanded sequence of lower and middle Eocene sediments on J Anomaly Ridge. Furthermore, the gradational relationship of this sequence into overlying strata may mean that there is a complete EOT in the drilling transect on Southeast Newfoundland Ridge (Fig. F7). Piston core samples show the main lithology in the lower to middle Eocene section is a clay-rich, white to yellow nannofossil ooze. The absence of strong internal reflections suggests that the sequence is not punctuated by major hiatuses but was deposited steadily like many modern Pliocene–Pleistocene drifts in the North Atlantic. This sequence thins below ~4.5 km present water depth (~4 km in the Eocene), reflecting reduced sedimentation rates in the lysocline and below the calcite compensation depth (CCD). Thinning of the Eocene package at ~4 km paleodepth is broadly consistent with the position of the Eocene CCD estimated from prior North Atlantic drilling (Fig. F8) (Tucholke and Vogt, 1979).



The fourth sequence, bounded by reflection Horizons C and D (Fig. F3) of Cretaceous/Paleogene age, is >500 m thick and crops out on the base of J Anomaly Ridge (e.g., Site JA-1; Fig. F6) and in numerous places on the crest of Southeast Newfoundland Ridge, including outcrops in moats around several seamounts. These strata also display driftlike morphology, albeit of smaller size than the Eocene drifts, and mostly well-defined parallel reflections like the Pleistocene cover section. This sequence was drilled at DSDP Site 384 (Fig. F9), which recovered Campanian to lowermost Eocene beige calcareous ooze and soft chalk with excellent magnetic stratigraphy, well-preserved foraminifers and calcareous nannofossils, as well as radiolarians in the late Paleocene (Berggren et al., 2000). The unconformities at the Cretaceous/Paleogene boundary and the Paleocene/Eocene boundary at DSDP Site 384 are to be expected because the site is located in a condensed section on top of a ridge. All recent Paleogene/Cretaceous drilling expeditions (ODP Legs 171B, 198, 199, 207, and 208 [Norris, Kroon, Klaus, et al., 1998; Bralower, Premoli Silva, Malone, et al., 2002; Lyle, Wilson, Janecek, et al., 2002; Erbacher, Mosher, Malone, et al., 2004; Zachos, Kroon, Blum, et al., 2004]) recovered one or more of these boundary sections despite their absence in older DSDP holes upon which the new drilling legs were based.

The fifth sequence, underlying reflection Horizon D, displays dense but parallel reflections (Fig. F3) and crops out on the northwest slope of J Anomaly Ridge, the crest and flanks of Southeast Newfoundland Ridge, and apparently in the pelagic caps of several seamounts. It consists of several discrete seismic sequences separated by possible unconformities that are indicated by truncations of reflectors. The entire seismic package is likely of mid-Cretaceous to early Late Cretaceous age on the basis of seismic ties to DSDP Site 384. Some of these sequences lap up against seismically identified buried reefs and are as thick as 450 m. The reefs and surrounding sediments are probably Barremian/Albian in age on the basis of results from DSDP Site 384 (Tucholke and Vogt, 1979) and Sr isotope stratigraphy (P. Wilson, unpubl. data), in keeping with the estimated ages of buried reefs off Florida (Hutchinson et al., 1995; Norris et al., 2001a). Representative summaries of our interpretations of the sequence of sedimentary packages on J Anomaly and Southeast Newfoundland Ridges are given in Figures F10 and F11, respectively.

## The modern Deep Western Boundary Current

The area east of the Grand Banks is a region critical to understanding the history of deepwater circulation in the North Atlantic because it is the gateway between bottom water sources in the Norwegian-Greenland and Labrador Seas and the main basins of

the North Atlantic to the south. Denmark Strait overflow water is the main deep-water mass, centered at ~3500 m and overlain by Labrador Sea water at ~1500 m (Pickart et al., 1999). Southeast Newfoundland Ridge is a major barrier to deep southward flow, and it diverts the Deep Western Boundary Current offshore into the path of the northeasterly flow of the Gulf Stream. The deepest part of the bottom current follows submarine contours around the southeastern end of the ridge and continues west around J Anomaly Ridge and along the Nova Scotian continental rise (Fig. F1). Shallower portions of the current follow contours around the crest of Southeast Newfoundland Ridge and also interact with seamounts on the ridge, forming local moats and drifts.

The Gulf Stream actually reaches the seafloor over Southeast Newfoundland Ridge and may contribute to bottom scouring. East of the ridge, Meinen and Watts (2000) found that the mean North Atlantic Current clearly extends to the bottom. Their measured bottom currents are strong enough to suspend sediments but probably not strong enough to cause extensive erosion. Still, we must bear in mind the possibility that erosion on J Anomaly and Southeast Newfoundland Ridges is related to a southward-flowing deep boundary current and/or a northward-flowing surface current that regionally extends to the bottom.

## History of the Deep Western Boundary Current

Something akin to modern North Atlantic Deep Water appears not to have been produced until the late Miocene or early Pliocene, when a combination of tectonic subsidence of the Greenland-Scotland Ridge and Northern Hemisphere refrigeration began to form cold, dense overflow waters in the Nordic seas and the Labrador Sea (Oppo et al., 1995; Wright and Miller, 1993; Wright et al., 1992). However, northern-component deep waters clearly formed in the North Atlantic throughout the Neogene and Oligocene, judging from geochemical differences between Atlantic and Indo-Pacific waters (Wright et al., 1992). Intensification of deepwater formation in the North Atlantic is proposed to account for acceleration of the Deep Western Boundary Current during the Oligocene, leading to widespread erosion along continental margins and formation of the seismic reflection, Horizon A<sup>u</sup> in the western North Atlantic; subsequent current-controlled sedimentation formed major sediment drifts throughout the North Atlantic (Arthur et al., 1989; Miller and Fairbanks, 1985; Miller et al., 1987; Tucholke and Mountain, 1986; Tucholke, 1979; Tucholke and Vogt, 1979).

Direct evidence for significant flow in a deep boundary current before the Oligocene is sparse (Davies et al., 2001). Tucholke and Mountain (1986) suggested that the Eirik and Gloria Drifts south of Greenland may have begun to grow in the middle Eocene, based on interpreted ages of deep reflections in the drifts. The presence of onlapping reflectors and depositional structures on Blake Nose along the mid-Atlantic margin suggest erosion by an intermediate water mass centered above 2000 m water depth in the early Eocene (Katz et al., 1999; Norris et al., 2001a, 2001b). The seismic record from Blake Nose also shows evidence of condensed sections and slumps on the tip of Blake Nose (~2600 m) that could indicate deeper erosional flow along the Blake Escarpment in the early Eocene (Norris, Kroon, Klaus, et al., 1998). Erosion on Blake Nose may have been caused by shallow parts of the Deep Western Boundary Current rather than by the northward-flowing Gulf Stream. The area of erosion is more than 100 km east of the main flow of the Gulf Stream, which is constrained by the location of the Florida Straight and Suwanee Channel. In the deep basin, Mountain and Miller (1992) presented seismic evidence for late Paleocene bottom currents over the Bermuda Rise that could have a source analogous to Antarctic Bottom Water. Although limited, all of these data suggest that both a southern-source water mass and a northern-source water mass may have been present in the deep North Atlantic and circulated strongly enough to control seafloor deposition and erosion during the relatively warm climates of the early Paleogene. This eventuality raises the possibility that our drilling operations can expand upon some of the extraordinary paleoclimate results yielded during IODP coring in the Arctic (e.g., Brinkhuis et al., 2006; Moran et al., 2006; Pagani et al., 2006b; Sluijs et al., 2006).

## **Newfoundland sediment drifts**

One of the main advantages of drilling the Newfoundland sediment drift complex is the near-absence of Neogene sedimentary cover. Most areas were swept by sufficiently strong currents during the later Cenozoic to prevent extensive deposition of younger strata on the southern side of the ridges or in patches around the seamounts. Although we do not have firm dates on when these strong currents were initiated, they are probably a post-Oligocene feature (on the basis of sedimentation rate changes at ODP Site 1267 in the Newfoundland Basin) and may reflect the full development of North Atlantic Deep Water, possibly in combination with a strengthened Gulf Stream. Before this time, the remarkable thickness, absence of internal reflections, and drift morphology suggest that the Paleogene section is likely to be hugely expanded, with sedimentation rates much higher than the 1–2 cm/k.y. typically encountered in the

deep sea (Figs. F6, F7). A similar transition from drift deposition to nondeposition was encountered on Blake Plateau off the Florida-South Carolina margin during ODP Leg 171B (Norris, Kroon, Klaus, et al., 1998) in the latest Eocene. On Blake Nose, the Eocene and older sections were unusually expanded, with deposition rates as high as 6 cm/k.y. throughout the Eocene (Norris et al., 2001a, 2001b). We view the Leg 171B results as a favorable prognosis for the outcome of drilling the Newfoundland ridges.

The primary drilling targets for Expedition 342 are in plastered drifts that exist in three places: (1) the southern toe and eastern flank of J Anomaly Ridge, (2) the southern flank of Southeast Newfoundland Ridge, and (3) the north-facing slopes of seamounts on Southeast Newfoundland Ridge. In addition, we target the pelagic cap of one of the seamounts to obtain the shallow end-member of the depth transect.

Drift sedimentation clearly has a complex history on the Newfoundland ridges, with an initial phase of drift formation on the eastern flank of J Anomaly Ridge in the Late Cretaceous (probably starting in the Campanian or early Maastrichtian, judging from DSDP Site 384 drilling results [Berggren et al., 2000; Tucholke and Ludwig, 1982]) and continuing through most or all of the Paleocene. DSDP Site 384 was spot cored in a highly condensed section, and the Paleocene/Eocene boundary was not obtained. However, acoustic character does change at some point in the late Paleocene or early to middle Eocene with the creation of an acoustically transparent layer (seismic Unit 3). This transparent seismic unit is our primary drilling target because the absence of internal reflectors suggests that it is a conformable sequence with a good likelihood of being correlative across the depth transect.

Drift morphology suggests that the primary drift deposits formed mostly under a southward-flowing bottom current in the Eocene. This current formed plastered drifts on the north faces of seamounts on Southeast Newfoundland Ridge, as well as a long episodically growing and accreting ridge system between J Anomaly Ridge and Southeast Newfoundland Ridge. The southeastern flank of Southeast Newfoundland Ridge has a very thick seismically transparent drift (part of seismic Unit 3) that is overlain by a younger drift deposit that displays complex internal reflectors suggestive of sediment waves (seismic Unit 2). We provisionally assign the transition between these drift packages to the EOT.

The considerable thickness of the middle Eocene to ?upper Eocene seismically transparent interval (seismic Unit 3) means that traditional methods of coring Paleogene targets will have to give way to more focused drilling objectives. Most previous Paleo-

gene and Cretaceous drilling was designed to obtain records spanning tens of millions of years. In contrast, previous drilling legs that targeted Pleistocene drifts typically cored the upper parts of the sediment packages in order to obtain highly expanded records of the late Pleistocene. Our goal will be to follow the “Pleistocene strategy” in which we will core expanded drift records at the expense of long time series.

## Scientific objectives

Expedition 342 is focused on Paleogene records on the Newfoundland ridges. Although there is an extensive Cretaceous record of both drifts and fossil reefs evident in the seismic record, we do not have time to do justice to Cretaceous objectives without sacrificing our studies of the Paleogene system. Furthermore, although we are likely to obtain a record of the majority of the Paleogene during the expedition, a particular interval of focus is the middle Eocene to Oligocene, where there are thick sediment drift deposits that should preserve unusually expanded records of the transition from the greenhouse world of the Eocene climatic optimum to the glaciated world of the Oligocene. Drilling the Newfoundland sediment drifts will allow us to address key problems in paleoceanography, paleoclimate, and biotic evolution.

1. *Recover data on the history of the Paleogene carbonate compensation depth and forcing factors for Paleogene hyperthermals.*

One of the primary objectives of Expedition 342 is to provide data on the history and dynamics of the Paleogene carbon cycle. A particular goal is to use the carbon isotope data sets in combination with depth reconstructions of the carbonate lysocline to provide constraints for carbon cycle models. An extremely successful result of ODP Leg 208 (Zachos, Kroon, Blum, et al., 2004) was the acquisition of a ~2000 m depth transect that permitted estimation of the magnitude of CCD fluctuations in the Paleogene, particularly the Paleocene/Eocene Thermal Maximum (PETM) (Zachos et al., 2005). This depth transect showed that the CCD excursion associated with the PETM was >2000 m and suggested that the amount of CO<sub>2</sub> added to the biosphere during the PETM must have been much greater than previously documented (Panchuk et al., 2008). In turn, these data have been interpreted to suggest that the source of greenhouse gases could not have been primarily gas hydrates because the combined magnitude of the temperature excursion, the CCD fluctuation, and the size of the  $\delta^{13}\text{C}$  anomaly all suggest a carbon source more similar to marine organic carbon than bacterial methane (Panchuk et al., 2008). This example emphasizes how important it is to capture the magnitude of these carbonate preservation excursions because they

provide a direct estimate of the change in ocean undersaturation and hence the transient change in CO<sub>2</sub> storage during extreme climate events. Further, when combined with δ<sup>13</sup>C data sets, the size of the CCD excursion can be used to study the source of isotopically light carbon transferred during such events and, ultimately, climate sensitivity to CO<sub>2</sub> forcing (e.g., Pagani et al., 2006a; Goodwin et al., 2009; Dunkley Jones et al., 2010).

Understanding the spatial and depth dimensions of the CCD change is clearly key to modeling the likely sources and amounts of carbon added to the biosphere during the PETM, but our current observational data do not yet provide a clear picture of either variable. If the methane hydrate hypothesis is untenable for the PETM and other hyperthermals, then it becomes even more important to identify a viable alternative—a task that would be made much easier if we had a clear idea of the total amount of CO<sub>2</sub> put into the ocean and atmosphere during the PETM and other Paleogene hyperthermal events. A well-resolved depth transect that could be used to identify the full depth range of the CCD excursion is critical to resolving the amount and type of carbon introduced into the biosphere during Paleogene hyperthermals. Recent evidence that the PETM and Paleogene global warming events may be orbitally forced or at least conditioned (Lourens et al., 2005; Galeotti et al., 2010; Sexton et al., 2011) implies that the source of carbon was not an impact or one-time volcanic eruption (Kent et al., 2003; Svensen et al., 2004). Thus, long astronomically calibrated records of CCD changes through the warm Eocene may be critical to unraveling the origins of the PETM and other Paleogene events (e.g., the middle Eocene climatic optimum, a prominent reversal in the long-term global cooling trend from peak Cenozoic warmth in the early Eocene) (Bohaty et al., 2009; Bilj et al., 2010).

In addition to reconstructing the sources and fate of carbon that produces extreme climate events, we also need to know the rate and full magnitude of these events and the response of marine biota. In most deep-sea records, slow sedimentation rates mean that the full magnitude of the events may have been bioturbated or dissolved away (Zeebe and Zachos, 2007). As has long been capitalized on by the Pleistocene paleoclimate community, the first solution to the problem of resolving transient events is to target sites where sedimentation rates are higher than the ocean average. Expedition 342 is aimed first and foremost at obtaining highly expanded records suitable for studies of Paleogene climate by targeting drift sediments of hypothesized Oligocene–middle Eocene age. The depth transect approach and acquisition of expanded carbonate-rich sections near the limits of their northern extent will allow us to study faunal and floral processes such as population turnover and latitudinal and strati-

graphic range expansion during intervals of ocean acidification and global warming (e.g., Gibbs et al., 2006; Edgar et al., 2010).

The record on the Newfoundland ridges should allow a companion study to Walvis Ridge drilling (Leg 208) to be conducted under the flow path of northern-source deep waters. We have not previously obtained a good record of the history of the carbonate chemistry of the Deep Western Boundary Current because the Leg 208 transect on Walvis Ridge is likely influenced mainly by southern source waters by virtue of its location on the eastern side of the South Atlantic Basin. Furthermore, we can see in the Newfoundland seismic data that the toe of J Anomaly Ridge (at ~5 km depth) lies close to the average depth of the CCD because the drift package thins markedly at this point. Therefore, proposed drilling on J Anomaly Ridge, combined with the shallower sites on Southeast Newfoundland Ridge, should position us to recover a depth transect spanning ~4 km. It is of course possible that the amplitude of CCD shift during the most extreme Paleogene transient events could still exceed our transect, but we are better placed to obtain a record of the full magnitude of CCD excursions than previous studies. Our proposed transect is particularly suited to resolving fluctuations in the carbonate chemistry of the truly deep ocean—a big change from most Paleogene sites, which rarely have been targeted at paleodepths below ~2500 m.

The carbonate content of deep-sea sediments is a sensitive measure of the productivity, weathering, and fluxes of carbon within the biosphere. The CCD reflects changes in carbon erosion, deposition, and silicate weathering and in association with  $\delta^{13}\text{C}$  of marine and terrestrial proxies (benthic foraminifers, terrestrial biomarkers, and planktonic-benthic gradients) can be used to gauge changes in the size and distribution of carbon reservoirs (Higgins and Schrag, 2006; Leon-Rodriguez and Dickens, 2010). However, although the general form of CCD changes is moderately well known for the various ocean basins (Peterson et al., 1992), we have little information on the rates and amplitude of change in the CCD on short timescales, which are so important to understanding transient episodes such as the various extinction events, hyperthermals, and glacial events of the Paleogene.

Although the PETM marks a pronounced global warming and ocean acidification event, the obverse is true of the EOT, where the Pacific Ocean appears to undergo pronounced de-acidification associated with the onset of major Cenozoic polar ice sheets (Fig. F12) (Coxall et al., 2005; Merico et al., 2008). Ultimately, ice sheet initiation appears to have been triggered by an orbitally forced interval of cool summers, but some other factor, probably long-term drawdown in atmospheric carbon dioxide levels,

must have conditioned the climate system (DeConto and Pollard, 2003; Coxall et al., 2005; DeConto et al., 2008). Records from the tropical Pacific (ODP Leg 199 [Lyle, Wilson, Janecek, et al., 2002]) demonstrate that the CCD deepened permanently (by ~1 km) in the earliest Oligocene—much faster than previously documented—in two 40 k.y. “jumps” and in lockstep with the stepwise onset of Antarctic glaciation, as recorded in benthic foraminifer  $\delta^{18}\text{O}$  (Coxall and Wilson, 2011; Coxall et al., 2005). However, it is unclear to what extent this lockstep behavior represents the global picture because sufficiently complete EOT depth transects from other ocean basins and latitudes are not available. Comparatively low-resolution records across a highly condensed and reworked Eocene/Oligocene boundary from Walvis Ridge (Leg 208 [Zachos, Kroon, Blum, et al., 2004]) have been interpreted in terms of a much smaller (~200 m) and nonpermanent CCD deepening. Thus, it is not clear whether CCD behavior in the equatorial Pacific represents the global picture, driven by wholesale change in deep-sea  $\text{CO}_3$  ion concentration, or is to some extent a regional signal driven by changes in export production with important implications for our understanding of contemporaneous carbon cycling (Dunkley Jones et al., 2008; Coxall and Wilson, 2011).

Additional large, but temporary, CCD deepening events are also documented in the middle Eocene of the equatorial Pacific (Lyle et al., 2005). These calcium carbonate accumulation events have been interpreted (by analogy with the EOT and on the basis of discontinuous stable isotope records) to be a lithologic expression of large-scale bipolar continental glaciation (Tripathi et al., 2005, 2007), but this interpretation is contested (Edgar et al., 2007; Eldrett et al., 2007, 2009; DeConto et al., 2008). The middle Eocene to lower Oligocene depth transect on the Newfoundland ridges presents an ideal opportunity to generate high-resolution records of changes in mass accumulation of  $\text{CaCO}_3$  needed to test the hypothesis that the CCD changes recently documented in the equatorial Pacific are globally representative and intimately associated with the onset of continental glaciation. Together with the floral, faunal, and geochemical proxy records such as compound-specific  $\delta^{13}\text{C}_{\text{org}}$  and  $\delta^{11}\text{B}$  in foraminiferal calcite (e.g., Pagani et al., 2005; Pearson et al., 2009) that could be generated, it would be possible to test for biotic turnover and  $\text{pCO}_2$  drawdown across these intervals, with important implications for our understanding of the causes and consequences of Cenozoic climate deterioration.



*2. Determine the flow history of the Atlantic Deep Western Boundary Current.*

Deep ocean circulation is critical to defining the global climatic regime and its stability for two reasons. First, the sinking of surface waters distributes thermal energy around the globe. Second, the chemistry and nutrient composition of the dominant deepwater masses influence the partitioning of CO<sub>2</sub> between the deep ocean and the atmosphere. The pattern, strength, and stability of thermohaline circulation arise from a combination of wind forcing (Toggweiler and Samuels, 1995) and thermal or salinity density contrasts.

Numerous models suggest that thermohaline circulation can exist in multiple equilibrium states (e.g., Marotzke and Willebrand, 1991), with the potential for catastrophic disruption or collapse. For example, in the recent past the warmth and stability of interglacial climates is notably distinct from the rapid and abrupt cycles of warming and cooling that pepper the cold of glacial periods (e.g., Dansgaard et al., 1993). It has been proposed that enhanced climate instability during cold periods may originate from salinity feedbacks, which set up multiple thermohaline modes (Keeling and Stephens, 2001; Rahmstorf, 1995; Stommel and Arons, 1960), or from instabilities that lead to periodic purges and the collapse of large ice sheets (Alley and Clark, 1999). Analogues to Pleistocene ice sheet-driven cycles could exist in Oligocene climate records where geochemical studies suggest that both poles may have been glaciated, although other evidence suggests that only Antarctica supported major ice sheets (DeConto et al., 2008; Edgar et al., 2007). Salinity-driven feedbacks are a potential source of rapid climate shifts in Eocene and older records before the large-scale development of polar ice caps.

The proposed drilling transect lies directly under the flow path of the Atlantic Deep Western Boundary Current and therefore is ideally placed to monitor the chemistry and temperature of waters exiting the Nordic basins in the Paleogene. Therefore, the J Anomaly and Southeast Newfoundland Ridge sites are perfectly placed to act as end-members for studying the contribution of northern source waters to the rest of the global ocean. We already have a South Atlantic/Southern Ocean end-member site (ODP Site 690, Weddell Sea) and Pacific end-member sites (Shatsky Rise, ODP Leg 198), but we have nothing equivalent in the North Atlantic except for the subtropical Blake Nose (ODP Leg 171B) sites, many of which are located in water depths that are too shallow to truly record Deep Western Boundary Current properties.

Why do we need end-members? If all we had were equatorial sites (far from the high-latitude sites of deepwater formation) we could still determine whether Atlantic waters were being exported into the Pacific and vice versa, but we would not know where those waters originated. Barring the unexpected revival of models of warm saline deep water (Brass et al., 1982; Friedrich et al., 2008), it seems most likely that deep waters dominantly form at high latitudes (Bice and Marotzke, 2002; Bice et al., 1997), as is the case today and as is predicted in ocean circulation models for the Paleogene. Hence, in order to offer any concrete observational data to test ocean modeling for past warm climates, we must know where deep waters are sourced and how deepwater production varies during different climate states. Drilling Newfoundland Ridge sediment drifts offers a first-rate opportunity to obtain a true North Atlantic end-member for these studies. The large depth range covered by the proposed depth transect also will allow studies of the full range of ocean properties from the abyss to thermocline waters, really for the first time anywhere in the Paleogene.

In order to capture such nuances and rapid shifts in circulation patterns, it is critical to obtain records that allow us to reconstruct climate at suborbital temporal resolution. The Newfoundland sediment drifts offer an unprecedented opportunity to achieve this goal from sites close to the source of northern overflow waters in the Paleogene and to resolve the changes in circulation that accompany various Paleogene extreme climate events.

A case in point is the inferred reversal in deepwater overturning during the PETM (Nuñez and Norris, 2006; Tripathi and Elderfield, 2005). A compilation of  $\delta^{13}\text{C}$  data from benthic foraminifers suggests that the “aging-gradient” in  $\delta^{13}\text{C}$  between Southern Ocean and Northern Hemisphere sites abruptly reverses during this interval of global warming (Fig. F13) (Nuñez and Norris, 2006). Southern Ocean overturning in the late Paleocene is interpreted to give way to northern overturning during the PETM and then gradually revert to Southern Ocean deepwater formation over the next ~100–150 k.y. An alternative explanation is that the reconstructed gradient reversal is a stratigraphic artifact created by the effects of dissolution on sediment accumulation in northern Atlantic sites (Zeebe and Zachos, 2007). A reversal in deep ocean circulation is seen in global climate model experiments of the PETM (e.g., Bice and Marotzke, 2001) and may have occurred during other Paleogene climate events. Drilling on the Newfoundland ridges can be used to look for such reversals in deepwater formation during a host of extreme climate events using three techniques. First, we can use depth transects to produce highly resolved records of the vertical structure of deep waters at critical sites such as the Newfoundland Ridges. Second, we can examine geo-

graphic gradients in benthic foraminifer geochemistry (e.g.,  $\delta^{13}\text{C}$ ) using the Newfoundland sites as a northern end-member for comparison with sites elsewhere in the world. Third, we can use the history of drift formation itself to qualitatively monitor the strength of the Deep Western Boundary Current and estimate the rate of formation of deep waters in the North Atlantic.

Depth transects have been shown to produce highly resolved records of changes in the source of deep waters in the Pleistocene (e.g., ODP Leg 154 [Curry, Shackleton, Richter, et al., 1995]) and the Paleogene (Legs 198, 207, and 208). For example, the hypothesized change in deepwater circulation during the PETM may have similarities to changes in deepwater formation during Pleistocene interstadials, in which outflows from the Nordic seas shift from deepwater formation to intermediate water formation as North Atlantic overturning waxes and wanes. In the Pleistocene, reduced North Atlantic overturning is associated with the intrusion of Antarctic Bottom Water well into the northern North Atlantic beneath Glacial North Atlantic Intermediate Water (Oppo and Lehman, 1993). We can look for similar changes in deepwater source areas by geochemical analysis of benthic foraminiferal calcite along depth transects. Appropriately well-preserved material can also be used to generate proxy records for the total  $\text{CO}_3^{2-}$  content of the deep and intermediate waters using planktonic foraminifer weight and percent fragmentation.

Our deepest sites lie within the carbonate lysocline in the Paleogene. None of our sites are strictly below the depth of carbonate accumulation, but the deepest site may have very little carbonate given the condensed nature of the transparent (Eocene) horizon. Foraminifer preservation will clearly suffer in sediments that have been subjected to extensive calcite dissolution and may well preclude foraminifer-based geochemical studies, particularly in planktonic foraminifers. However, if the sites can be correlated (by physical property records) to well-dated upslope sites (as was done during ODP Leg 154), we can use the deepwater site to pin the depth of the CCD and therefore evaluate the full magnitude of CCD variations throughout the Paleogene. The deepwater sites should also preserve a record of more refractory substrates such as fish teeth that can be used in Nd isotope studies of deep ocean flow paths (e.g., Via and Thomas 2006; Scher et al., 2011; Thomas et al., 2003).

An additional approach for identifying patterns of deepwater formation relies on dating drift sedimentary packages and analyzing their thicknesses and distributions in seismic profiles. The dates we currently have for the sediment drifts on the Newfoundland ridges strongly suggest that major drift formation began in the early Eo-

cene with the deposition of thick acoustically transparent sequences and then changed character in the early Oligocene to a more mud-wave dominated system. Verification of early Eocene drift formation would require a major reassessment of our inferences of the relationship between the rates of deepwater formation and polar glaciation because it has been generally held that drift formation began at the major onset of Antarctic glaciation in the earliest Oligocene (Davies et al., 2001).

Studies of deposition rates, sediment sources, and grain size would do much to evaluate the origins and current regimes under which these drifts formed, as well as provide precise dates for changes in drift formation that could be compared with geochemical evidence for changes in deepwater sources. To achieve these primary goals we propose to combine proxies from sedimentology, clay mineralogy, and organic/isotope geochemistry to be applied specifically to the current-sensitive silt fraction. Continuous granulometric records will provide direct information on the variability of current strength and thus the history of the Deep Western Boundary Current. Clay mineral assemblages are excellent tracers for provenance studies, and organic matter composition will support the identification of source areas of fine-grained material and the presence of allochthonous organic matter from higher northern latitudes. As a working hypothesis we consider that periods of enhanced strength of the Deep Western Boundary Current should have resulted in stronger advection of a higher latitude component and generally coarser grain sizes in the silt fraction, whereas periods of reduced current activity should primarily record more local sediment sources and surface-ocean signatures as well as finer grained sediments.

### *3. Obtain high-resolution records of the onset and development of Cenozoic glaciation.*

The canonical view of the onset of Cenozoic glaciation is that it took place in two main steps: (east) Antarctic ice sheets were established around the time of the EOT (~33 Ma), whereas Northern Hemisphere glaciation was not triggered until ~3–7 Ma (e.g., Miller et al., 1987; Zachos et al., 2001). However, on the basis of sediments recovered in the last phase of ODP and the initial phase of IODP, it has been suggested that this view of Earth's climate history may need revision. Dropstones have been reported from the Arctic (IODP Expedition 303) in sediments of ~45 Ma age (Backmann et al., 2005). Discontinuous  $\delta^{18}\text{O}$  records in bulk and benthic foraminiferal calcite from the equatorial Pacific (ODP Leg 199) have been interpreted in terms of extensive ice sheet development in both hemispheres, together with a huge (>150 m) eustatic sea level fall around 42 Ma (Tripathi et al., 2005, 2007). This interpretation is controversial (Lear et al., 2004; Edgar et al., 2007; DeConto et al., 2008). Records from the

Norwegian-Greenland Sea and the Arctic Lomonosov Ridge suggest that winter sea ice formation was initiated around the start of the middle Eocene and that isolated alpine outlet glaciers existed on Greenland by the late Eocene (Eldrett et al., 2007; Stickley et al., 2009). In contrast with early interpretations (Lear et al., 2000), it is now also clear that the magnitude of the  $\delta^{18}\text{O}$  increase across the EOT (~33.5 Ma; Fig. F11) is too large to reflect ice growth on Antarctica alone (Coxall et al., 2005), and there is growing evidence for contemporaneous global cooling (Lear et al., 2004, 2008; Liu et al., 2009; Eldrett et al., 2009).

Expedition 342 provides an opportunity to shed new light on these aspects of Paleogene climate in the high northern latitudes in unprecedented stratigraphic detail. The middle to upper Eocene and lower Oligocene sections targeted here will allow us to generate the high-resolution records of changes in sedimentation rate, clay mineral assemblage, and occurrence and provenance of ice-rafted debris (IRD) that are needed. A potential problem exists with differentiating between putative Paleogene IRD and sediment eroded from the continental margin. In Pleistocene strata, IRD is often identified because of its coarse grain size (sand-sized and larger) and its distinctive provenance (e.g., “red-coated grains” from Labrador; basalt from Iceland) (Bond and Lotti, 1995; Hemming et al., 1998). IRD in the silt fraction has been identified by a number of techniques, including modeling of end-member components using a wide spectrum of grain-size analyses (Weltje, 1997; Weltje and Prins, 2003; Prins et al., 2002). IRD might also be identified by combining grain-size (especially sand content) and mineralogical information during “cold” events inferred from light stable isotope studies and geochemical assessment of provenance.

Clay minerals are excellent tracers of provenance in the modern North Atlantic and should have broadly similar distributions in the Paleogene. Continental-sourced clays should dominate the west Greenland and Canadian margins, whereas volcanic-sourced clays should be more typical of the Paleogene flood basalt province in eastern Greenland. In the modern North Atlantic, smectite, illite, chlorite, and kaolinite constitute the major proportion of the clay fraction. Smectite has been regarded as a major tracer for Iceland-Faeroe-derived material (Fagel et al., 1996) and could be expected from the Greenland volcanic province in the Paleogene. Where smectites are lacking, chlorite is the typical high-latitude clay from old metamorphic sources. A lack of volcanogenic and weathered basalt-derived clays (nontronite and amorphous minerals) would suggest a rather restricted contribution from eastern Greenland and mid-ocean-ridge sources. Clay mineral type (e.g., montmorillonite versus beidellite) and percentage data and Sm-Nd ratios in the clay fraction of Reykjanes

Ridge sediments indicate a dominant terrigenous contribution from young continental crust that may derive from Europe and/or the Arctic (Fagel et al., 2001; Innocent et al., 2000). Today, the clay fraction may also contain terrigenous calcites and dolomites deriving from glacier milk in the Hudson Bay area. Such a signal could be transported for much longer distances than sand-sized IRD.

*4. Extend the astronomical calibration of biostratigraphic and magnetostratigraphic markers and the geological timescale.*

A detailed geological timescale that can be applied widely has always been a primary goal. Indeed, a highly resolved timescale is becoming increasingly critical in studies of Paleogene paleoceanography as we extend work on millennial timescales into deep time and require increasingly high-resolution correlation to evaluate the evolution of interbasin geochemical gradients. Determination of the rates at which Earth processes take place and how these rates change are key not only to developing an understanding of Earth history but also to accurately describing the nature and rate of the processes themselves.

The discovery of orbitally driven variations in Earth's climate, and their preservation in the marine sedimentary record, has been the latest advance in chronostratigraphy. The application of this technique is not without assumptions, including the predictability of the exact beat of the climatic metronome (Pälike et al., 2000, 2004). However, if constrained by a paleomagnetic reversal stratigraphy, and if the same ages are obtained for geologic boundaries in different regions with different sensitivities to each of the different orbital forcings, we can develop a strong confidence in the timescale. A complete orbitally tuned Cenozoic timescale can provide estimates of process rates that have comparable precision throughout the Cenozoic.

We are working toward an astronomically tuned Cenozoic timescale. There is a semi-anchored astronomical timescale back to 30 Ma (mostly from ODP Leg 154). No magnetostratigraphy was recovered during Leg 154 (Curry, Shackleton, Richter, et al., 1995), but investigations from ODP Legs 177 (Gersonde, Hodell, Blum, et al., 1999) and 199 have resulted in verification and refinement of results from Leg 154 (e.g., Bilups et al., 2004; Wade and Pälike, 2004), as well as an extension of the tuning across the EOT (Coxall et al., 2005). Several other ODP legs and IODP expeditions have provided suitable data for work of this sort—most recently from the Pacific Equatorial Age Transect (Expedition 320/321 [Pälike, Lyle, Nishi, Raffi, Gamage, Klaus, and the Expedition 320/321 Scientists, 2010]). Additional records are available for the time intervals of 35–42 Ma (Pälike et al., 2001; ODP Legs 171B and 177), ~45–56 Ma (ODP

Leg 207; Westerhold and Röhl, 2009), 53–57 Ma (Norris and Röhl, 1999; Lourens et al., 2005; ODP Legs 171B, 198, and 208), and 62–65 Ma (ODP Legs 165 [Sigurdsson, Leckie, Acton, et al., 1997], 171B, 198, and 208). From this perspective, acquisition of an astronomically tuned record of the late Eocene and the early middle Eocene would be extremely important to span existing gaps in our tuning efforts and to provide single-site, high-resolution data that allow splicing, verification, and extension of previous efforts.

For the Paleocene and Eocene, a shallow CCD has hampered efforts to get long, uninterrupted carbonate sequences that allow high-resolution paleoclimatic studies with traditional geochemical studies (e.g., stable isotope analysis). The tectonic setting of the sites targeted by Expedition 342 is likely to overcome this problem because the proposed sites track above the CCD for the critical time slices needed, with potentially very expanded Paleocene, Eocene, and Oligocene sedimentary deposits. In addition, for the time intervals that have already been astronomically tuned, a comparison between low-latitude sites from the Pacific and Atlantic will be complemented by the North Atlantic setting of Expedition 342, offering the chance to decipher the processes controlling the amplification of, for example, ~41 k.y. obliquity versus ~100 and 405 k.y. eccentricity cycles and to test the hypothesis that there are different dominant astronomical forcings between Earth's warm and cool periods.

## Drilling strategy

Expedition 342 will begin with a 2 day transit to ODP Site 1073 to conduct a 2 day engineering test of the newly developed Motion Decoupled Hydraulic Delivery System (MDHDS), a device that should enhance the quality of formation temperature and pressure measurements (see “[MDHDS tool testing](#)”). After an additional ~4 days of transit, the vessel will arrive at the main operations area (Fig. [F14](#)). An overview of primary and alternate drill sites, including links to figures showing site positions along the single-channel, high-resolution seismic survey lines, is given in Table [T1](#). Additional operational planning detail is given in Tables [T2](#) (primary sites) and [T3](#) (alternate sites).

Our primary goal is to drill a depth transect in high deposition rate, middle Eocene–?upper Eocene and ?Oligocene drift sites. Our depth transect consists of six drill sites, each of which will be cored three times to obtain continuous spliced sections (Tables [T1](#), [T2](#)). We propose to start with the deepest end of the depth transect on J Anomaly

Ridge to pin the deep end of the depth transect (Fig. F1) This first site (JA-1A) will be drilled 400 meters below seafloor (mbsf) through the middle and ?upper Eocene sediment package into the lower Eocene and Paleocene (Figs. F4, F6, F10). Two additional sites (JA-14A and JA-5A) will be drilled to ~250 mbsf on this same drift higher on the flank of J Anomaly Ridge (Figs. F4, F6, F10). These sites are intended to sample a very expanded record of the ?upper Eocene and upper middle Eocene. We will then move to Southeast Newfoundland Ridge to drill the ?upper Eocene and ?Oligocene boundary sections at Site SENR-16A to 400 mbsf (Figs. F4, F7, F11). Next, we will move to Site SENR-11A, where we will drill the upper part of one of the plastered drifts on the north flank of one of the seamounts to sample the ?upper Eocene and middle Eocene (300 mbsf) (Figs. F4, F15). We will then finish drilling operations by coring the ?upper Eocene to middle Eocene pelagic cap of the seamount (Site SENR-19B; 250 mbsf) (Figs. F4, F16). All holes will be triple cored, with the option to extend two holes to 400 m subbottom and log them. Advanced piston corer (APC) penetration will be maximized by “drilling over” the APC barrel until this is no longer safe or practical, at which point the extended core barrel (XCB) will be used to achieve the depth objective.

Two alternative scenarios have also been considered and may be implemented in some form depending on the results from Sites JA-1A and SENR-16A. In both alternate scenarios we would drill both Sites JA-1A (targeting the Paleocene–Eocene drift section at the deep end of the transect) and SENR-16A (to target the EOT).

In the first alternative scenario, we may find that drilling at Site JA-1A makes a compelling case to prioritize Paleocene–lower Eocene sections over upper Eocene drift deposits. A Paleocene–lower Eocene depth transect could be obtained by drilling a 400 m section at alternate Site JA-15A, a 400 m section at alternate Site SENR-18A, and a 200 m section at alternate Site SENR-1B (Figs. F4, F6, F17, F18). This strategy would yield a four-point depth transect only slightly (280 m) shorter than the transect focused on middle Eocene–?upper Eocene sediments. However, we would likely encounter more unconformities in the section (likely near the lower Eocene/middle Eocene boundary) and more chert.

In the second alternative scenario, we may find that drilling results make a compelling case to prioritize capturing a continuous high deposition–rate section in the middle Eocene–Oligocene record over the depth transect aspect of our plan. This would involve drilling Site JA-1A (400 m penetration) and then a combination of Site JA-14A (250 m penetration) in the middle Eocene–?upper Eocene, followed by ~200 m pen-



etration at alternate Site JA-15A (to the lower Eocene/middle Eocene boundary) (Figs. **F4, F6, F10**). The combined record of Sites JA-14A and JA-15A would provide a complete record of the acoustically transparent drift package on J Anomaly Ridge. Coring would then switch to Site SENR-16A to obtain the 400 m thick Oligocene–upper Eocene section, followed by Site SENR-11A to 400 m to obtain the lower part of the middle Eocene (Figs. **F4, F7, F10, F15**). If time allowed, we would core the pelagic cap at either Sites SENR-19B or SENR-1B (both ~200–250 m penetration; Figs. **F4, F16, F17, F18**). We would obtain a four-point depth transect with this strategy in the middle Eocene and a three-point transect in the ?upper Eocene as long as there were time to core both pelagic caps. A further possibility under this alternative scenario targeted at capturing a continuous high deposition–rate section in the middle Eocene to Oligocene would involve drilling alternate Site SENR-10A to 200 m, depending on the results of drilling at Site SENR-16A.

Our drilling strategy depends on maintaining a balance between (1) multiple coring at sites to obtain continuous sections, (2) collecting long enough records to capture numerous “critical boundaries,” (3) maximizing the total depth range captured by our coring transect, (4) obtaining logging records to fill gaps in discontinuously cored sections, and (5) providing log data to create synthetic seismograms to tie cores to seismic records. Two additional considerations are (1) to produce logs that will help us tackle the problem of differential compaction in cores and (2) to maximize the logged record relative to hole depth. These objectives are not fully compatible because all require trade-offs in operations time. We rank these priorities in favor of (1) obtaining the depth transect, (2) maximizing sedimentation rate in local sections instead of targeting long time series records, (3) collecting spliced records of physical core, (4) obtaining logging records to bridge core gaps, and (5) constructing synthetic seismograms for core-seismic integration. We rank the effort to tackle the differential compaction problem and acquire logs in shallow holes as a lower priority.

## Downhole measurements strategy

### Wireline logging

On the basis of the drilling strategy outlined above, we propose to prioritize logging operations according to the accumulated value of each of the logging-related criteria for expedition science. Hence, we will give less consideration to logging shallow penetration holes where we anticipate complete core recovery and sites that sample the

acoustically transparent Eocene drift sediment package where we have no acoustic reflection record to compare with synthetic seismograms. Conversely, sites that have deep penetration, sample acoustically complex sections, and those where the core recovery is incomplete will be higher priorities for logging. Therefore, our priority logging sites are JA-1A, SENR-16A, and SENR-11A. Other sites (JA-14A, JA-5A, and SENR-19B) have lower priority for logging because they have shallow penetration, are proposed for triple coring, and are in acoustically transparent sections.

Two standard IODP tool string configurations will be deployed in each logging hole: the triple combination (triple combo) and the Formation MicroScanner (FMS)-sonic tool strings (Fig. F21). The first run will be the triple combo tool string, which logs formation resistivity, density, porosity, natural gamma radiation (NGR), and borehole diameter. The diameter log provided by the caliper on the density tool will allow assessment of hole conditions (e.g., any washouts of sandy beds), log quality, and the potential for success of the following runs. The second run will be the FMS-sonic tool string, which provides an oriented 360° resistivity image of the borehole wall and logs of formation acoustic velocity, NGR, and borehole diameter.

The Magnetic Susceptibility Sonde (MSS) currently under development at Lamont-Doherty Earth Observatory Borehole Research Group is anticipated to be available for deployment during Expedition 340 Lesser Antilles, and therefore also during Expedition 342. If the MSS is available, the triple combo will be modified to replace the Dual Induction Tool (DIT) resistivity tool with the MSS; this modified tool string will be called the “paleo combo” (Fig. F22). Details of the logging tools are available at [iodp.ldeo.columbia.edu/TOOLS\\_LABS/tools.html](http://iodp.ldeo.columbia.edu/TOOLS_LABS/tools.html).

Downhole logging data will provide the only stratigraphic data where core is not recovered and aims to provide characterization of in situ formation properties and establish the link between features in the borehole and reflectors in the seismic sections. To provide the link between borehole stratigraphy and the seismic section, sonic velocity and density data will be combined to generate synthetic seismograms for detailed well-seismic correlations.

Logging time estimates for each site are given in Tables T1, T2, and T3.

## **Formation temperature measurements**

The downhole measurement plan includes a depth series of reconnaissance temperature measurements for all sites. Typically, ~3–5 measurements are made in one hole per site using the advanced piston corer temperature tool (APCT-3). The scientific objective of the temperature measurement plan is to provide sufficient data to reconstruct the thermal gradient at each site.

## **MDHDS tool testing**

### **Background and summary**

Approximately two days of ship time during Expedition 342 will be spent testing the Motion Decoupled Hydraulic Delivery System (MDHDS). The MDHDS is an IODP-funded engineering development led by the University of Texas in conjunction with the USIO and Mohr Engineering. The MDHDS will serve as a foundation for future penetrometer and other downhole tool deployments. We will test the MDHDS at ODP Site 1073 (Leg 174A), offshore New Jersey, by deploying both the SET-P and T2P pore pressure penetrometers. Because of previous drilling at Site 1073, we know the lithology and material properties of this site. This sea trial is the culmination of multiple land-based tests, and a successful deployment will mean this tool can be reliably deployed during future expeditions. There is also significant scientific value to the test. During Leg 174A, the presence of pore overpressure near the seafloor was predicted (Dugan and Flemings, 2000). A successful test of the MDHDS and recovery of pore pressure measurements in this shallow section would illuminate at what depth pore pressure starts and the current stability of the sediments near the seafloor, which are critical questions for both hydrodynamic models of shallow sedimentary sections and our understanding of the process of slope failure. The MDHDS will be run with a real-time data link through the logging wireline to observe system behavior.

### **Motivation for testing and relevance to IODP goals**

The ability to measure pressure and permeability in mudstone is critical to achieving the scientific goals of IODP as expressed in the Initial Science Plan (ISP) (IODP International Working Group, 2001). In the ISP, issues directly related to fluid pressure/flow include the occurrence, stability, and dissociation of gas hydrate (Hyndman and Davis, 1992; Kvenvolden, 1993; Dickens et al., 1997; Ruppel, 1997; Dillon et al., 2000;

Liu and Flemings, 2009) and the geometry, structure, fluxes, and earthquake mechanics of accretionary complexes (Davis et al., 1983; Dahlen et al., 1984; Bekins and Dreiss, 1992; Saffer and Bekins, 2002; Screaton et al., 2002). Models of these systems await validation because of the lack of direct pressure measurements; IODP has started to implement short-term measurements via penetrometers (Flemings et al., 2008) and downhole formation testers (Saffer, McNeill, Byrne, Araki, Toczko, Eguchi, Takahashi, and the Expedition 319 Scientists, 2010) and long-term observatories (Fisher et al., 2005). The Engineering Development Panel prioritized measurements of in situ pressure as one of the critical technologies in need of development and supported the development of the MDHDS. The Science and Technology Panel defines the measurement of in situ pressure as a “standard measurement,” which shall, whenever practical, be carried out.

The new science plan for future scientific drilling emphasizes the need for observatory science relating to pore pressure, gas hydrate dynamics, and geohazards, including those related to fluid flow and slope failure ([www.iodp.org/Science-Plan-for-2013-2023/](http://www.iodp.org/Science-Plan-for-2013-2023/)). Our pore pressure measurements will illuminate the role of pore fluids in continental slope geomorphology (Johnson, 1939; Rona, 1969), the cause of low-angle landslides (Terzaghi, 1950; Bombolakis, 1981), and the effect of focused flow along permeable layers on the timing and distribution of failure (Haneberg, 1995; Dugan and Flemings, 2000, 2002; Boehm and Moore, 2002; Flemings et al., 2002).

## Why the MDHDS?

Previously, the T2P and the SET-P (formerly the DVTP-P), the two penetrometers used by IODP, were deployed by wireline on the Collected Delivery System (CDS). The CDS is analogous to an old-style pointer, in which a series of cylinders slide past each other to increase or decrease the system’s length. In this configuration, the penetrometer is pushed in by the drill string, and then the drill string is raised to decouple the drill string from the formation; however, the penetrometer remains connected to the drill string through the CDS, which should expand and contract during ship heave. Analysis of previous deployments showed that when the drill string was raised, the penetrometer was pulled out of the formation >80% of the time (Fig. F23). When this occurs, the measured pressure drops rapidly and the measurement is compromised (Fig. F23E–F23G). This occurs with both the T2P and the SETP.

The MDHDS (Fig. F24) was specifically designed to overcome this problem. More broadly, it is envisioned to be the foundation for future downhole tool deployment

and is designed to allow real-time communication between the tool and the rig floor via the logging wireline. It is a wireline-deployed system that uses mud pressure to advance a penetrometer into the formation (Fig. F24). After hydraulic deployment of the penetrometer, the bottom-hole assembly (BHA) is raised to completely decouple the tool from the BHA, thus eliminating the adverse effects of pipe heave. The MDHDS also uses mud pressure to insert the tool rather than lowering the BHA, which eliminates the mud plugging problem that has plagued the CDS.

The MDHDS can be deployed either on the coring wireline or on an armored conductor cable such as the logging line. If deployed on the wireline, complete decoupling will occur because of separation of the wireline from the tool. Alternatively, if deployed on the conductor cable, a continuous signal can communicate with the tool. The capability of a “hotline” to the tool opens a range of exciting possibilities for future tool developments. Unlike the CDS, which is driven into the formation by lowering the BHA to the bottom of the borehole, the MDHDS allows the BHA to remain 2 m off the bottom of the borehole (Fig. F24). This clearance greatly reduces the possibility of jamming borehole cuttings or other detritus inside the BHA, which could result in coupling between the tool and the BHA. The penetrometer is extracted from the formation by lowering the wireline through the upper latch union, allowing the RS (the RS or “Running Shoe” is designed to retrieve downhole tools by wireline) overshot to latch onto the RS fishing neck attached to the upper piston rod. In the case of a “hotline” deployment, the soft tether will recoil itself inside the upper piston rod, allowing the RS overshot to latch onto the RS fishing neck.

## Operations at Site 1073

Prior to arrival at Site 1073, considerable time will be spent with Schlumberger personnel, core technicians, and the drilling crew to review the rig floor procedure for deploying the MDHDS.

Site 1073 is at 639 m water depth (Fig. F25). Sediments encountered will be soft mudstone (Fig. F26). We will wash down (or core) to ~100 m before deploying the MDHDS and associated penetrometers multiple times. We will also test the real-time data link via the logging wireline. Before each new deployment we will need to wash down ~10 m. The T2P will need to be tested with and without the logging wireline. The SET-P will be tested without the wireline. We have requested six penetrometer deployments. The core technicians will also need time to work out the field deployment of the tool and the deck-handling procedure.

## Risks and contingencies

Three principal factors could affect implementation of the drilling plan:

1. Adverse hole conditions at the principal sites because of dropstones and chert and adverse formation conditions (e.g., if we were to encounter sediments that do not allow generation of high-quality composite sections suited to modern paleoceanographic analysis).
2. Weather conditions that could limit the ability to drill, particularly hurricanes early in the hurricane season.
3. Time delays arising from equipment breakdowns, tools lost downhole, or measures taken to respond to hole conditions.

## Hole conditions

Poor hole conditions at all sites will be dealt with in the first instance by using frequent high-viscosity mud sweeps and or heavy mud to condition the holes. The only possible remedial action if hole conditions prove to be insurmountable is to plug and abandon the hole and move to an alternate hole/site. In the event that we encounter formations that do not allow us to build high-quality composite sections suited to modern paleoceanographic analysis, a primary site may be shortened or dropped from the schedule. Such a decision will only be made following consultation with the science party.

## Weather conditions

Hurricane season at the operation area is between August and November; thus, Expedition 342 is scheduled (mid-June to mid-August) to be largely outside this window. However, we had to abandon the site survey for 3 days to run south into the North Atlantic Gyre due to Hurricane Alex in mid-August 2004.

## Timing

If significant time is spent responding to poor hole conditions, slower-than-expected penetration rates, or weather-related delays, a primary site may be shortened or dropped from the schedule. Such a decision will only be made following consultation with the science party.

## Alternate sites

Alternate sites may be cored and logged if poor hole conditions or other operational difficulties are encountered at the respective primary sites and if better conditions are expected at the alternate sites. Seismic profiles of all proposed alternate sites (as well as of all primary sites discussed above) are included in “[Site summaries](#).” The operations plans for the alternate sites can be found in Tables [T1](#) and [T3](#).

## Sample and data sharing strategy

Shipboard and shore-based researchers should refer to the IODP Sample, Data, and Obligations Policy ([www.iodp.org/program-policies/](http://www.iodp.org/program-policies/)). This document outlines the policy for distributing IODP samples and data. It also defines the obligations incurred by sample and data recipients. All requests for data and core samples must be approved by the Sample Allocation Committee (SAC). The SAC is composed of the Co-Chief Scientists, Staff Scientist, and IODP Curator on shore and curatorial representatives in place of the Curator on board the ship.

Every member of the science party is obligated to carry out scientific research for the expedition and publish. For this purpose, shipboard scientists are expected to submit sample requests (at [smcs.iodp.org:8080/smcs/](http://smcs.iodp.org:8080/smcs/)) detailing their science plan ~3–4 months before the beginning of the expedition (exact time line will be established when staffing is complete). On the basis of sample requests (shore based and shipboard) submitted by this deadline and input from the scientific party, the SAC will prepare a tentative sampling plan that will be revised on the ship as dictated by recovery and cruise objectives. The sampling plan will be subject to modification depending on the actual material recovered and collaborations that may evolve between scientists during the expedition. This planning process is necessary to coordinate the research to be conducted and to ensure that the scientific objectives are achieved. Modifications to the sampling plan and access to samples and data during the expedition and the 1 y postexpedition moratorium period require the approval of the SAC.

All sample frequencies and sizes must be justified on a scientific basis and will depend on core recovery, the full spectrum of other requests, and the expedition objectives. Some redundancy of measurement is unavoidable, but minimizing the duplication of measurements among the shipboard party and identified shore-based collaborators will be a factor in evaluating sample requests. Success will require collaboration, inte-

gration of complementary data sets, and consistent methods of analysis. Substantial collaboration and cooperation are highly encouraged.

Shipboard sampling will be restricted to acquiring ephemeral data types and to low-resolution sampling for shipboard data acquisition (e.g., biostratigraphic sampling, pore waters, and shipboard geochemistry) so that we can rapidly produce age-model data critical to the overall objectives of the expedition and plan for higher resolution sampling postcruise. Sampling may also include “toothpick” (~0.5 cm<sup>3</sup>) samples for preliminary shore-based stable isotope investigations where they are likely to materially aid the identification of critical intervals for the sampling party, as long as they do not threaten the integrity of the core. The bulk of sampling for scientists’ personal research will be postponed until a shore-based sampling party to be implemented ~4–5 months after the expedition at the Bremen Core Repository (BCR) in Bremen, Germany. The BCR houses cores collected from the Atlantic and Arctic Oceans.

There may be considerable demand for samples from a limited amount of cored material for some critical intervals. Critical intervals may require special handling, a higher sampling density, reduced sample size, or continuous core sampling for a set of particular high-priority research objectives. The SAC may require an additional formal sampling plan before critical intervals are sampled, and a special sampling plan will be developed to maximize scientific return and scientific participation and to preserve some material for future studies. The SAC can decide at any stage during the expedition or during the 1 y moratorium period to identify recovered intervals as “critical.”

All collected data and samples will be protected by a 1 y postexpedition moratorium, during which time data and samples are available only to the Expedition 342 Science Party and approved shore-based participants. Because of the decision to hold a sampling party ~4–5 months postcruise, the moratorium will in fact extend to 1 y following the completion of the sampling party.



## References

- Alley, R.B., and Clark, P.U., 1999. The deglaciation of the Northern Hemisphere: a global perspective. *Annu. Rev. Earth Planet. Sci.*, 27(1):149–182. doi:10.1146/annurev.earth.27.1.149
- Arthur, M.A., Srivastava, S.P., Kaminski, M., Jarrard, R., and Osler, J., 1989. Seismic stratigraphy and history of deep circulation and sediment drift development in Baffin Bay and the Labrador Sea. In Srivastava, S.P., Arthur, M., Clement, B., et al., *Proc. ODP, Sci. Results*, 105: College Station, TX (Ocean Drilling Program), 957–988. doi:10.2973/odp.proc.sr.105.118.1989
- Austin, J.A., Jr., Christie-Blick, N., Malone, M.J., et al., 1998. *Proc. ODP, Init. Repts.*, 174A: College Station, TX (Ocean Drilling Program). doi:10.2973/odp.proc.ir.174a.1998
- Backman, J., Moran, K., McInroy, D., and the IODP Expedition 302 Scientists, 2005. IODP Expedition 302, Arctic Coring Expedition (ACEX): a first look at the Cenozoic paleoceanography of the central Arctic Ocean. *Sci. Drill.*, 1:12–17. doi:10.2204/iodp.sd.1.02.2005
- Bekins, B.A., and Dreiss, S.J., 1992. A simplified analysis of parameters controlling dewatering in accretionary prisms. *Earth Planet. Sci. Lett.*, 10(3–4):275–287. doi:10.1016/0012-821X(92)90092-A
- Berggren, W.A., Aubry, M.-P., van Fossen, M., Kent, D.V., Norris, R.D., and Quillévéré, F., 2000. Integrated Paleocene calcareous plankton magnetobiochronology and stable isotope stratigraphy: DSDP Site 384 (NW Atlantic Ocean). *Palaeogeogr., Palaeoclimatol., Palaeoecol.*, 159(1–2):1–51. doi:10.1016/S0031-0182(00)00031-6
- Bice, K.L., Barron, E.J., and Peterson, W.H., 1997. Continental runoff and early Cenozoic bottom-water sources. *Geology*, 25(10):951–954. doi:10.1130/0091-7613(1997)025<0951:CRAECB>2.3.CO;2
- Bice, K.L., and Marotzke, J., 2001. Numerical evidence against reversed thermohaline circulation in the warm Paleocene/Eocene ocean. *J. Geophys. Res., [Oceans]*, 106(C6):11529–11542. doi:10.1029/2000JC000561
- Bice, K.L., and Marotzke, J., 2002. Could changing ocean circulation have destabilized methane hydrate at the Palaeocene/Eocene boundary? *Paleoceanography*, 17(2):1018–1039. doi:10.1029/2001PA000678
- Bijl, P.K., Houben, A.J.P., Schouten, S., Bohaty, S.M., Sluijs, A., Reichert, G.-J., Sinninghe Damsté, J.S., and Brinkhuis, H., 2010. Transient middle Eocene atmospheric CO<sub>2</sub> and temperature variations. *Science*, 330(6005):819–821. doi:10.1126/science.1193654
- Billups, K., Pälike, H., Channell, J.E.T., Zachos, J.C., and Shackleton, N.J., 2004. Astronomic calibration of the late Oligocene through early Miocene geomagnetic polarity time scale. *Earth Planet. Sci. Lett.*, 224(1–2):33–44. doi:10.1016/j.epsl.2004.05.004
- Boehm, A., and Moore, J.C., 2002. Fluidized sandstone intrusions as an indicator of paleo-stress orientation, Santa Cruz, California. *Geofluids*, 2(2):147–161. doi:10.1046/j.1468-8123.2002.00026.x
- Bohaty, S.M., Zachos, J.C., Florindo, F., and Delaney, M.L., 2009. Coupled greenhouse warming and deep-sea acidification in the middle Eocene. *Paleoceanography*, 24(2):PA2207–PA2222. doi:10.1029/2008PA001676
- Bombolakis, E.G., 1981. Analysis of a horizontal catastrophic landslide. In Carter, N.L., Friedman, M., Logan, J.M., and Stearns, D.W. (Eds.), *Mechanical Behavior of Crustal Rocks*. Geophys. Monogr., 24:251–258. doi:10.1029/GM024p0251

- Bond, G.C., and Lotti, R., 1995. Iceberg discharges into the North Atlantic on millennial time scales during the last glaciation. *Science*, 276(5200):1005–1010. [doi:10.1126/science.267.5200.1005](https://doi.org/10.1126/science.267.5200.1005)
- Bralower, T.J., Premoli Silva, I., Malone, M.J., et al., 2002. *Proc. ODP, Init. Repts.*, 198: College Station, TX (Ocean Drilling Program). [doi:10.2973/odp.proc.ir.198.2002](https://doi.org/10.2973/odp.proc.ir.198.2002)
- Brass, G.W., Southam, J.R., and Peterson, W.H., 1982. Warm saline bottom water in the ancient ocean. *Nature (London, U. K.)*, 296(5858):620–623. [doi:10.1038/296620a0](https://doi.org/10.1038/296620a0)
- Brinkhuis, H., Schouten, S., Collinson, M.E., Sluijs, A., Sinninghe Damsté, J.S., Dickens, G.R., Huber, M., Cronin, T.M., Onodera, J., Takahashi, K., Bujak, J.P., Stein, R., van der Burgh, J., Eldrett, J.S., Harding, I.C., Lotter, A.F., Sangiorgi, F., van Konijnenburg-van Cittert, H., de Leeuw, J.W., Matthiessen, J., Backman, J., Moran, K., and the Expedition 302 Scientists, 2006. Episodic fresh surface waters in the Eocene Arctic Ocean. *Nature (London, U. K.)*, 441(7093):606–609. [doi:10.1038/nature04692](https://doi.org/10.1038/nature04692)
- Channell, J.E.T., Sato, T., Kanamatsu, T., Stein, R., and Alvarez Zarikian, C., 2010. Expedition 303/306 synthesis: North Atlantic climate. In Channell, J.E.T., Kanamatsu, T., Sato, T., Stein, R., Alvarez Zarikian, C.A., Malone, M.J., and the Expedition 303/306 Scientists, *Proc. IODP, 303/306*: College Station, TX (Integrated Ocean Drilling Program Management International, Inc.). [doi:10.2204/iodp.proc.303306.214.2010](https://doi.org/10.2204/iodp.proc.303306.214.2010)
- Coxall, H.K., and Wilson, P.A., 2011. Early Oligocene glaciation and productivity in the eastern equatorial Pacific: insights into global carbon cycling. *Paleoceanography*, 26(2):PA2221–PA2238. [doi:10.1029/2010PA002021](https://doi.org/10.1029/2010PA002021)
- Coxall, H.K., Wilson, P.A., Pälike, H., Lear, C.H., and Backman, J., 2005. Rapid stepwise onset of Antarctic glaciation and deeper calcite compensation in the Pacific Ocean. *Nature (London, U. K.)*, 433(7021):53–57. [doi:10.1038/nature03135](https://doi.org/10.1038/nature03135)
- Curry, W.B., Shackleton, N.J., Richter, C., et al., 1995. *Proc. ODP, Init. Repts.*, 154: College Station, TX (Ocean Drilling Program). [doi:10.2973/odp.proc.ir.154.1995](https://doi.org/10.2973/odp.proc.ir.154.1995)
- Dahlen, F.A., Suppe, J., and Davis, D., 1984. Mechanics of fold-and-thrust belts and accretionary wedges: cohesive Coulomb theory. *J. Geophys. Res., [Solid Earth]*, 89(B12):10087–10101. [doi:10.1029/JB089iB12p10087](https://doi.org/10.1029/JB089iB12p10087)
- Dansgaard, W., Johnsen, S.J., Clausen, H.B., Dahl-Jensen, D., Gundestrup, N.S., Hammer, C.U., Hvidberg, C.S., Steffensen, J.P., Sveinbjörnsdottir, A.E., Jouzel, J., and Bond, G., 1993. Evidence for general instability of past climate from a 250-kyr ice-core record. *Nature (London, U. K.)*, 364(6434):218–220. [doi:10.1038/364218a0](https://doi.org/10.1038/364218a0)
- Davies, R., Cartwright, J., Pike, J., and Line, C., 2001. Early Oligocene initiation of North Atlantic Deep Water formation. *Nature (London, U. K.)*, 410(6831):917–920. [doi:10.1038/35073551](https://doi.org/10.1038/35073551)
- Davis, D., Suppe, J., and Dahlen, F.A., 1983. Mechanics of fold-and-thrust belts and accretionary wedges. *J. Geophys. Res., [Solid Earth]*, 88(B2):1153–1172. [doi:10.1029/JB088iB02p01153](https://doi.org/10.1029/JB088iB02p01153)
- DeConto, R.M., and Pollard, D., 2003. Rapid Cenozoic glaciation of Antarctica induced by declining atmospheric CO<sub>2</sub>. *Nature (London, U. K.)*, 421(6920):245–249. [doi:10.1038/nature01290](https://doi.org/10.1038/nature01290)
- DeConto, R.M., Pollard, D., Wilson, P.A., Pälike, H., Lear, C.H., and Pagani, M., 2008. Thresholds for Cenozoic bipolar glaciation. *Nature (London, U. K.)*, 455(7213):652–656. [doi:10.1038/nature07337](https://doi.org/10.1038/nature07337)

- Dickens, G.R., Castillo, M.M., and Walker, J.C.G., 1997. A blast of gas in the latest Paleocene: simulating first-order effects of massive dissociation of oceanic methane hydrate. *Geology*, 25(3):259–262. doi:10.1130/0091-7613(1997)025<0259:ABOGIT>2.3.CO;2
- Dillon, W.P., Nealon, J.W., Taylor, M.H., Lee, M.W., Drury, R.M., and Anton, C.H., 2000. Seafloor collapse and methane venting associated with gas hydrate on the Blake Ridge: causes and implications to seafloor stability and methane release. In Paull, C.K., and Dillon, W.P. (Eds.), *Natural Gas Hydrates: Occurrence, Distribution, and Detection*. Geophys. Monogr., 124:211–233. doi:10.1029/GM124p0211
- Dugan, B., and Flemings, P.B., 2000. Overpressure and fluid flow in the New Jersey continental slope: implications for slope failure and cold seeps. *Science*, 289(5477):288–291. doi:10.1126/science.289.5477.288
- Dugan, B., and Flemings, P.B., 2002. Fluid flow and stability of the US continental slope offshore New Jersey from the Pleistocene to the present. *Geofluids*, 2(2):137–146. doi:10.1046/j.1468-8123.2002.00032.x
- Dunkley Jones, T., Bown, P.R., Pearson, P.N., Wade, B.S., Coxall, H.K., and Lear, C.H., 2008. Major shifts in calcareous phytoplankton assemblages through the Eocene–Oligocene transition of Tanzania and their implications for low-latitude primary production. *Paleoceanography*, 23(4):PA4204–PA4217. doi:10.1029/2008PA001640
- Dunkley Jones, T., Ridgwell, A., Lunt, D.J., Maslin, M.A., Schmidt, D.N., and Valdes, P.J., 2010. A Palaeogene perspective on climate sensitivity and methane hydrate instability. *Philos. Trans. R. Soc., A*, 368(1919):2395–2415. doi:10.1098/rsta.2010.0053
- Edgar, K.M., Wilson, P.A., Sexton, P.F., Gibbs, S.J., Roberts, A.P., and Norris, R.D., 2010. New biostratigraphic, magnetostratigraphic and isotopic insights into the Middle Eocene Climatic Optimum in low latitudes. *Palaeogeogr., Palaeoclimatol., Palaeoecol.*, 297(3–4):670–682. doi:10.1016/j.palaeo.2010.09.016
- Edgar, K.M., Wilson, P.A., Sexton, P.F., and Suganuma, Y., 2007. No extreme bipolar glaciation during the main Eocene calcite compensation shift. *Nature (London, U. K.)*, 448(7156):908–911. doi:10.1038/nature06053
- Eldrett, J.S., Greenwood, D.R., Harding, I.C., and Huber, M., 2009. Increased seasonality through the Eocene to Oligocene transition in northern high latitudes. *Nature (London, U. K.)*, 459(7249):969–973. doi:10.1038/nature08069
- Eldrett, J.S., Harding, I.C., Wilson, P.A., Butler, E., and Roberts, A.P., 2007. Continental ice in Greenland during the Eocene and Oligocene. *Nature (London, U. K.)*, 446(7132):176–179. doi:10.1038/nature05591
- Erbacher, J., Mosher, D.C., Malone, M.J., et al., 2004. *Proc. ODP, Init. Repts.*, 207: College Station, TX (Ocean Drilling Program). doi:10.2973/odp.proc.ir.207.2004
- Fagel, N., Robert, C., and Hillaire-Marcel, C., 1996. Clay mineral signature of the NW Atlantic boundary undercurrent. *Mar. Geol.*, 130(1–2):19–28. doi:10.1016/0025-3227(95)00134-4
- Fagel, N., Robert, C., Preda, M., and Thorez, J., 2001. Smectite composition as a tracer of deep circulation: the case of the northern North Atlantic. *Mar. Geol.*, 172(3–4):309–330. doi:10.1016/S0025-3227(00)00123-7
- Fisher, A.T., Wheat, C.G., Becker, K., Davis, E.E., Jannasch, H., Schroeder, D., Dixon, R., Pettigrew, T.L., Meldrum, R., McDonald, R., Nielsen, M., Fisk, M., Cowen, J., Bach, W., and Edwards, K., 2005. Scientific and technical design and deployment of long-term seafloor observatories for hydrogeologic and related experiments, IODP Expedition 301, eastern flank of Juan de Fuca Ridge. In Fisher, A.T., Urabe, T., Klaus, A., and the Expedition 301 Scientists, *Proc. IODP*, 301: College Station, TX (Integrated Ocean Drilling Program Management International, Inc.). doi:10.2204/iodp.proc.301.103.2005

- Flemings, P.B., Long, H., Dugan, B., Germaine, J., John, C.M., Behrmann, J.H., Sawyer, D., and IODP Expedition 308 Scientists, 2008. Pore pressure penetrometers document high overpressure near the seafloor where multiple submarine landslides have occurred on the continental slope, offshore Louisiana, Gulf of Mexico. *Earth Planet. Sci. Lett.*, 269(3–4):309–325. doi:10.1016/j.epsl.2007.12.005
- Flemings, P.B., Stump, B.B., Finkbeiner, T., and Zoback, M., 2002. Flow focusing in overpressured sandstones: theory, observations, and applications. *Am. J. Sci.*, 302:827–855. doi:10.2475/ajs.302.10.827
- Friedrich, O., Erbacher, J., Moriya, K., Wilson, P.A., and Kuhnert, H., 2008. Warm saline intermediate waters in the Cretaceous tropical Atlantic Ocean. *Nat. Geosci.*, 1(7):453–457. doi:10.1038/ngeo217
- Galeotti, S., Krishnan, S., Pagani, M., Lanci, L., Gaudio, A., Zachos, J.C., Monechi, S., Morelli, G., and Lourens, L., 2010. Orbital chronology of early Eocene hyperthermals from the Contessa Road section, central Italy. *Earth Planet. Sci. Lett.*, 290(1–2):192–200. doi:10.1016/j.epsl.2009.12.021
- Gersonde, R., Hodell, D.A., Blum, P., et al., 1999. *Proc. ODP, Init. Repts.*, 177: College Station, TX (Ocean Drilling Program). doi:10.2973/odp.proc.ir.177.1999
- Gibbs, S.J., Bown, P.R., Sessa, J.A., Bralower, T.J., and Wilson, P.A., 2006. Nannoplankton extinction and origination across the Paleocene–Eocene Thermal Maximum. *Science*, 314(5806):1770–1773. doi:10.1126/science.1133902
- Goodwin, P., Williams, R.G., Ridgwell, A., and Follows, M.J., 2009. Climate sensitivity to the carbon cycle modulated by past and future changes in ocean chemistry. *Nat. Geosci.*, 2(2):145–150. doi:10.1038/ngeo416
- Greenwood, D.R., Basinger, J.F., and Smith, R.Y., 2010. How wet was the Arctic Eocene rain forest? Estimates of precipitation from Paleogene Arctic macrofloras. *Geology*, 38(1):15–18. doi:10.1130/G30218.1
- Hampson, J.C., Jr., and Robb, J.M., 1984. A geologic map of the continental slope off New Jersey: Lindenköhl Canyon to Toms Canyon. *U.S. Geol. Surv. Misc. Invest. Ser.*, Map I-1608.
- Haneberg, W.C., 1995. Groundwater flow and the stability of heterogeneous infinite slopes underlain by impervious substrata. In Haneberg, W.C., and Anderson, S.A. (Eds.), *Clay and Shale Slope Instability*. Rev. Eng. Geol., 10:63–78.
- Haywood, A.M., Ridgwell, A., Lunt, D.J., Hill, D.J., Pound, M.J., Dowsett, H.J., Dolan, A.M., Francis, J.E., and Williams, M., 2011. Are there pre-Quaternary geological analogues for a future greenhouse warming? *Philos. Trans. R. Soc., A*, 369(1938):933–956. doi:10.1098/rsta.2010.0317
- Hemming, S.R., Broecker, W.S., Sharp, W.D., Bond, G.C., Gwiazda, R.H., McManus, J.F., Klas, M., and Hajdas, I., 1998. Provenance of Heinrich layers in core V28-82, northeastern Atlantic:  $^{40}\text{Ar}/^{39}\text{Ar}$  ages of ice-rafted hornblende, Pb isotopes in feldspar grains, and Nd-Sr-Pb isotopes in the fine sediment fraction. *Earth Planet. Sci. Lett.*, 164(1–2):317–333. doi:10.1016/S0012-821X(98)00224-6
- Higgins, J.A., and Schrag, D.P., 2006. Beyond methane: towards a theory for the Paleocene–Eocene Thermal Maximum. *Earth Planet. Sci. Lett.*, 245(3–4):523–537. doi:10.1016/j.epsl.2006.03.009
- Hutchinson, D.R., Poag, C.W., and Popenoe, P., 1995. Geophysical database of the east coast of the United States: southern Atlantic margin—stratigraphy and velocity from multi-channel seismic profiles. *Open-File Rep.—U.S. Geol. Surv.*, 95-27.

- Hyndman, R.D., and Davis, E.E., 1992. A mechanism for the formation of methane hydrate and seafloor bottom-simulating reflectors by vertical fluid expulsion. *J. Geophys. Res., [Solid Earth]*, 97(B5):7025–7041. doi:10.1029/91JB03061
- IODP International Working Group, 2001. *Earth, Ocean, and Life: Scientific Investigation of the Earth System Using Multiple Drilling Platforms and New Technologies—Integrated Ocean Drilling Program Initial Science Plan, 2003–2013*: Washington, DC (International Working Group Support Office). <http://www.iodp.org/isp/>
- Innocent, C., Fagel, N., and Hillaire-Marcel, C., 2000. Sm–Nd isotope systematics in deep-sea sediments: clay-size versus coarser fractions. *Mar. Geol.*, 168(1–4):79–87. doi:10.1016/S0025-3227(00)00052-9
- Johnson, D.W., 1939. *The Origin of Submarine Canyons: A Critical Review of Hypotheses*: New York (Hafner).
- Katz, M.E., Pak, D.K., Dickens, G.R., and Miller, K.G., 1999. The source and fate of massive carbon input during the latest Paleocene thermal maximum. *Science*, 286(5444):1531–1533. doi:10.1126/science.286.5444.1531
- Keeling, R.F., and Stephens, B.B., 2001. Antarctic sea ice and the control of Pleistocene climate instability. *Paleoceanography*, 16(1):112–131. doi:10.1029/2000PA000529
- Kent, D.V., Cramer, B.S., Lanci, L., Wang, D., Wright, J.D., and Van der Voo, R., 2003. A case for a comet impact trigger for the Paleocene/Eocene Thermal Maximum and carbon isotope excursion. *Earth Planet. Sci. Lett.*, 211(1–2):13–26. doi:10.1016/S0012-821X(03)00188-2
- Kvenvolden, K.A., 1993. Gas hydrates—geological perspective and global change. *Rev. Geophys.*, 31(2):173–187. doi:10.1029/93RG00268
- Lear, C.H., Bailey, T.R., Pearson, P.N., Coxall, H.K., and Rosenthal, Y., 2008. Cooling and ice growth across the Eocene–Oligocene transition. *Geology*, 36(3):251–254. doi:10.1130/G24584A.1
- Lear, C.H., Elderfield, H., and Wilson, P.A., 2000. Cenozoic deep-sea temperatures and global ice volumes from Mg/Ca in benthic foraminiferal calcite. *Science*, 287(5451):269–272. doi:10.1126/science.287.5451.269
- Lear, C.H., Rosenthal, Y., Coxall, H.K., and Wilson, P.A., 2004. Late Eocene to early Miocene ice sheet dynamics and the global carbon cycle. *Paleoceanography*, 19(4):PA4015–PA4025. doi:10.1029/2004PA001039
- Leon-Rodriguez, L., and Dickens, G.R., 2010. Constraints on ocean acidification associated with rapid and massive carbon injections: the early Paleogene record at Ocean Drilling Program Site 1215, equatorial Pacific Ocean. *Palaeogeogr., Palaeoclimatol., Palaeoecol.*, 298(3–4):409–420. doi:10.1016/j.palaeo.2010.10.029
- Liu, X., and Flemings, P., 2009. Dynamic response of oceanic hydrates to sea level drop. *Geophys. Res. Lett.*, 36(17):L17308–L173012. doi:10.1029/2009GL039821
- Liu, Z., Pagani, M., Zinniker, D., DeConto, R., Huber, M., Brinkhuis, H., Shah, S.R., Leckie, R.M., and Pearson, A., 2009. Global cooling during the Eocene–Oligocene climate transition. *Science*, 323(5918):1187–1190. doi:10.1126/science.1166368
- Lourens, L.J., Sluijs, A., Kroon, D., Zachos, J.C., Thomas, E., Röhl, U., Bowles, J., and Raffi, I., 2005. Astronomical pacing of late Palaeocene to early Eocene global warming events. *Nature (London, U. K.)*, 435(7045):1083–1087. doi:10.1038/nature03814
- Lyle, M., Olivarez Lyle, A., Backman, J., and Tripathi, A., 2005. Biogenic sedimentation in the Eocene equatorial Pacific—the stuttering greenhouse and Eocene carbonate compensa-

- tion depth. In Lyle, M., Wilson, P.A., Janecek, T.R., et al., *Proc. ODP, Init. Repts.*, 199: College Station, TX (Ocean Drilling Program), 1–35. [doi:10.2973/odp.proc.sr.199.219.2005](https://doi.org/10.2973/odp.proc.sr.199.219.2005)
- Lyle, M., Wilson, P.A., Janecek, T.R., et al., 2002. *Proc. ODP, Init. Repts.*, 199: College Station, TX (Ocean Drilling Program). [doi:10.2973/odp.proc.ir.199.2002](https://doi.org/10.2973/odp.proc.ir.199.2002)
- Marotzke, J., and Willebrand, J., 1991. Multiple equilibria of the global thermohaline circulation. *J. Phys. Oceanogr.*, 21(9):1372–1385. [doi:10.1175/1520-0485\(1991\)021<1372:MEOTGT>2.0.CO;2](https://doi.org/10.1175/1520-0485(1991)021<1372:MEOTGT>2.0.CO;2)
- Meinen, C.S., and Watts, D.R., 2000. Vertical structure and transport on a transect across the North Atlantic Current near 42°N: time series and mean. *J. Geophys. Res., [Oceans]*, 105(C9):21869–21891. [doi:10.1029/2000JC900097](https://doi.org/10.1029/2000JC900097)
- Merico, A., Tyrrell, T., and Wilson, P.A., 2008. Eocene/Oligocene ocean de-acidification linked to Antarctic glaciation by sea-level fall. *Nature (London, U. K.)*, 452(7190):979–982. [doi:10.1038/nature06853](https://doi.org/10.1038/nature06853)
- Miller, K.G., and Fairbanks, R.G., 1985. Oligocene to Miocene carbon isotope cycles and abyssal circulation changes. In Sundquist, E.J., and Broecker, W.S. (Eds.), *The Carbon Cycle and Atmospheric CO<sub>2</sub>: Natural Variations Archean to Present*. Geophys. Monogr., 32:469–486.
- Miller, K.G., Fairbanks, R.G., and Mountain, G.S., 1987. Tertiary oxygen isotope synthesis, sea-level history, and continental margin erosion. *Paleoceanography*, 2(1):1–19. [doi:10.1029/PA002i001p00001](https://doi.org/10.1029/PA002i001p00001)
- Mountain, G.S., and Miller, K.G., 1992. Seismic and geologic evidence for early Paleogene deepwater circulation in the western North Atlantic. *Paleoceanography*, 7(4):423–439. [doi:10.1029/92PA01268](https://doi.org/10.1029/92PA01268)
- Moran, K., Backman, J., Brinkhuis, H., Clemens, S.C., Cronin, T., Dickens, G.R., Eynaud, F., Gattacceca, J., Jakobsson, M., Jordan, R.W., Kaminski, M., King, J., Koc, N., Krylov, A., Martinez, N., Matthiessen, J., McInroy, D., Moore, T.C., Onodera, J., O'Regan, M., Pälike, H., Rea, B., Rio, D., Sakamoto, T., Smith, D.C., Stein, R., St. John, K., Suto, I., Suzuki, N., Takahashi, K., Watanabe, M., Yamamoto, M., Farrell, J., Frank, M., Kubik, P., Jokat, W., and Kristoffersen, Y., 2006. The Cenozoic palaeoenvironment of the Arctic Ocean. *Nature (London, U. K.)*, 441(7093):601–605. [doi:10.1038/nature04800](https://doi.org/10.1038/nature04800)
- National Research Council, 2011. *Understanding Earth's Deep Past: Lessons for Our Climate Future*: Washington DC (National Academies Press).
- Norris, R.D., Klaus, A., and Kroon, D., 2001a. Mid-Eocene deep water, the Late Palaeocene Thermal Maximum and continental slope mass wasting during the Cretaceous–Palaeogene impact. In Kroon, D., Norris, R.D., and Klaus, A. (Eds.), *Western North Atlantic Paleogene and Cretaceous Paleooceanography*. Geol. Soc. Spec. Publ., 183(1):23–48. [doi:10.1144/GSL.SP.2001.183.01.02](https://doi.org/10.1144/GSL.SP.2001.183.01.02)
- Norris, R.D., Kroon, D., Huber, B.T., and Erbacher, J., 2001b. Cretaceous–Palaeogene ocean and climate change in the subtropical North Atlantic. In Kroon, D., Norris, R.D., and Klaus, A. (Eds.), *Western North Atlantic Paleogene and Cretaceous Paleooceanography*, Geol. Soc. Spec. Publ., 183(1):1–22. [doi:10.1144/GSL.SP.2001.183.01.01](https://doi.org/10.1144/GSL.SP.2001.183.01.01)
- Norris, R.D., Kroon, D., Klaus, A., et al., 1998. *Proc. ODP, Init. Repts.*, 171B: College Station, TX (Ocean Drilling Program). [doi:10.2973/odp.proc.ir.171B.1998](https://doi.org/10.2973/odp.proc.ir.171B.1998)
- Norris, R.D., and Röhl, U., 1999. Carbon cycling and chronology of climate warming during the Palaeocene/Eocene transition. *Nature (London, U. K.)*, 401(6755):775–778. [doi:10.1038/44545](https://doi.org/10.1038/44545)

- Nuñez, F., and Norris, R.D., 2006. Abrupt reversal in ocean overturning during the Palaeocene/Eocene warm period. *Nature (London, U. K.)*, 439(7072):60–63. doi:10.1038/nature04386
- Oppo, D.W., and Lehman, S.J., 1993. Mid-depth circulation of the subpolar North Atlantic during the last glacial maximum. *Science*, 259(5098):1148–1152. doi:10.1126/science.259.5098.1148
- Oppo, D.W., Raymo, M.E., Lohmann, G.P., Mix, A.C., Wright, J.D., and Prell, W.L., 1995. A  $\delta^{13}\text{C}$  record of upper North Atlantic deep water during the past 2.6 million years. *Paleoceanography*, 10(3):373–394. doi:10.1029/95PA00332
- Pagani, M., Caldeira, K., Archer, D., and Zachos, J.C., 2006a. ATMOSPHERE: an ancient carbon mystery. *Science*, 314(5805):1556–1557. doi:10.1126/science.1136110
- Pagani, M., Pedentchouk, N., Huber, M., Sluijs, A., Schouten, S., Brinkhuis, H., Sinninghe Damsté, J.S., Dickens, G.R., and Expedition 302 Scientists, 2006b. Arctic hydrology during global warming at the Palaeocene/Eocene Thermal Maximum. *Nature (London, U. K.)*, 443(7103):671–675. doi:10.1038/nature05043
- Pagani, M., Zachos, J.C., Freeman, K.H., Tipple, B., and Bohaty, S., 2005. Marked decline in atmospheric carbon dioxide concentrations during the Paleogene. *Science*, 309(5734):600–603. doi:10.1126/science.1110063
- Pälike, H., Lyle, M., Nishi, H., Raffi, I., Gamage, K., Klaus, A., and the Expedition 320/321 Scientists, 2010. *Proc. IODP*, 320/321: Tokyo (Integrated Ocean Drilling Program Management International, Inc.). doi:10.2204/iodp.proc.320321.2010
- Pälike, H., Norris, R.D., Herrle, J.O., Wilson, P.A., Coxall, H.K., Lear, C.H., Shackleton, N.J., Tripathi, A.K., and Wade, B.S., 2006. The heartbeat of the Oligocene climate system. *Science*, 314(5807):1894–1898. doi:10.1126/science.1133822
- Pälike, H., Laskar, J., and Shackleton, N.J., 2004. Geologic constraints of the chaotic diffusion of the solar system. *Geology*, 32(11):929–932. doi:10.1130/G20750.1
- Pälike, H., and Shackleton, N.J., 2000. Constraints on astronomical parameters from the geological record for the last 25 Myr. *Earth Planet. Sci. Lett.*, 182(1):1–14. doi:10.1016/S0012-821X(00)00229-6
- Pälike, H., Shackleton, N.J., and Röhl, U., 2001. Astronomical forcing in late Eocene marine sediments. *Earth Planet. Sci. Lett.*, 193(3–4):589–602. doi:10.1016/S0012-821X(01)00501-5
- Panchuk, K., Ridgwell, A., and Kump, L.R., 2008. Sedimentary response to Paleocene–Eocene Thermal Maximum carbon release: a model-data comparison. *Geology*, 36(4):315–318. doi:10.1130/G24474A.1
- Pearson, P.N., Foster, G.L., and Wade, B.S., 2009. Atmospheric carbon dioxide through the Eocene–Oligocene climate transition. *Nature (London, U. K.)*, 461(7267):1110–1113. doi:10.1038/nature08447
- Peterson, L.C., Murray, D.W., Ehrmann, W.U., and Hempel, P., 1992. Cenozoic carbonate accumulation and compensation depth changes in the Indian Ocean. In Duncan, R.A., Rea, D.K., Kidd, R.B., von Rad, U., and Weissel, J.K. (Eds.), *Synthesis of Results from Scientific Drilling in the Indian Ocean*. Geophys. Monogr., 70:311–333.
- Pickart, R.S., McKee, T.K., Torres, D.J., and Harrington, S.A., 1999. Mean structure and interannual variability of the slope water system south of Newfoundland. *J. Phys. Oceanogr.*, 29(10):2541–2558. doi:10.1175/1520-0485(1999)029<2541:MSAIVO>2.0.CO;2
- Prins, M.A., Bouwer, L.M., Beets, C.J., Troelstra, S.R., Weltje, G.J., Kruk, R.W., Kuijpers, A., and Vroon, P.Z., 2002. Ocean circulation and iceberg discharge in the glacial North Atlantic:

- inferences from unmixing of sediment size distributions. *Geology*, 30(6):555–558. doi:10.1130/0091-7613(2002)030<0555:OCAIDI>2.0.CO;2
- Quillévéré, F., Norris, R.D., Kroon, D., and Wilson, P.A., 2008. Transient ocean warming and shifts in carbon reservoirs during the early Danian. *Earth Planet. Sci. Lett.*, 265(3–4):600–615. doi:10.1016/j.epsl.2007.10.040
- Rahmstorf, S., 1995. Bifurcations of the Atlantic thermohaline circulation in response to changes in the hydrological cycle. *Nature (London, U. K.)*, 378(6553):145–149. doi:10.1038/378145a0
- Rona, P.A., 1969. Middle Atlantic continental slope of the United States: deposition and erosion. *AAPG Bull.*, 53(7):1453–1465. doi:10.1306/5D25C85F-16C1-11D7-8645000102C1865D
- Ruppel, C., 1997. Anomalously cold temperatures observed at the base of the gas hydrate stability zone on the U.S. Atlantic passive margin. *Geology*, 25(8):699–702. doi:10.1130/0091-7613(1997)025<0699:ACTOAT>2.3.CO;2
- Saffer, D., McNeill, L., Byrne, T., Araki, E., Toczko, S., Eguchi, N., Takahashi, K., and the Expedition 319 Scientists, 2010. *Proc. IODP*, 319: Tokyo (Integrated Ocean Drilling Program management International, Inc.). doi:10.2204/iodp.proc.319.2010
- Saffer, D.M., and Bekins, B.A., 2002. Hydrologic controls on the morphology and mechanics of accretionary wedges. *Geology*, 30(3):271–274. doi:10.1130/0091-7613(2002)030<0271:HCOTMA>2.0.CO;2
- Scher, H.D., Bohaty, S.M., Zachos, J.C., and Delaney, M.L., 2011. Two-stepping into the ice-house: East Antarctic weathering during progressive ice-sheet expansion at the Eocene–Oligocene transition. *Geology*, 39(4):383–386. doi:10.1130/G31726.1
- Screaton, E., Saffer, D., Henry, P., and Hunze, S., 2002. Porosity loss within the underthrust sediments of the Nankai accretionary complex: implications for overpressures. *Geology*, 30(1):19–22. doi:10.1130/0091-7613(2002)030<0019:PLWTUS>2.0.CO;2
- Sexton, P.F., Norris, R.D., Wilson, P.A., Pälike, H., Westerhold, T., Röhl, U., Bolton, C.T., and Gibbs, S., 2011. Eocene global warming events driven by ventilation of oceanic dissolved organic carbon. *Nature (London, U. K.)*, 471(7338):349–352. doi:10.1038/nature09826
- Sigurdsson, H., Leckie, R.M., Acton, G.D., et al., 1997. *Proc. ODP, Init. Repts.*, 165: College Station, TX (Ocean Drilling Program). doi:10.2973/odp.proc.ir.165.1997
- Sluijs, A., Schouten, S., Pagani, M., Woltering, M., Brinkhuis, H., Sinninghe Damsté, J.S., Dickens, G.R., Huber, M., Reichert, G.-J., Stein, R., Matthiessen, J., Lourens, L.J., Pedentchouk, N., Backman, J., Moran, K., and the Expedition 302 Scientists, 2006. Subtropical Arctic Ocean temperatures during the Palaeocene/Eocene Thermal Maximum. *Nature (London, U. K.)*, 441(7093):610–613. doi:10.1038/nature04668
- Stickley, C.E., St. John, K., Koç, N., Jordan, R.W., Passchier, S., Pearce, R.B., and Kearns, L.E., 2009. Evidence for middle Eocene Arctic sea ice from diatoms and ice-rafted debris. *Nature (London, U. K.)*, 460(7253):376–379. doi:10.1038/nature08163
- Stommel, H., and Arons, A.B., 1960. On the abyssal circulation of the world ocean—I. Stationary planetary flow patterns on a sphere. *Deep Sea Res.*, 6:140–154. doi:10.1016/0146-6313(59)90065-6
- Svensen, H., Planke, S., Malthes-Sørensen, A., Jamtveit, B., Myklebust, R., Eidem, T.R., and Rey, S.S., 2004. Release of methane from a volcanic basin as a mechanism for initial Eocene global warming. *Nature (London, U. K.)*, 429(6991):542–545. doi:10.1038/nature02566



- Terzaghi, K., 1950. Mechanism of landslides. In Paige, S. (Ed.), *Application of Geology to Engineering Practice: Berkeley Volume*: Baltimore (Geol. Soc. Am.), 83–123.
- Thomas, D.J., Bralower, T.J., and Jones, C.E., 2003. Neodymium isotopic reconstruction of late Paleocene–early Eocene thermohaline circulation. *Earth Planet. Sci. Lett.*, 209(3–4):309–322. doi:10.1016/S0012-821X(03)00096-7
- Toggweiler, J.R., and Samuels, B., 1995. Effect of Drake Passage on the global thermohaline circulation. *Deep-Sea Res., Part I*, 42(4):477–500. doi:10.1016/0967-0637(95)00012-U
- Tripati, A., Backman, J., Elderfield, H., and Ferretti, P., 2005. Eocene bipolar glaciation associated with global carbon cycle changes. *Nature (London, U. K.)*, 436(7049):341–346. doi:10.1038/nature03874
- Tripati, A.K., Eagle, R.A., Morton, A., Dowdeswell, J.A., Atkinson, K.L., Bahé, Y., Dawber, C.F., Khadun, E., Shaw, R.M.H., Shorttle, O., and Thanabalasundaram, L., 2007. Evidence for glaciation in the Northern Hemisphere back to 44 Ma from ice-rafted debris in the Greenland Sea. *Earth Planet. Sci. Lett.*, 265(1–2):112–122. doi:10.1016/j.epsl.2007.09.045
- Tripati, A., and Elderfield, H., 2005. Deep-sea temperature and circulation changes at the Paleocene-Eocene Thermal Maximum. *Science*, 308(5730):1894–1898. doi:10.1126/science.1109202
- Tucholke, B.E., 1979. Relationships between acoustic stratigraphy and lithostratigraphy in the western North Atlantic Basin. In Tucholke, B.E., Vogt, P.R., et al., *Init. Repts. DSDP*, 43: Washington, DC (U.S. Govt. Printing Office), 827–846. doi:10.2973/dsdp.proc.43.141.1979
- Tucholke, B.E., and Ludwig, W.J., 1982. Structure and origin of the J Anomaly Ridge, western North Atlantic Ocean. *J. Geophys. Res., [Solid Earth]*, 87(B11):9389–9407. doi:10.1029/JB087iB11p09389
- Tucholke, B.E., and Mountain, G.S., 1986. Tertiary paleoceanography of the western North Atlantic Ocean. In Vogt, P.R., and Tucholke, B.E. (Eds.), *The Geology of North America: The Western North Atlantic Region* (Vol. M): Boulder (Geol. Soc. Am.), 631–650.
- Tucholke, B.E., and Vogt, P.R., 1979. Western North Atlantic: sedimentary evolution and aspects of tectonic history. In Tucholke, B.E., Vogt, P.R., et al., *Init. Repts. DSDP*, 43: Washington, DC (U.S. Govt. Printing Office), 791–825. doi:10.2973/dsdp.proc.43.140.1979
- Tucholke, B.E., Vogt, P.R., et al., 1979. *Init. Repts. DSDP*, 43: Washington, DC (U.S. Govt. Printing Office). doi:10.2973/dsdp.proc.43.1979
- Via, R.K., and Thomas, D.J., 2006. Evolution of Atlantic thermohaline circulation: early Oligocene onset of deep-water production in the North Atlantic. *Geology*, 34(6):441–444. doi:10.1130/G22545.1
- Wade, B.S., and Pälike, H., 2004. Oligocene climate dynamics. *Paleoceanography*, 19(4)PA4019–PA4034. doi:10.1029/2004PA001042
- Weltje, G.J., 1997. End-member modeling of compositional data: numerical-statistical algorithms for solving the explicit mixing problem. *Math. Geol.*, 29(4):503–549. doi:10.1007/BF02775085
- Weltje, G.J., and Prins, M.A., 2003. Muddled or mixed? Inferring palaeoclimate from size distributions of deep-sea clastics. *Sediment. Geol.*, 162(1–2):39–62. doi:10.1016/S0037-0738(03)00235-5
- Westerhold, T., and Röhl, U., 2009. High resolution cyclostratigraphy of the early Eocene—new insights into the origin of the Cenozoic cooling trend. *Clim. Past*, 5(3):309–327. doi:10.5194/cp-5-309-2009

- Wright, J.D., and Miller, K.G., 1993. Southern Ocean influences on late Eocene to Miocene deepwater circulation. *In* Kennett, J.P., and Warnke, D.A. (Eds.), *The Antarctic Paleoenvironment: A Perspective on Global Change*. Antarct. Res. Ser., 60:1–25.
- Wright, J.D., Miller, K.G., and Fairbanks, R.G., 1992. Early and middle Miocene stable isotopes: implications for deepwater circulation and climate. *Paleoceanography*, 7(3):357–389. [doi:10.1029/92PA00760](https://doi.org/10.1029/92PA00760)
- Zachos, J., Pagani, M., Sloan, L., Thomas, E., and Billups, K., 2001. Trends, rhythms, and aberrations in global climate 65 Ma to present. *Science*, 292(5517):686–693. [doi:10.1126/science.1059412](https://doi.org/10.1126/science.1059412)
- Zachos, J.C., Kroon, D., Blum, P., et al., 2004. *Proc. ODP, Init. Repts.*, 208: College Station, TX (Ocean Drilling Program. [doi:10.2973/odp.proc.ir.208.2004](https://doi.org/10.2973/odp.proc.ir.208.2004)
- Zachos, J.C., Röhl, U., Schellenberg, S.A., Sluijs, A., Hodell, D.A., Kelly, D.C., Thomas, E., Nicolo, M., Raffi, I., Lourens, L.J., McCarren, H., and Kroon, D., 2005. Rapid acidification of the ocean during the Paleocene–Eocene Thermal Maximum. *Science*, 308(5728):1611–1615. [doi:10.1126/science.1109004](https://doi.org/10.1126/science.1109004)
- Zeebe, R.E., and Zachos, J.C., 2007. Reversed deep-sea carbonate ion basin gradient during Paleocene-Eocene Thermal Maximum. *Paleoceanography*, 22(3):PA3201–PA3217. [doi:10.1029/2006PA001395](https://doi.org/10.1029/2006PA001395)

**Table T1. Expedition 342 operations summary.**

Proposed site	Location	Water depth (m)	TWT (s)	Target penetration depth (m)	Requested penetration depth (m)	Coring	Logging	Objective	Time (days)					Figure reference	
									Transit	Coring	Logging	On site	Total		
Primary								Port call						2.0	
1073	39°13.52'N, 72°16.55'W	650		100	300	single-APC		MDHDS test	2.2	2.0		2.0	4.2		
JA-1A	39°55.00'N, 51°47.00'W	4940	6.5	400	700	3-APC/XCB	TC, FMS	upper-middle Eocene to Paleogene, deep end	3.8	10.7	1.0	11.7	15.5	<a href="#">F6</a> , <a href="#">F10</a> , <a href="#">F19</a>	
JA-14A	40°3.00'N, 51°49.00'W	4250	5.7	250	700	3-APC/XCB		upper-middle Eocene drift	0.0	6.3		6.3	6.3	<a href="#">F6</a> , <a href="#">F10</a> , <a href="#">F19</a>	
JA-5A	40°13.00'N, 51°40.00'W	3900	5.1	250	700	3-APC/XCB		upper-middle Eocene drift	0.1	5.9		5.9	6.0	<a href="#">F6</a> , <a href="#">F20</a>	
SENR-16A	40°14.00'N, 47°30.00'W	4150	5.4	400	900	3-APC/XCB	TC, FMS	Oligocene to upper Eocene	0.8	9.4	1.0	10.4	11.2	<a href="#">F7</a> , <a href="#">F11</a>	
SENR-11A	41°37.00'N, 48°58.00'W	3300	4.4	300	600	3-APC/XCB	TC, FMS	upper-middle Eocene drift	0.4	6.3	0.8	7.1	7.5	<a href="#">F15</a>	
SENR-19B	41°40.00'N, 49°18.00'W	2470	3.3	250	300	3-APC/XCB		upper-middle Eocene drift, shallow	0.1	5.8		5.8	5.9	<a href="#">F16</a>	
								Transit to St. John's	1.5				1.5		
								Totals:	8.8	46.4	2.8	49.2	60.0		
Alternate															
JA-15A	40°10.00'N, 51°50.00'W	4290	5.7	200	500	3-APC/XCB		middle Eocene + Paleogene drift		4.9		4.9		<a href="#">F6</a> , <a href="#">F10</a> , <a href="#">F20</a>	
JA-15A	40°10.00'N, 51°50.00'W	4290	5.7	400	500	3-APC/XCB	TC, FMS	middle Eocene + Paleogene drift	9.4	1.0	10.4			<a href="#">F6</a> , <a href="#">F10</a> , <a href="#">F20</a>	
SENR-10A	40°4.00'N, 47°43.00'W	4250	5.7	200	800	3-APC/XCB		upper Eocene	4.8		4.8			<a href="#">F7</a> , <a href="#">F11</a>	
SENR-10A	40°4.00'N, 47°43.00'W	4250	5.7	400	800	3-APC/XCB	TC, FMS	upper Eocene	9.4	1.0	10.4			<a href="#">F7</a> , <a href="#">F11</a>	
SENR-11A	41°37.00'N, 48°58.00'W	3300	4.4	400	600	3-APC/XCB	TC, FMS	upper-middle Eocene drift	8.2	0.9	9.1			<a href="#">F15</a>	
SENR-1B	41°36.00'N, 49°18.00'W	2750	3.7	200	500	3-APC/XCB		Paleogene, shallow end	4.1		4.1			<a href="#">F17</a>	
SENR-18A	41°04.00'N, 49°17.00'W	3540	4.8	400	600	3-APC/XCB	TC, FMS	Paleogene	8.6	0.9	9.5			<a href="#">F18</a>	
JA-13A	40°0.00'N, 51°49.00'W	4710	6.2	250	600	3-APC/XCB		upper-middle Eocene drift	6.2		6.2			<a href="#">F6</a> , <a href="#">F10</a> , <a href="#">F19</a>	
JA-3A	40°3.00'N, 51°37.00'W	4725	6.3	250	700	3-APC/XCB		upper-middle Eocene drift, deep	6.3		6.3			<a href="#">F6</a> , <a href="#">F19</a>	
JA-4A	40°10.00'N, 51°38.00'W	4250	5.7	250	700	3-APC/XCB		upper-middle Eocene drift, 14A	5.8		5.8			<a href="#">F6</a> , <a href="#">F19</a>	

TWT = two-way traveltime. APC = advanced piston corer, XCB = extended core barrel. TC = triple combination tool string, FMS = Formation MicroScanner-sonic tool string. MDHDS = Motion Decoupled Hydraulic Delivery System.

Expedition 342 Scientific Prospectus

Table T2. Expedition 342 primary sites operations plan.

Site	Location (latitude, longitude)	Seafloor depth (mbrf)	Operations description	Transit (days)	Drilling/ Coring (days)	LWD/ MWD log (days)
<b>St. George, Bermuda</b>			<b><u>Begin Expedition</u></b>	<b>2.0</b>	<b>port call days</b>	
Transit ~552 nmi to Site 1073 @ 10.5				2.2		
<u>Site 1073</u>	39°13.52'N	650	Hole B - APC down to 100 m and begin testing MDHDS	0	2.0	0.0
EPSP	72°16.55'W					
to 0 mbsf						
<u>Subtotal days on site:</u>				2.0		
Transit ~947 nmi to JA-1A (400 m) @ 10.5				3.8		
<u>JA-1A (400 m)</u>	39°55.00'N	4951	Hole A - APC/XCB to 400 mbsf with orientation	0	3.7	0.0
EPSP	51°47.00'W		Hole B - APC/XCB to 400 mbsf	0	3.2	0.0
to 0 mbsf			Hole C - APC/XCB to 400 mbsf; log with triple combination and FMS-sonic	0	3.8	1.0
<u>Subtotal days on site:</u>				11.8		
Transit ~8 nmi to JA-14A (250 m) @ 10.5				0.0		
<u>JA-14A (250 m)</u>	40°3.00'N	4261	Hole A - APC/XCB to 250 mbsf with orientation	0	2.2	0.0
EPSP	51°49.00'W		Hole B - APC/XCB to 250 mbsf	0	1.8	0.0
to 0 mbsf			Hole C - APC/XCB to 250 mbsf	0	2.3	0.0
<u>Subtotal days on site:</u>				6.2		
Transit ~12 nmi to JA-5A (250 m) @ 10.5				0.1		
<u>JA-5A (250 m)</u>	40°13.00'N	3911	Hole A - APC/XCB to 250 mbsf with orientation	0	2.1	0.0
EPSP	51°40.00'W		Hole B - APC/XCB to 250 mbsf	0	1.7	0.0
to 0 mbsf			Hole C - APC/XCB to 250 mbsf	0	2.1	0.0
<u>Subtotal days on site:</u>				5.9		
Transit ~191 nmi to SENR-16A (400 m) @ 10.5				0.8		
<u>SENR-16A (400 m)</u>	40°14.00'N	4131	Hole A - APC/XCB to 400 mbsf with orientation	0	3.3	0.0
EPSP	47°30.00'W		Hole B - APC/XCB to 400 mbsf	0	2.8	0.0
to 0 mbsf			Hole C - APC/XCB to 400 mbsf; log with triple combination and FMS-sonic	0	3.3	0.9
<u>Subtotal days on site:</u>				10.4		
Transit ~106 nmi to SENR-11A (300 m) @ 10.5				0.4		
<u>SENR-11A (300 m)</u>	41°37.00'N	3311	Hole A - APC/XCB to 300 mbsf with orientation	0	2.2	0.0
EPSP	48°58.00'W		Hole B - APC/XCB to 300 mbsf	0	1.8	0.0
to 0 mbsf			Hole C - APC/XCB to 300 mbsf; log with triple combination and FMS-sonic	0	2.3	0.8
<u>Subtotal days on site:</u>				7.1		
Transit ~15 nmi to SENR-19B (250 m) @ 10.5				0.1		
<u>SENR-19B (250 m)</u>	41°40.00'N	4131	Hole A - APC to 250 mbsf with orientation	0	2.1	0.0
EPSP	49°18.00'W		Hole B - APC to 250 mbsf	0	1.6	0.0
to 0 mbsf			Hole C - APC to 250 mbsf	0	2.1	0.0
<u>Subtotal days on site:</u>				5.8		
Transit ~382 nmi to St. John's @ 10.5				1.5		
<b>St. John's</b>			<b><u>End expedition</u></b>	<b>8.8</b>	<b>46.4</b>	<b>2.8</b>

<b>Port call:</b>	<b>2.0</b>	<b>Total operating days:</b>	<b>58.0</b>
<b>Subtotal on site:</b>	<b>49.2</b>	<b>Total expedition:</b>	<b>60.0</b>

LWD = logging while drilling, MWD = measurement while drilling. EPSP = Environmental Protection and Safety Panel. MDHDS = Motion Decoupled Hydraulic Delivery System. APC = advanced piston corer, XCB = extended core barrel. FMS = Formation MicroScanner.

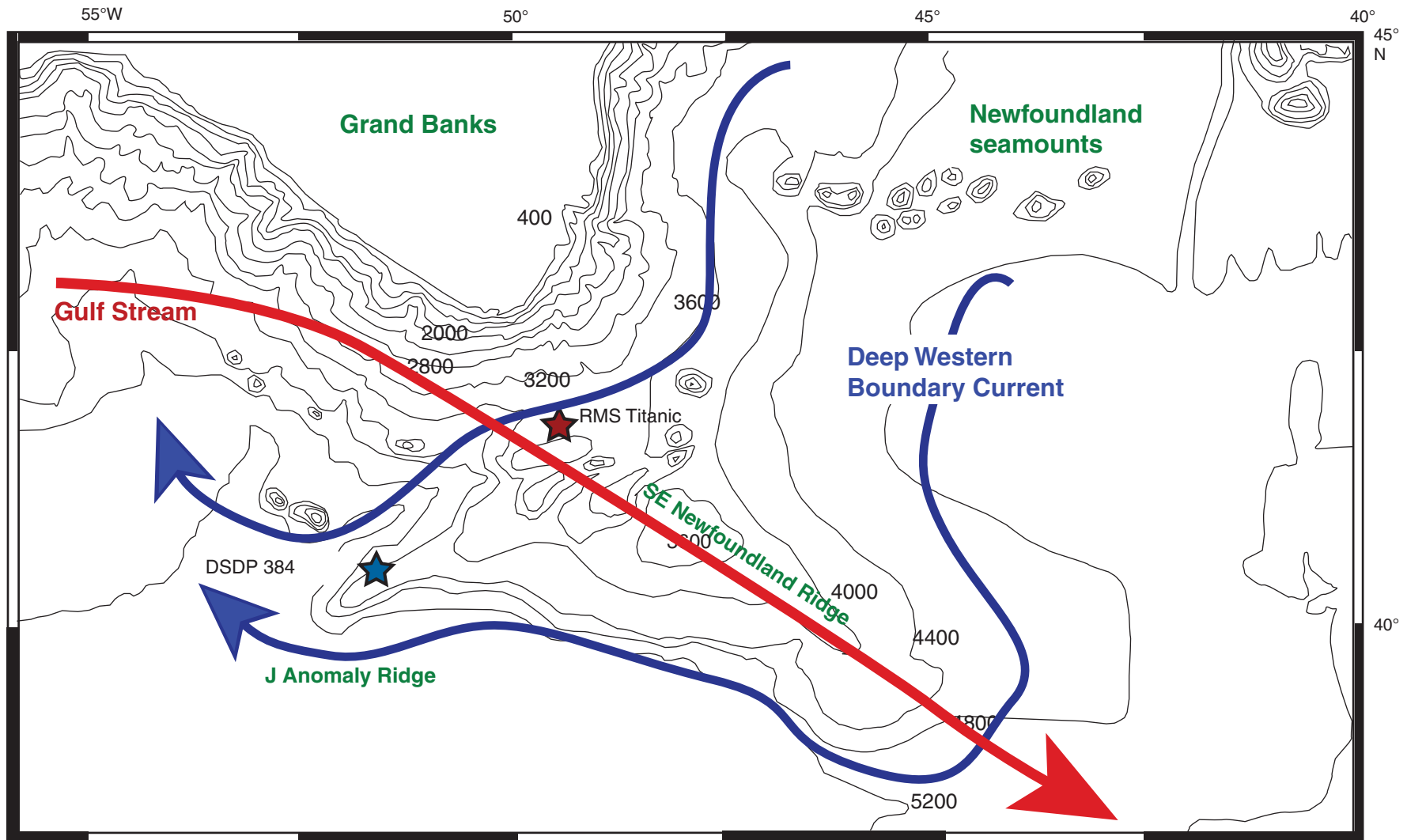
Expedition 342 Scientific Prospectus

Table T3. Expedition 342 alternate sites operations plan.

Site	Location (latitude, longitude)	Seafloor depth (mbrf)	Operations description	Drilling/ Coring (days)	LWD/ MWD log (days)
<u>JA-3A (250 m)</u>	40°3.00'N	4736	Hole A - APC to 250 mbsf with orientation and APCT-3 measurements	2.3	0.0
EPSP	51°37.00'W		Hole B - APC to 250 mbsf	1.7	0.0
to 0 mbsf			Hole C - APC to 250 mbsf	2.2	0.0
<u>Subtotal days on site:</u>				6.3	
<u>JA-4A (250 m)</u>	40°10.00'N	4261	Hole A - APC to 250 mbsf with orientation	2.1	0.0
EPSP	51°38.00'W		Hole B - APC to 250 mbsf	1.6	0.0
to 0 mbsf			Hole C - APC to 250 mbsf	2.1	0.0
<u>Subtotal days on site:</u>				5.8	
<u>JA-13A (250 m)</u>	40°0.00'N	4721	Hole A - APC to 250 mbsf with orientation and APCT-3 measurements	2.3	0.0
EPSP	51°49.00'W		Hole B - APC to 250 mbsf	1.7	0.0
to 0 mbsf			Hole C - APC to 250 mbsf	2.2	0.0
<u>Subtotal days on site:</u>				6.2	
<u>JA-15A (200 m)</u>	40°10.00'N	4301	Hole A - APC to 200 mbsf with orientation	1.8	0.0
EPSP	51°50.00'W		Hole B - APC to 200 mbsf	1.3	0.0
to 0 mbsf			Hole C - APC to 200 mbsf	1.9	0.0
<u>Subtotal days on site:</u>				4.9	
<u>JA-15A (400 m)</u>	40°10.00'N	4301	Hole A - APC/XCB to 400 mbsf with orientation	3.3	0.0
EPSP	51°50.00'W		Hole B - APC/XCB to 400 mbsf	2.8	0.0
to 0 mbsf			Hole C - APC/XCB to 400 mbsf; log with triple combination and FMS-sonic	3.3	1.0
<u>Subtotal days on site:</u>				10.4	
<u>SENR-1B (200 m)</u>	41°36.00'N	2761	Hole A - APC to 200 mbsf with orientation and APCT-3 measurements	1.7	0.0
EPSP	49°18.00'W		Hole B - APC to 200 mbsf	1.0	0.0
to 0 mbsf			Hole C - APC to 200 mbsf	1.3	0.0
<u>Subtotal days on site:</u>				4.1	
<u>SENR-10A (200 m)</u>	40°4.00'N	4261	Hole A - APC to 200 mbsf with orientation	1.8	0.0
EPSP	47°43.00'W		Hole B - APC to 200 mbsf	1.3	0.0
to 0 mbsf			Hole C - APC to 200 mbsf	1.7	0.0
<u>Subtotal days on site:</u>				4.8	
<u>SENR-10A (400 m)</u>	40°4.00'N	4261	Hole A - APC/XCB to 400 mbsf with orientation	3.3	0.0
EPSP	49°35.00'W		Hole B - APC/XCB to 400 mbsf	2.8	0.0
to 0 mbsf			Hole C - APC/XCB to 400 mbsf; log with triple combination and FMS-sonic	3.3	1.0
<u>Subtotal days on site:</u>				10.4	
<u>SENR-11A (400 m)</u>	41°37.00'N	3311	Hole A - APC/XCB to 400 mbsf with orientation	2.9	0.0
EPSP	48°58.00'W		Hole B - APC/XCB to 400 mbsf	2.4	0.0
to 0 mbsf			Hole C - APC/XCB to 400 mbsf; log with triple combination and FMS-sonic	2.8	0.9
<u>Subtotal days on site:</u>				9.1	
<u>SENR-18A (400 m)</u>	41°4.00'N	3551	Hole A - APC/XCB to 400 mbsf with orientation	3.0	0.0
EPSP	49°17.00'W		Hole B - APC/XCB to 400 mbsf	2.5	0.0
to 0 mbsf			Hole C - APC/XCB to 400 mbsf; log with triple combination and FMS-sonic	3.0	0.9
<u>Subtotal days on site:</u>				9.5	

LWD = logging while drilling, MWD = measurement while drilling, EPSP = Environmental Protection and Safety Panel, APC = advanced piston corer, XCB = extended core barrel, APCT-3 = advanced piston corer temperature tool, FMS = Formation MicroScanner.

**Figure F1.** Location of Southeast Newfoundland and J Anomaly Ridges relative to the flow paths of the Deep Western Boundary Current. Deep Sea Drilling Project (DSDP) Site 384 is the primary deep borehole that will provide stratigraphic control for Expedition 342 seismic records. Location of the RMS *Titanic* is also shown.



**Figure F2.** Paleogeographic map for the North Atlantic at the beginning of the Paleogene. Note the narrow, and mostly shallow, connections between the North Atlantic and Arctic Basins. The presence of sediment drifts on J Anomaly Ridge suggests that there was strong deepwater formation somewhere in the basins adjacent to Greenland or Norway or that there was overflow from the Arctic itself. Expedition 342 drilling will sample these sediment drifts with the objective to understand the paleoceanography and climate implications of deepwater formation in the northern basins of the Atlantic.

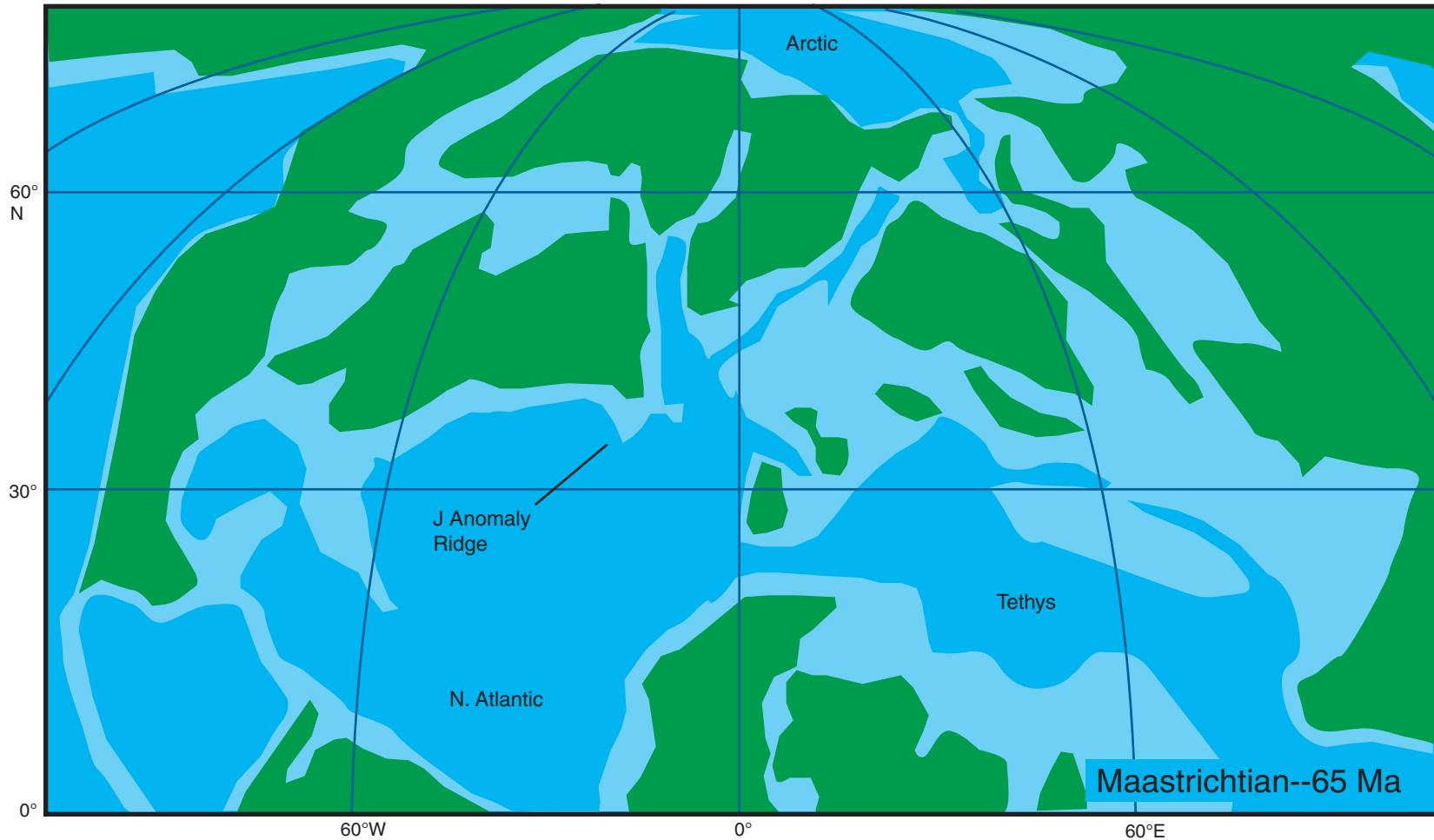


**Figure F3.** Reflection Profile V3202 over the crest of Southeast Newfoundland Ridge, with simplified interpretation (location in Fig. F4). Seismic sequences are discussed in the text. Differential deposition and moats around the seamounts were caused by seafloor currents and are responsible for seafloor outcrops and irregular thicknesses in seismic sequences for Reflections A, A-B, and B-C, the lowest of which may be as old as Eocene. The location of Reflection A is difficult to discern in this 1972 SCS line.

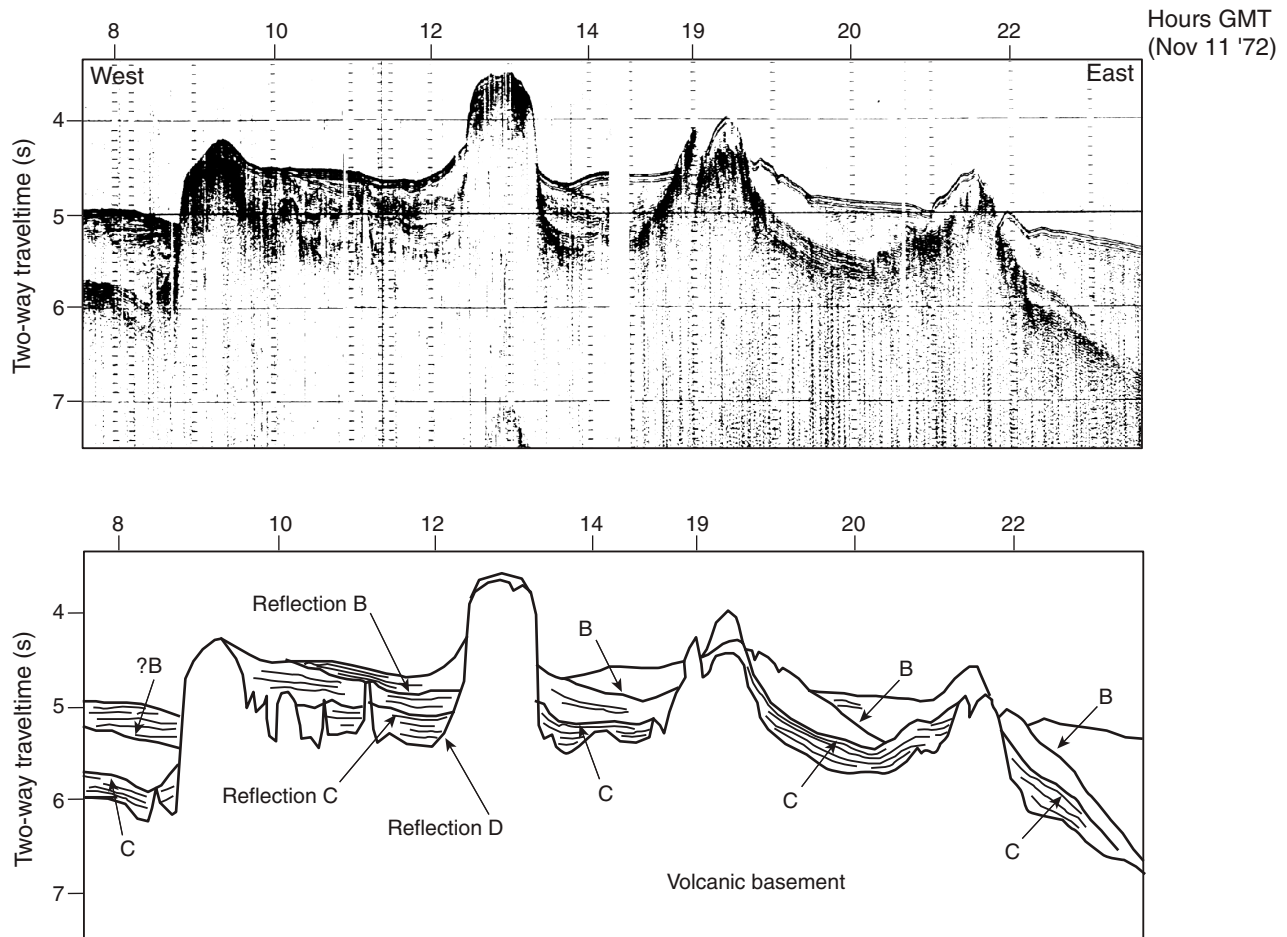




**Figure F4.** Track map for the Newfoundland ridges. Green lines are single-channel seismic (SCS) lines collected during R/V *Knorr* site survey Cruise 179-1. Additional seismic profiles (gray lines) that support Expedition 342 drilling are shown. Also shown is Deep Sea Drilling Project (DSDP) Site 384, which provides stratigraphic control for interpretation of the seismic data set. MCS = multichannel seismic.

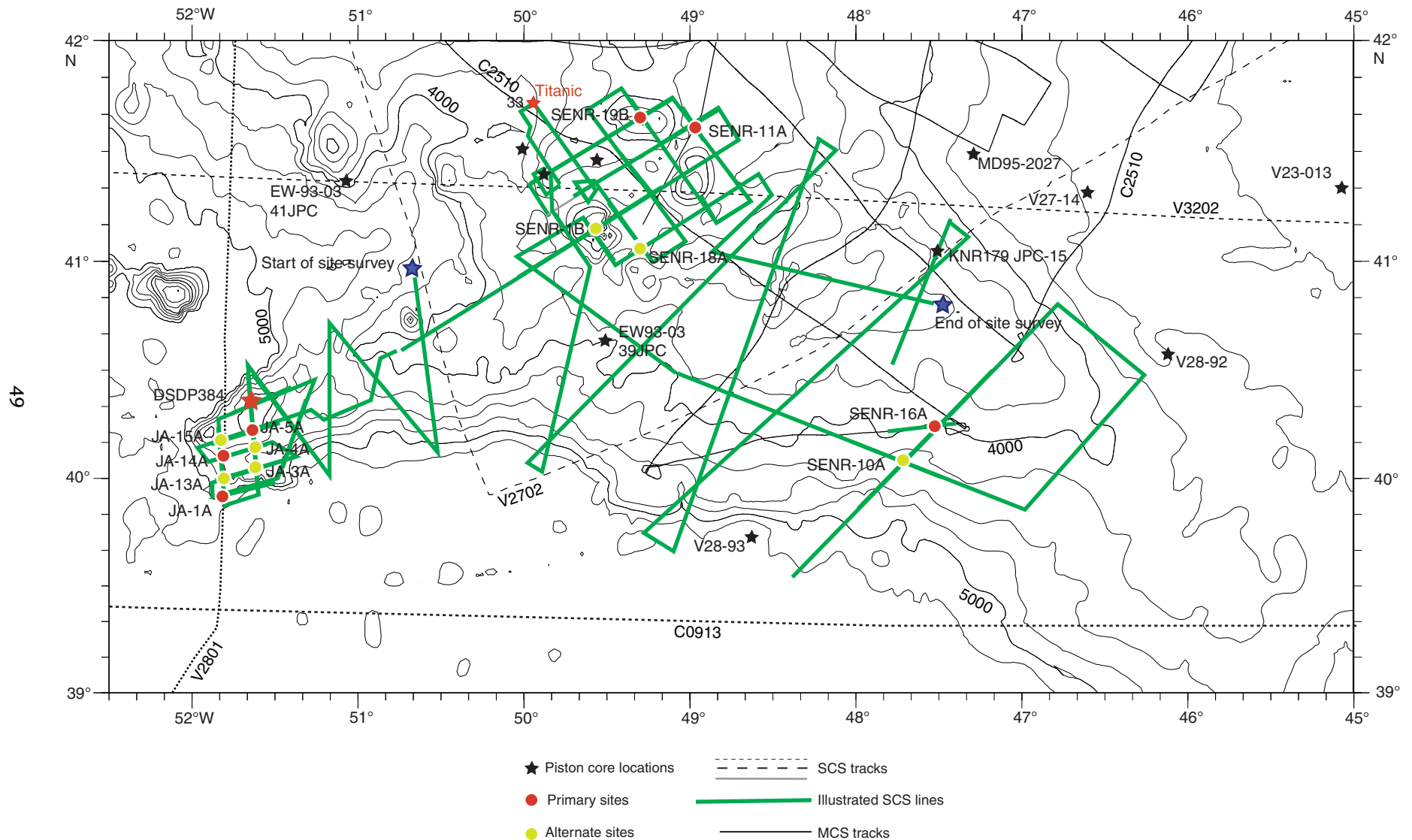


**Figure F5.** Bathymetry for the Newfoundland ridges. Red lines are interpreted single-channel seismic (SCS) profiles shown in Figures F10 and F11. SENR = Southeast Newfoundland Ridge. DSDP = Deep Sea Drilling Project. MCS = multichannel seismic.

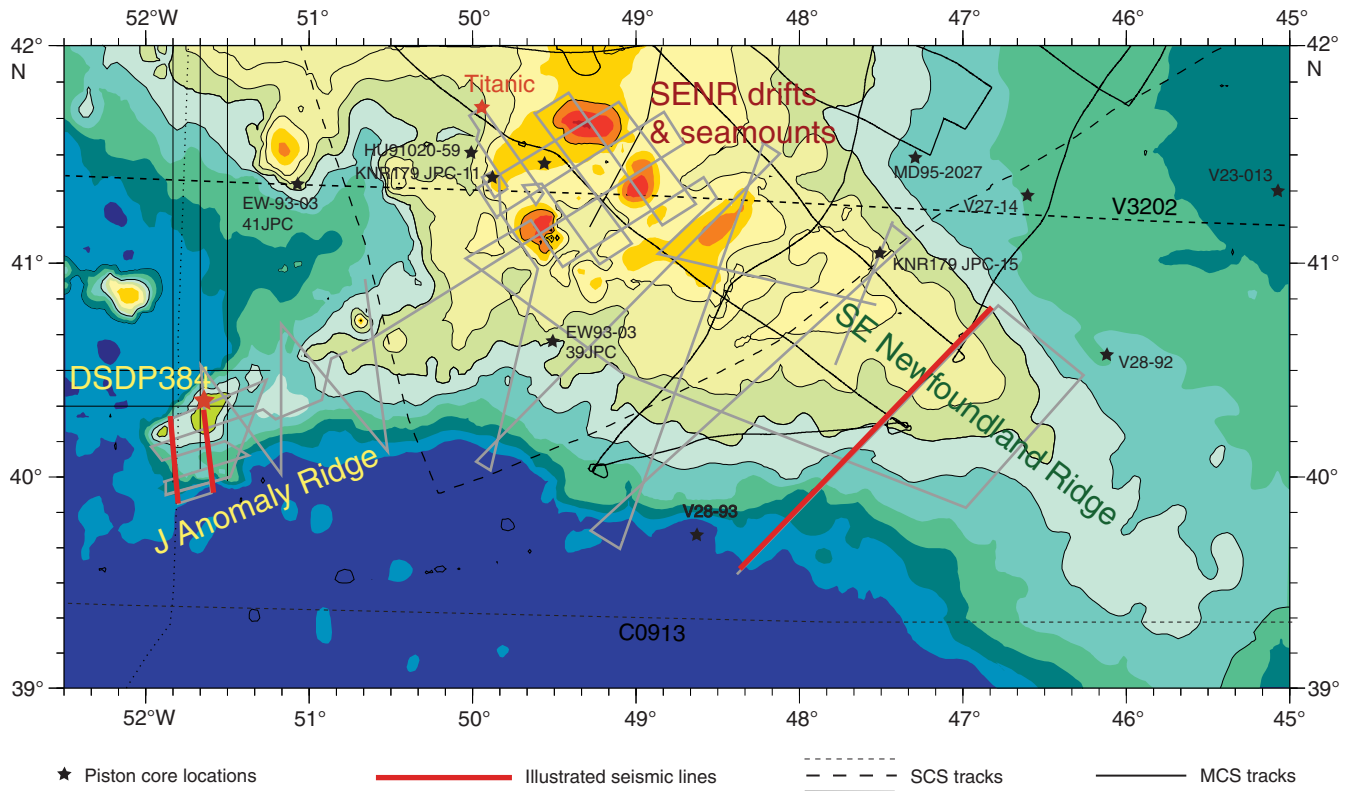


**Figure F6.** Single-channel seismic lines for J Anomaly Ridge running along-dip, with locations of related Expedition 342 drill sites. Profile KNR 179-1, Line 5, crosses J Anomaly Ridge through DSDP Site 384. Note the thinning of the transparent seismic unit of early?-late Eocene age between crossing Lines 10 and 12, here interpreted as erosional thinning of the carbonate section through the carbonate lysocline. Line 12 crosses Line 5 close to the depth of the CCD.

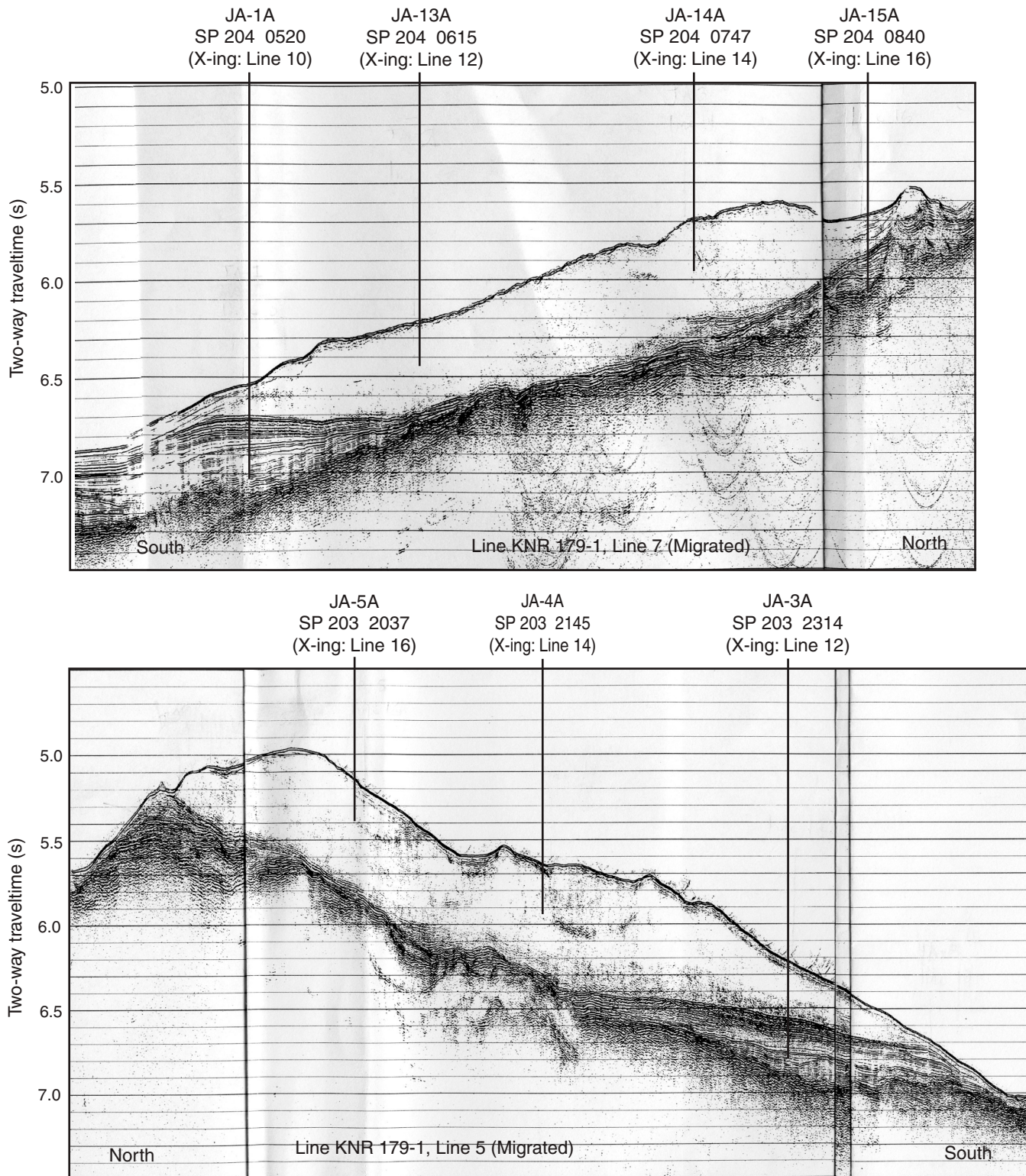


**Figure F7.** Single-channel seismic Profile KNR 179-1, Lines 46 and 49, for Southeast Newfoundland Ridge, with locations of related Expedition 342 drill sites.

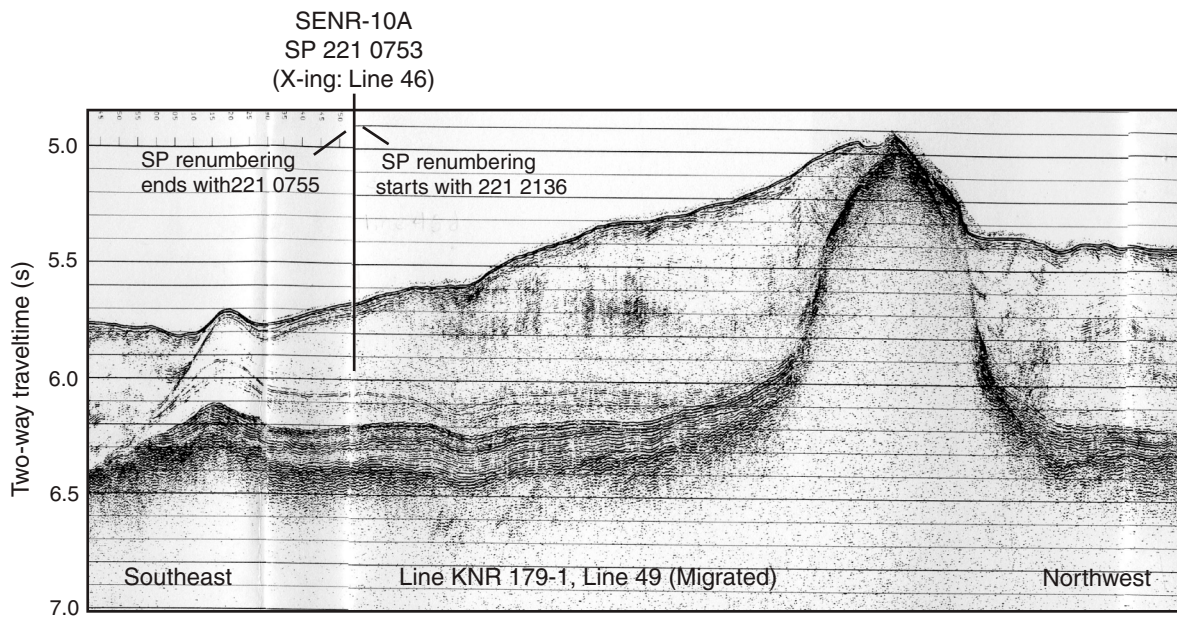
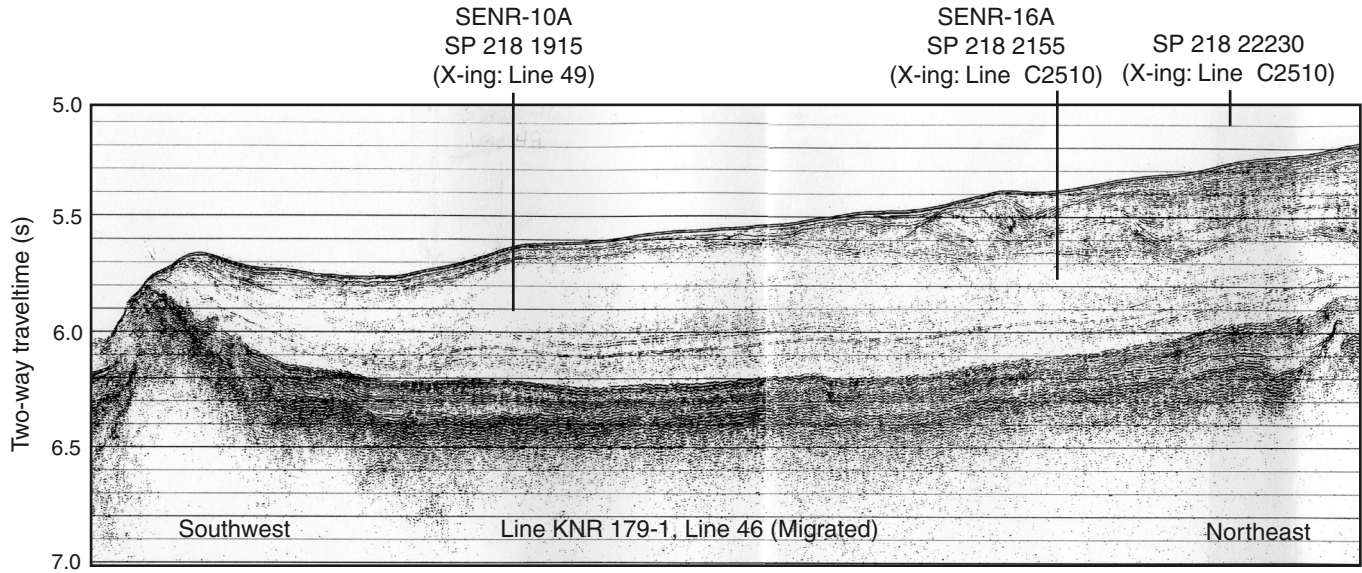


**Figure F8.** Subsidence estimates for North Atlantic Deep Sea Drilling Project (DSDP) records, with an interpretation of calcite compensation depth (CCD) history. Red dashed lines report the calculated subsidence history of the base of J Anomaly Ridge, DSDP Site 384 on the crest of J Anomaly Ridge, and the tops of the Southeast Newfoundland Ridge (SENR) seamounts. Seismic data suggest, in contrast to the reconstructed CCD record, that carbonate sediments extend nearly to the base of J Anomaly Ridge during the Paleogene (shown in the yellow band). Expedition 342 will core a depth transect in Paleogene sediments to refine our understanding of CCD history.

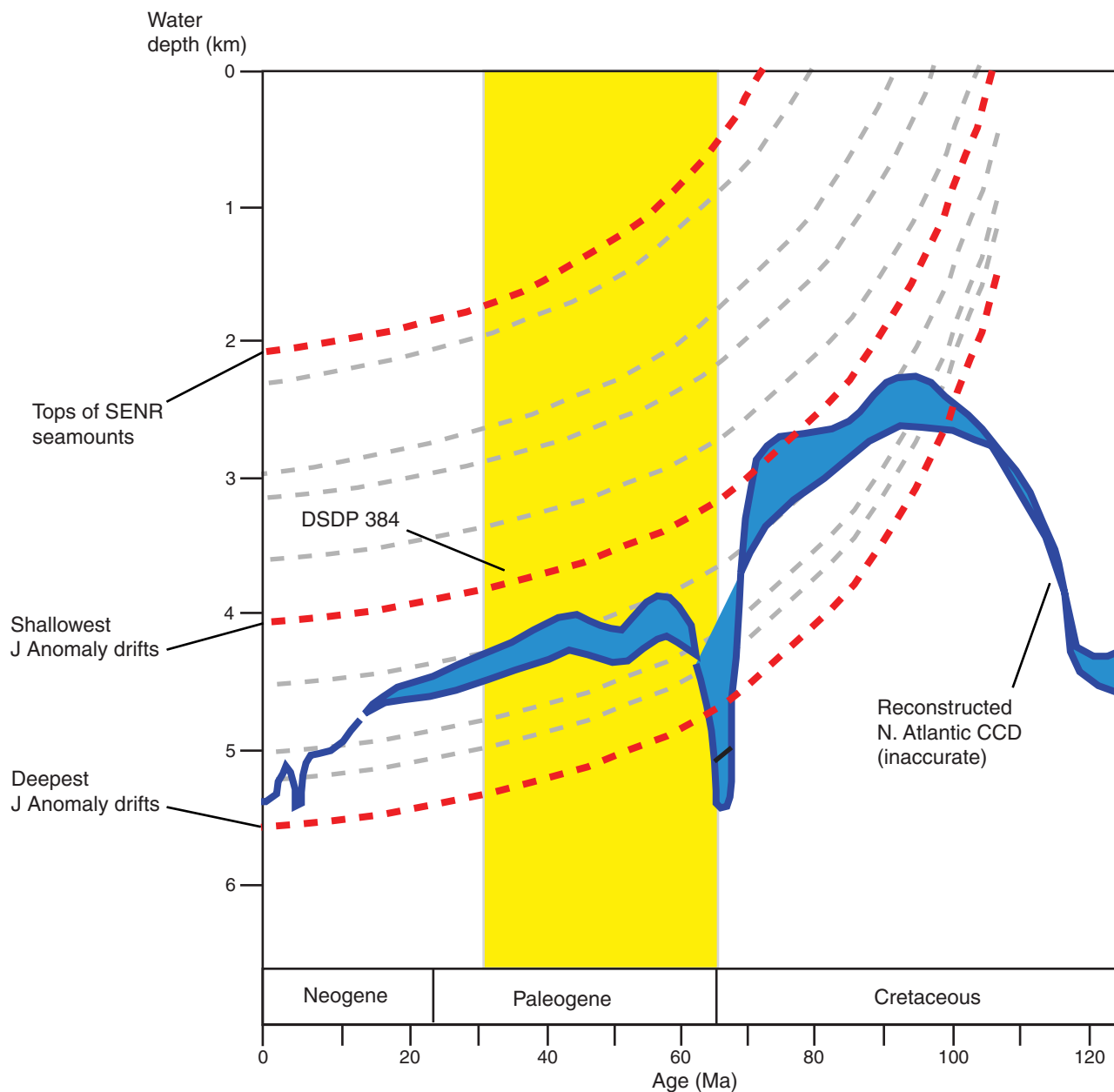


**Figure F9.** Generalized interpretation of seismic and sedimentary stratigraphy of the J Anomaly Ridge and adjacent Southeast Newfoundland Ridge. Sedimentary stratigraphy is based on the cored record in Deep Sea Drilling Project (DSDP) Site 384, whereas the seismic stratigraphy is based on seismic ties between single-channel seismic reflection profiles and DSDP Site 384.

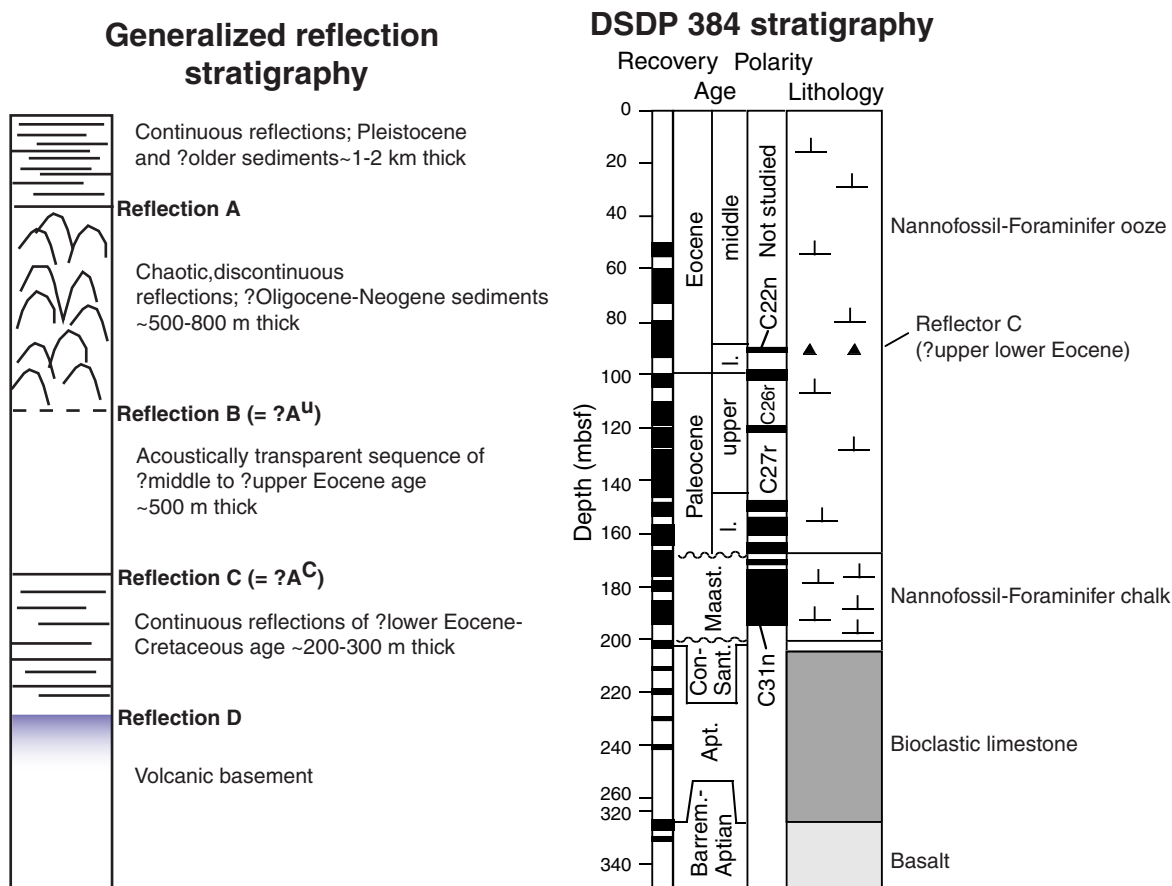


**Figure F10.** Single-channel seismic Profile KNR 179-1, Line 7, and interpretation. Cretaceous reefs (red) are overlain by pelagic sediment drifts (orange) and later by Eocene sediment drifts (green).

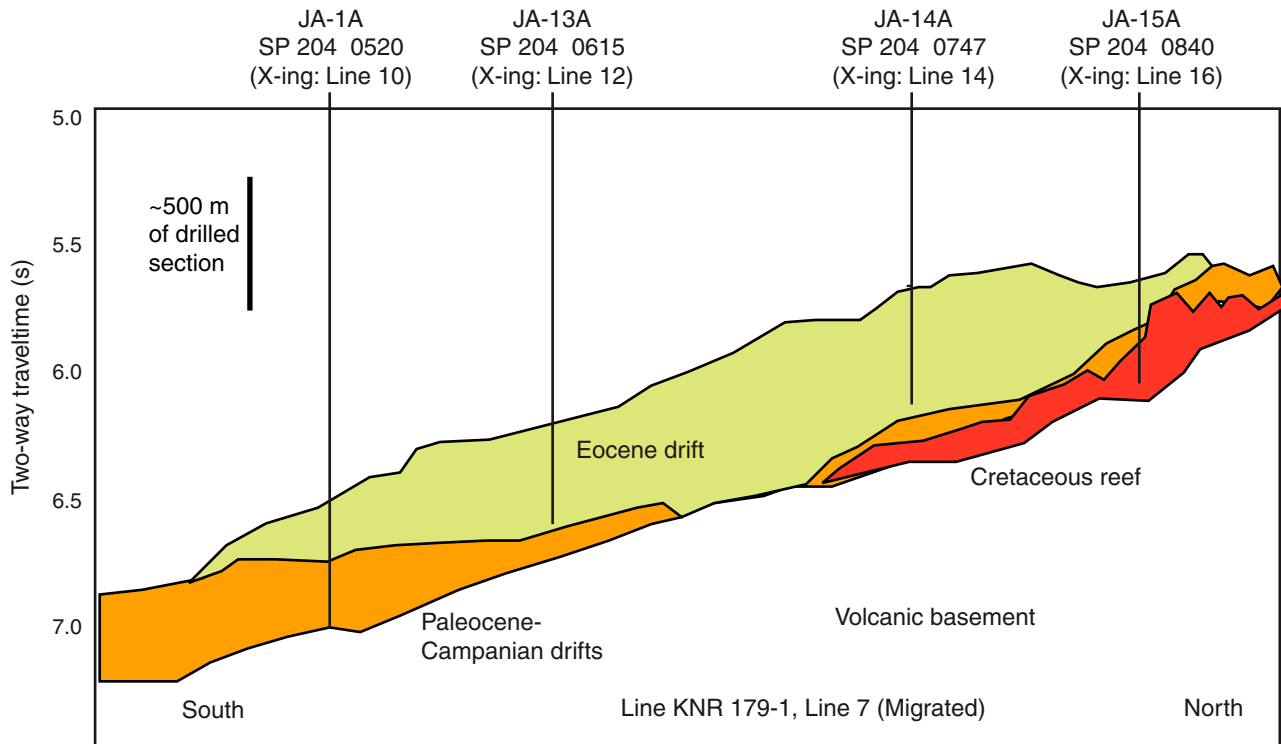
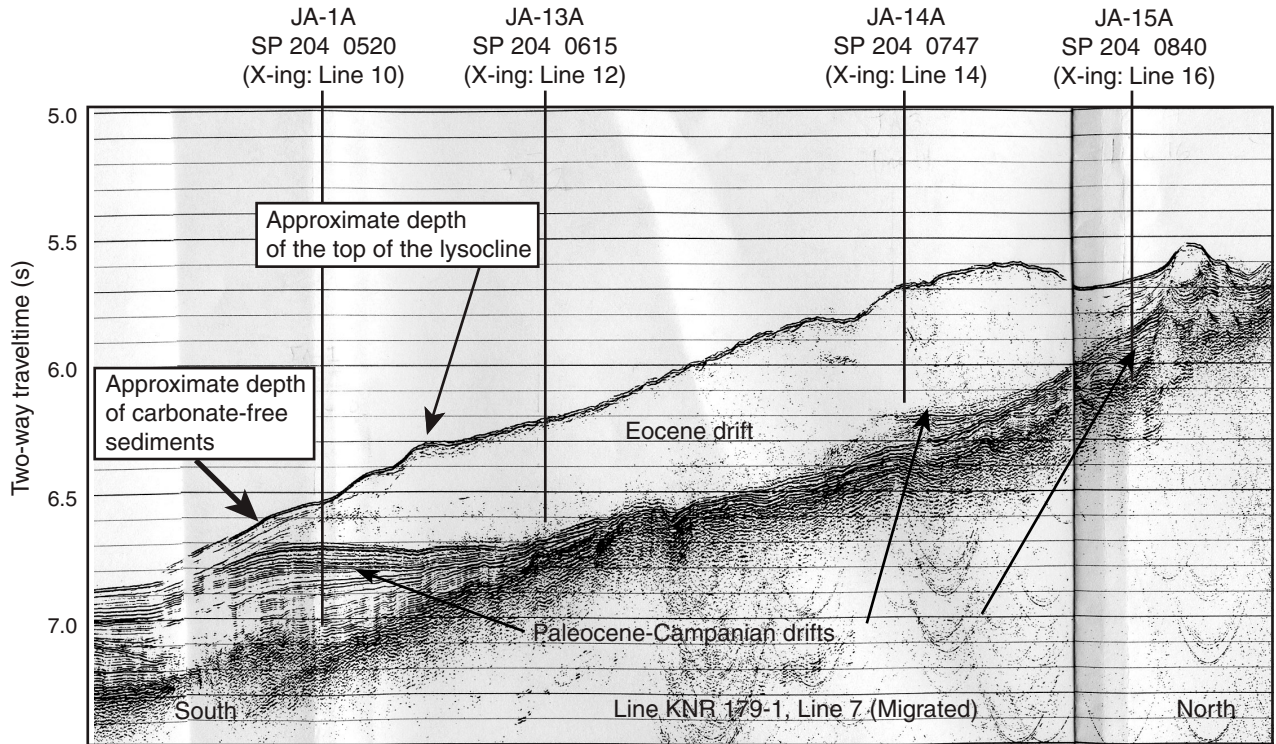


**Figure F11.** Single-channel seismic Profile KNR 179-1, Line 46B, and interpretation. Cretaceous sediments are overlain by Eocene through ?Oligocene–Miocene drifts.

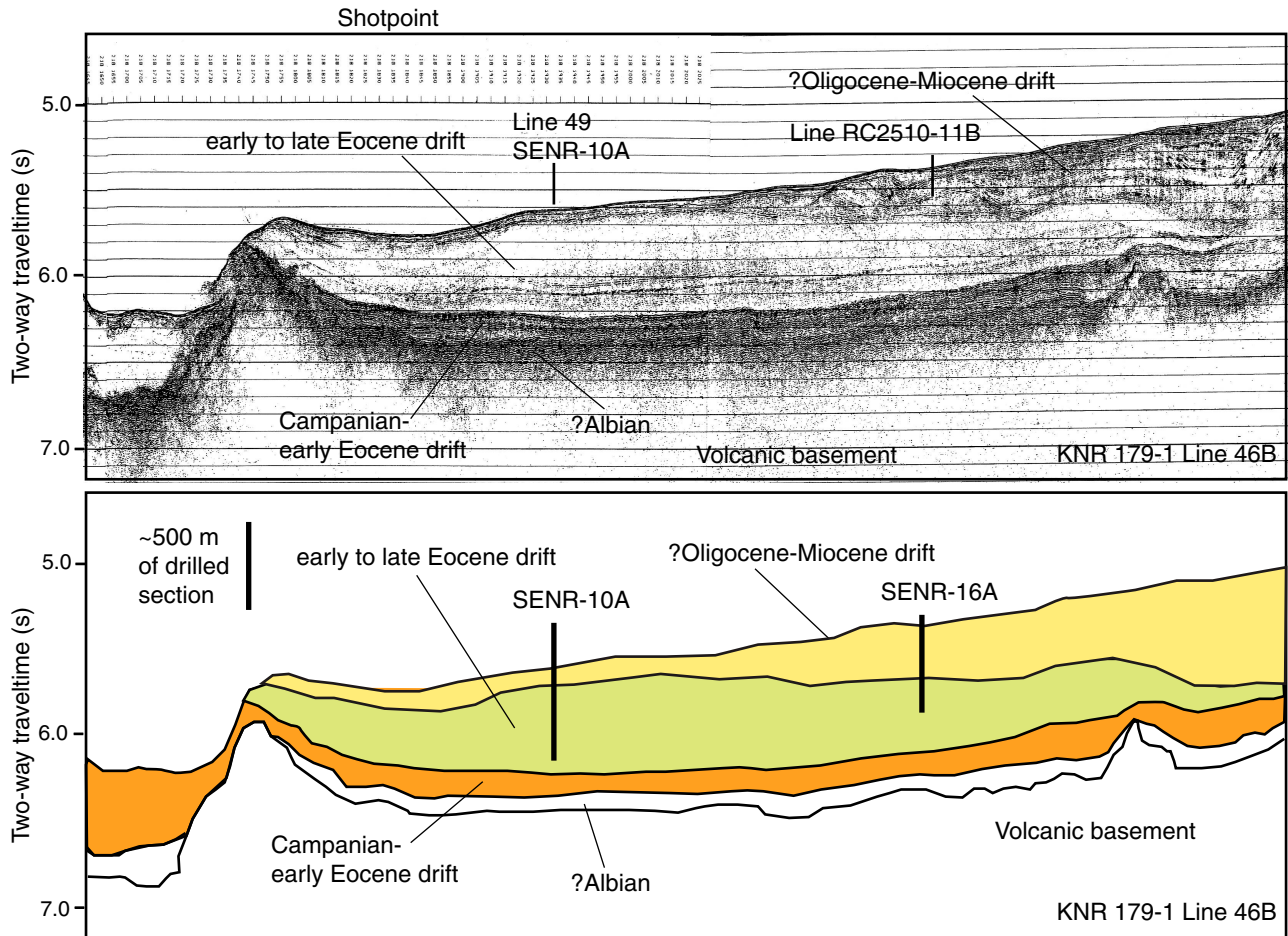




**Figure F12.** Eocene–Oligocene transition from the equatorial Pacific (ODP Site 1218), showing the lockstep-wise deepening of the CCD together with onset of major Antarctic glaciation (Coxall et al., 2005). MAR = mass accumulation rate, VPDB = Vienna Pee Dee belemnite.

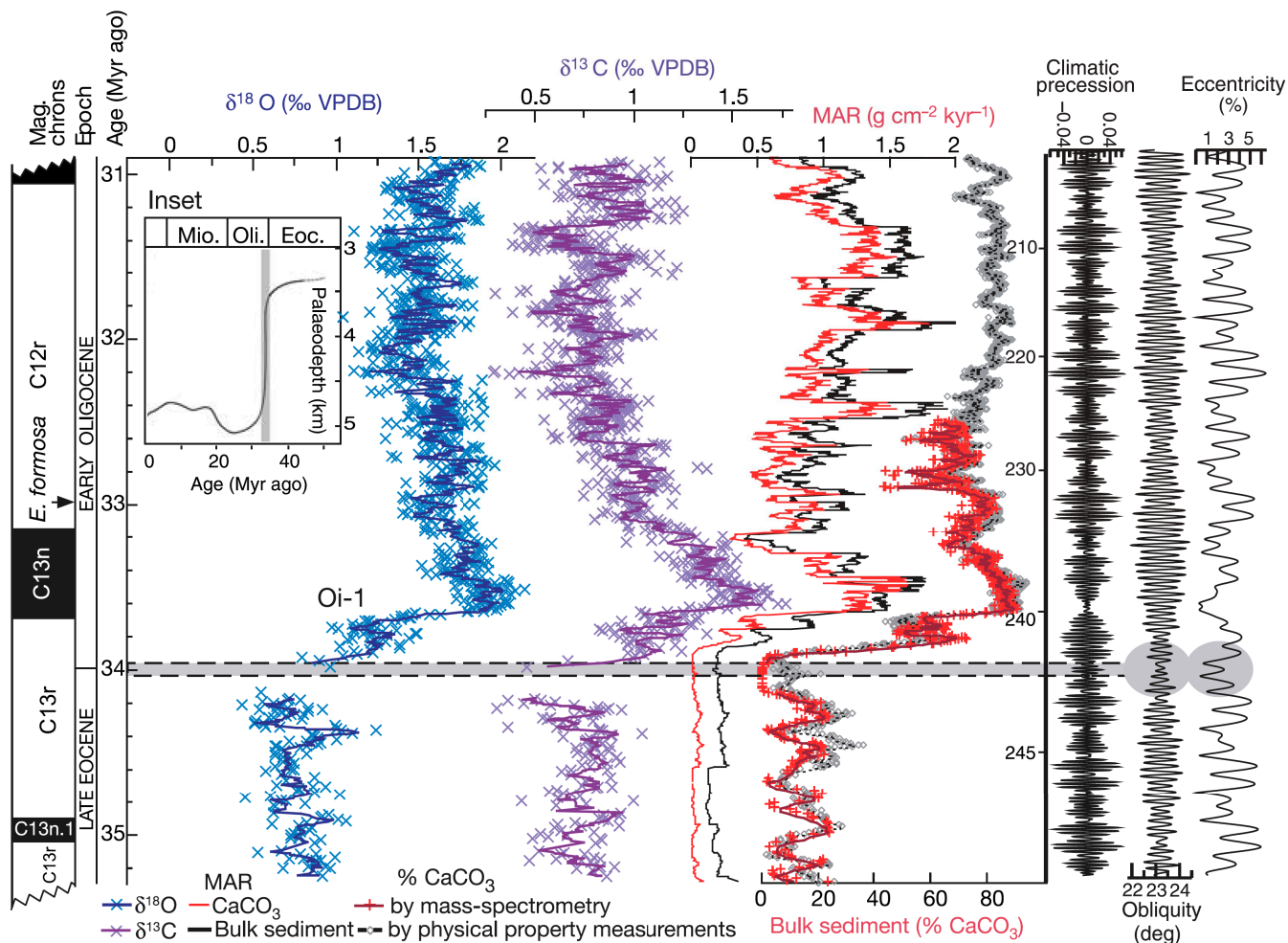


**Figure F13.** Compilation of benthic  $\delta^{13}\text{C}$  data through the PETM. Northern Hemisphere sites typically show more positive  $\delta^{13}\text{C}$  in the core of the PETM than Southern Ocean sites, indicating most deep water was formed in the northern basins. Before and after the PETM, however, the  $\delta^{13}\text{C}$  gradient is reversed, indicating southern sources of deep water. From Nuñez and Norris (2006). VPDB = Vienna Pee Dee belemnite. DSDP = Deep Sea Drilling Project, ODP = Ocean Drilling Program.

58

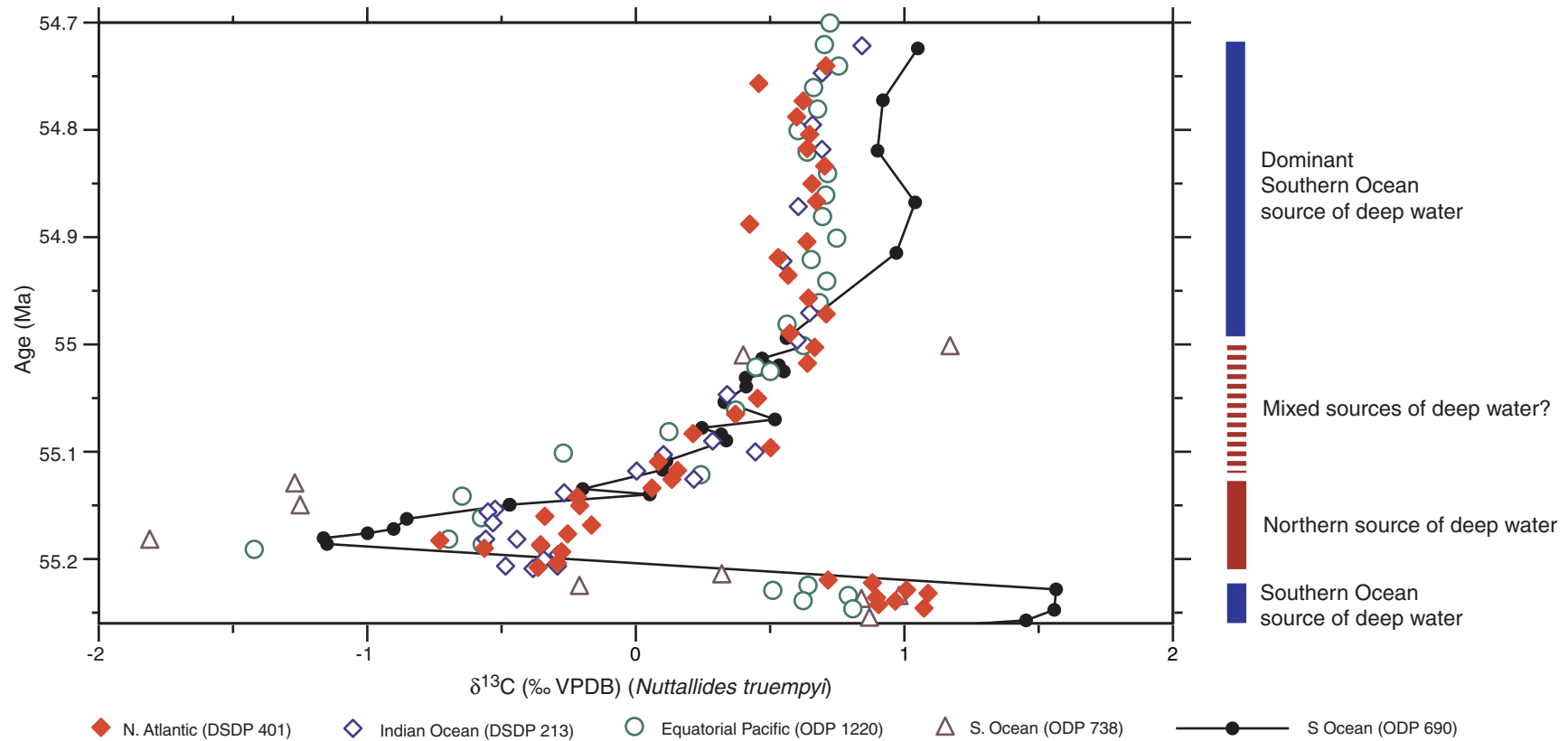


**Figure F14.** Overview of North Atlantic Ocean showing the location of Expedition 342 drill sites and port calls.

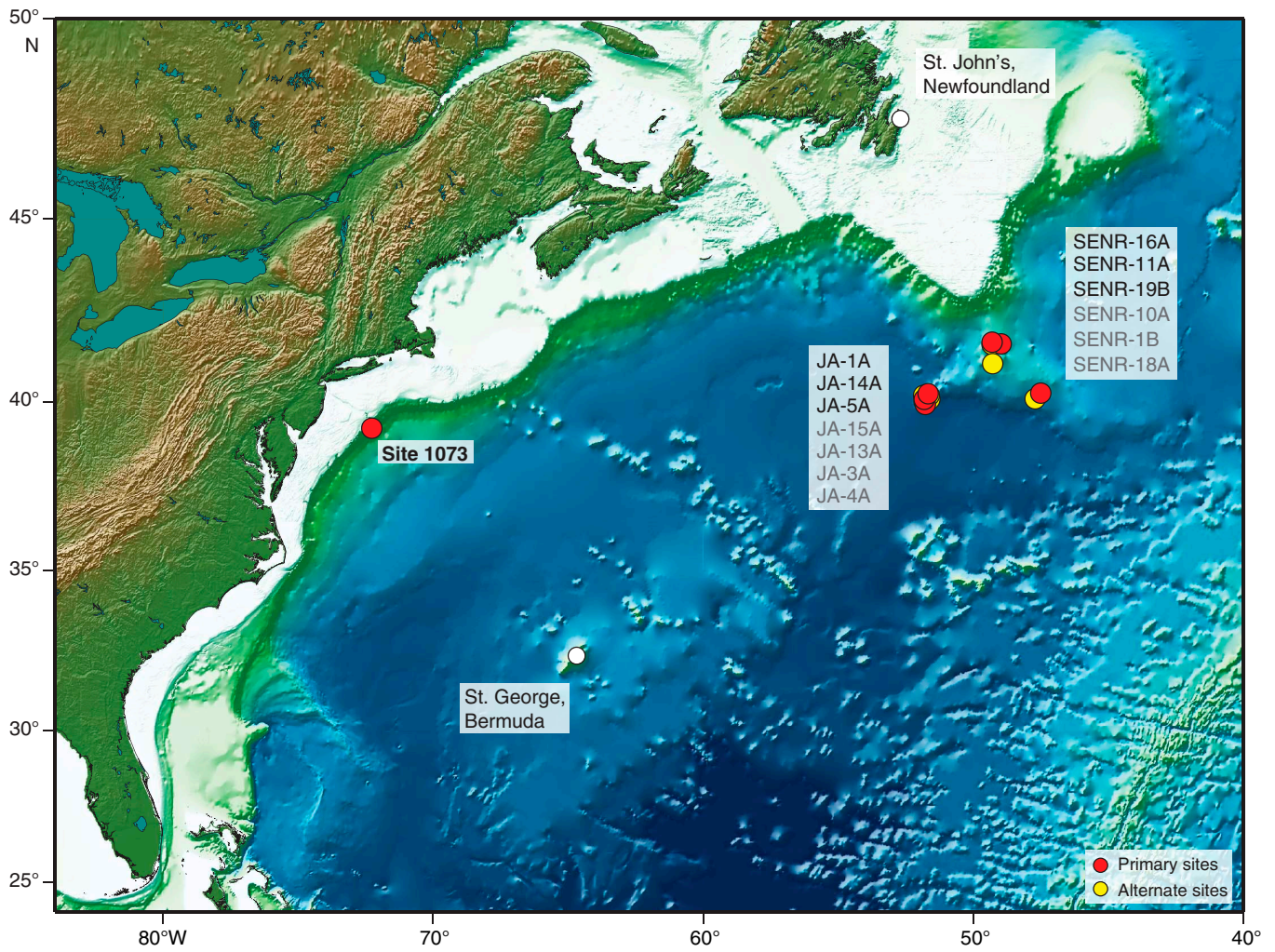


**Figure F15.** Single-channel seismic Profile KNR 179-1, Lines 22 and 25, showing Expedition 342 primary Site SENR-11A.

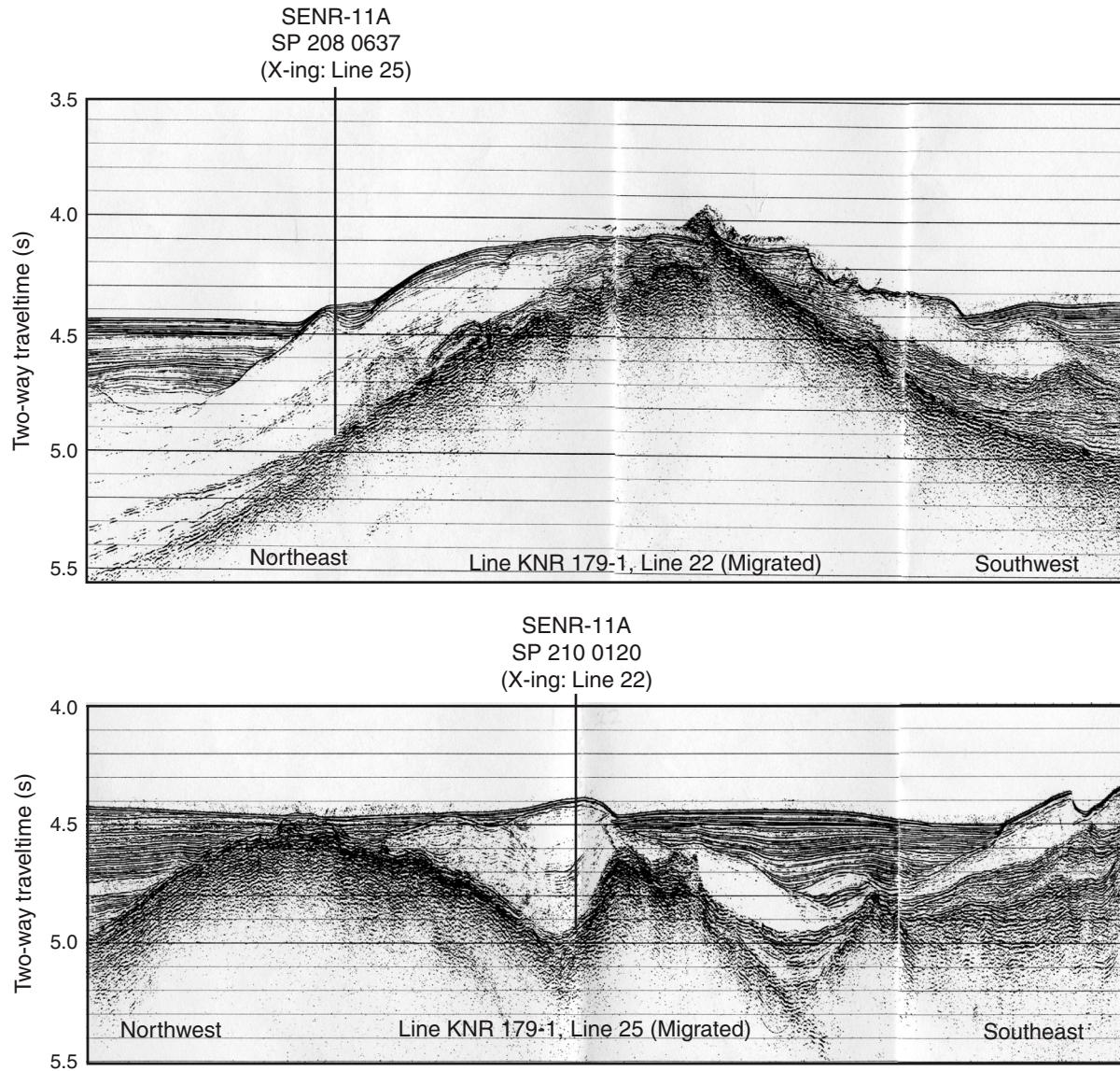


**Figure F16.** Single-channel seismic Profile KNR 179-1, Lines 27 and 24, showing Expedition 342 primary Site SENR-19B.

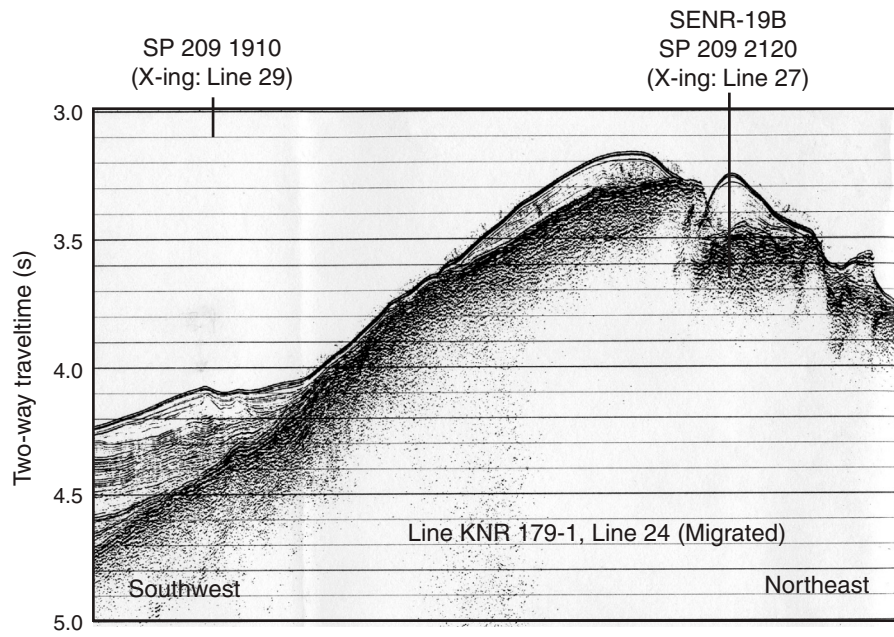
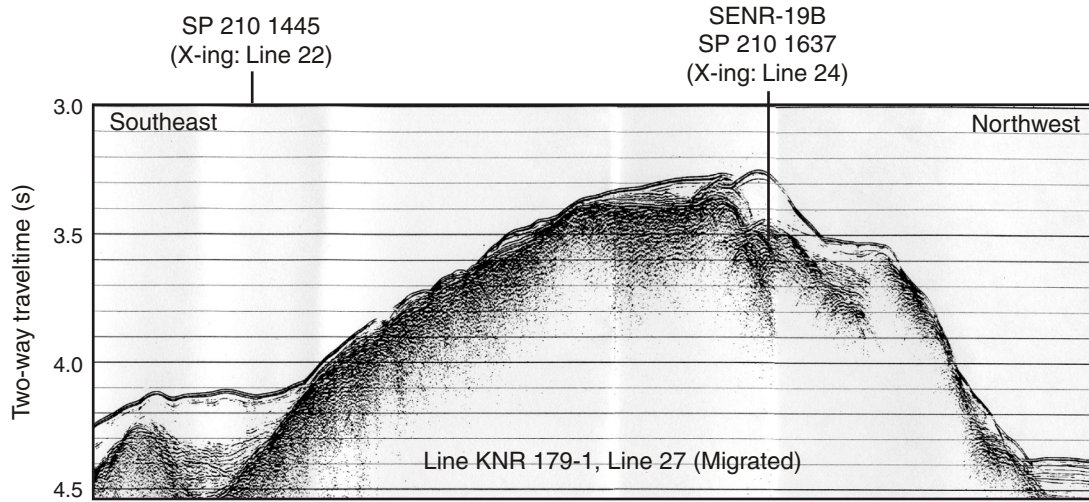


**Figure F17.** Single-channel seismic Profile KNR 179-1, Lines 52 and 20, showing Expedition 342 alternate Site SENR-1B.

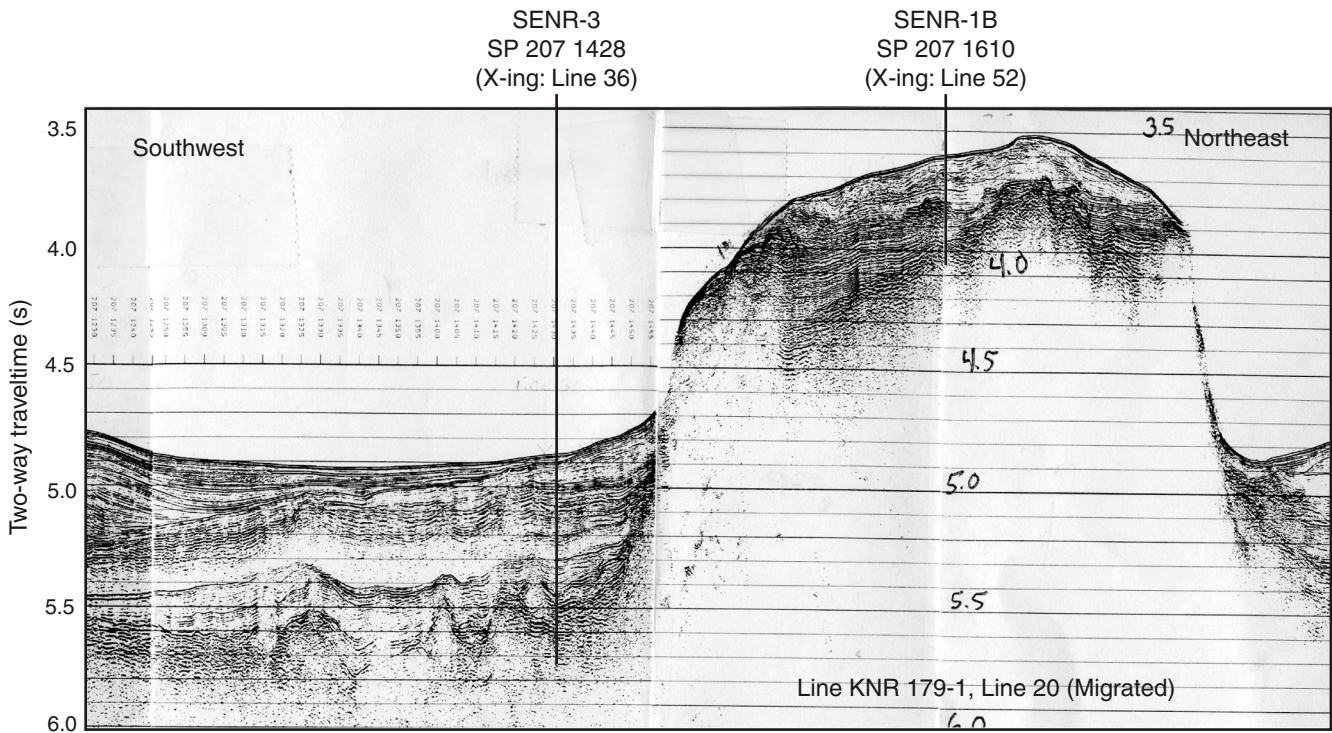
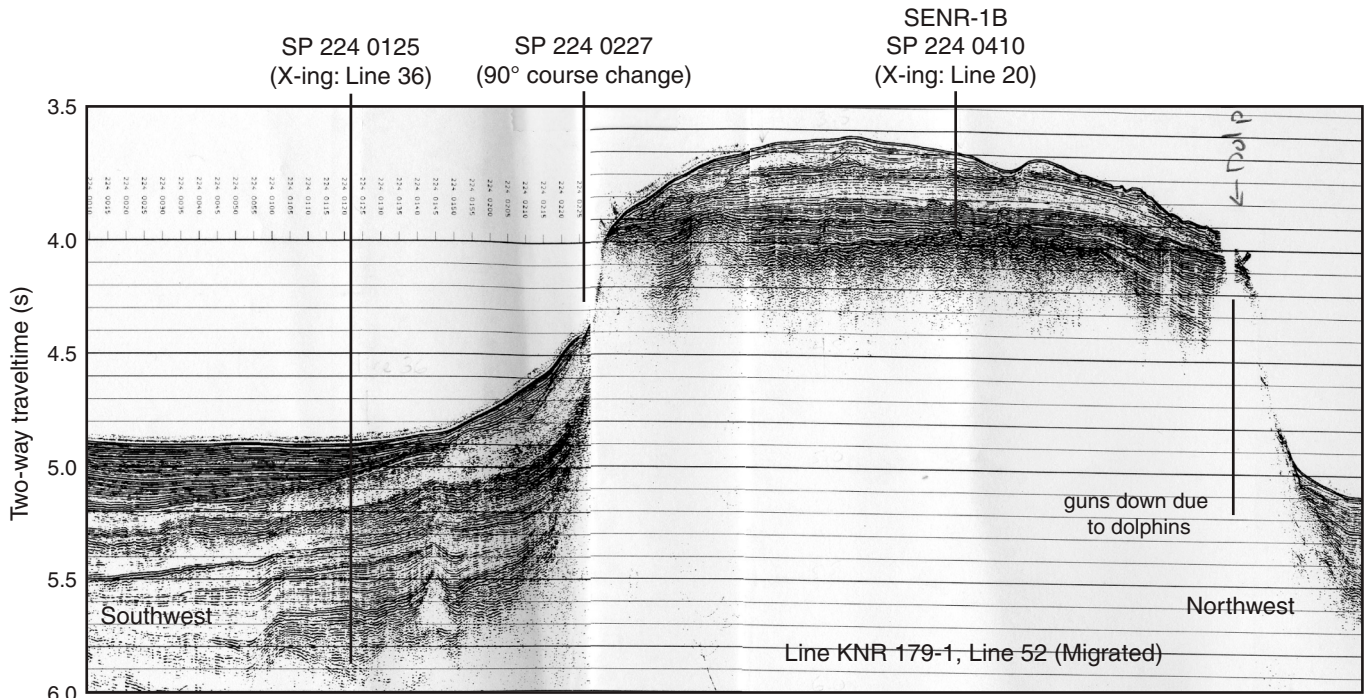


**Figure F18.** Single-channel seismic Profile KNR 179-1, Lines 53 and 31, showing Expedition 342 alternate Site SENR-18A.

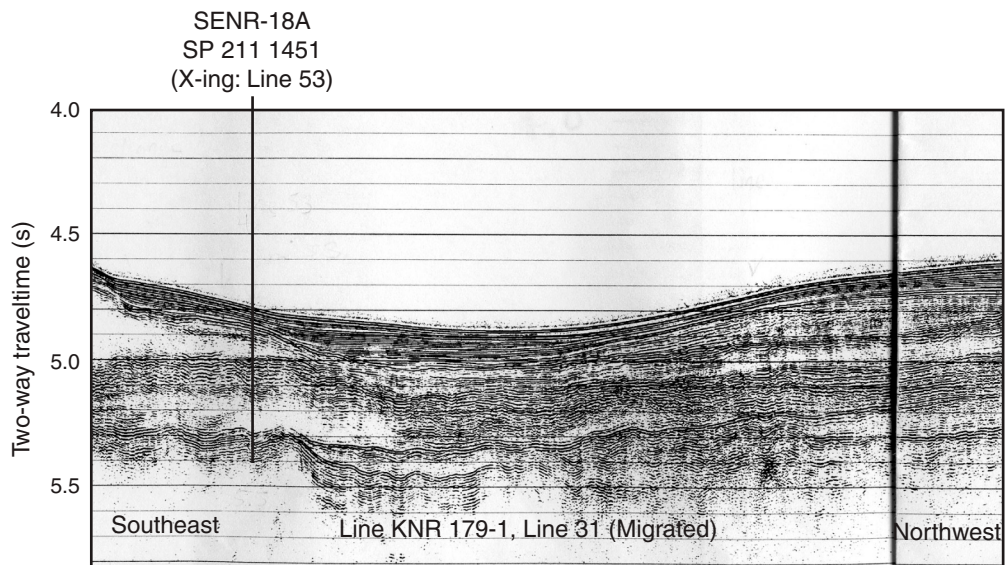
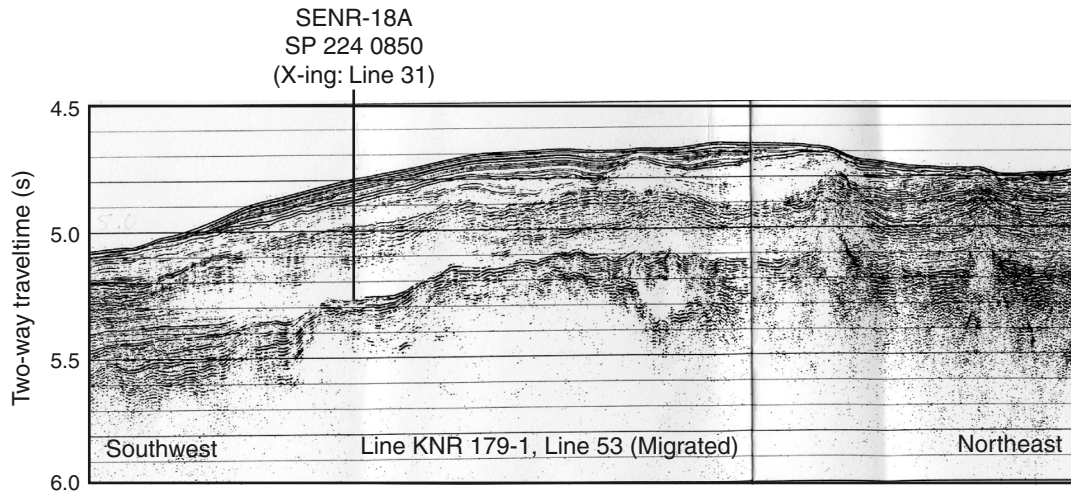


**Figure F19.** Single-channel seismic Profile KNR 179-1, Lines 10, 12, and 14, showing strike profiles of Expedition 342 primary Sites JA-1A and JA-14A, and alternate Sites JA-3A, JA-4A, and JA-13A.

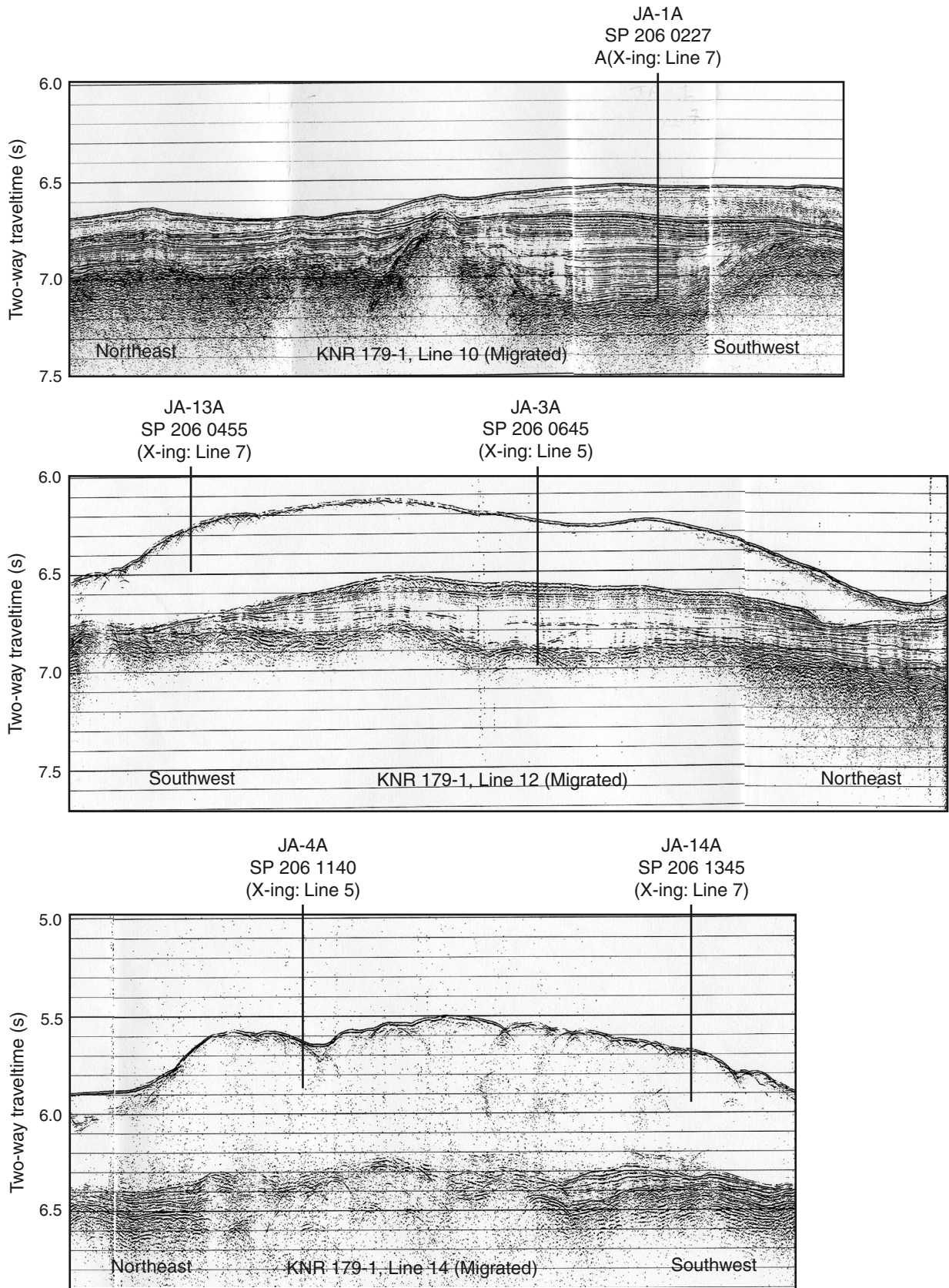




**Figure F20.** Single-channel seismic Profile KNR 179-1, Line 16, showing strike profiles of Expedition 342 primary Site JA-5A and alternate Site JA-15A.

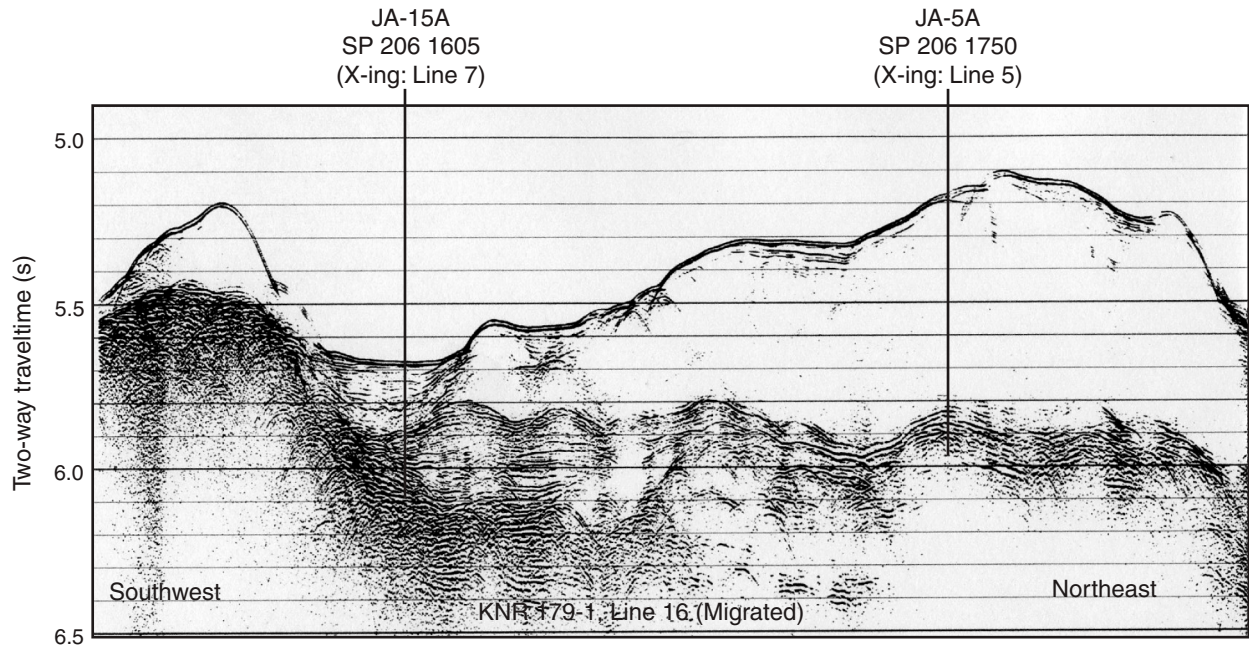


**Figure F21.** Triple combination (triple combo) and Formation MicroScanner (FMS)-sonic wireline logging tool strings. HNGS = Hostile Environment Natural Gamma Ray Sonde, HLDS = Hostile Environment Litho-Density Sonde, APS = Accelerator Porosity Sonde, GPIT = General Purpose Inclino-metry Tool, DIT = Dual Induction Tool, DSI = Dipole Sonic Imager.

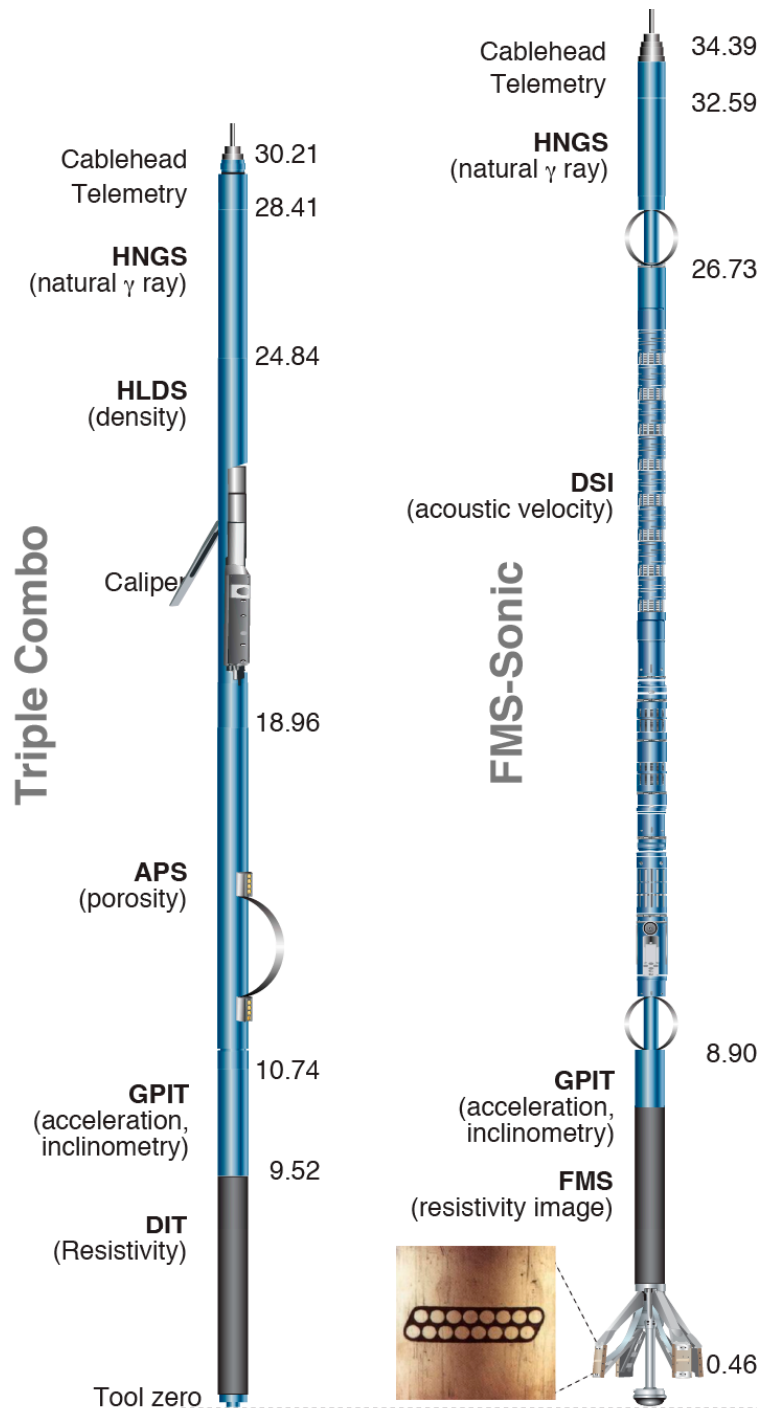


**Figure F22.** “Paleo combo” logging tool string, including the new Magnetic Susceptibility Sonde (MSS). GPIT = General Purpose Inclinerometry Tool, HNGS = Hostile Environment Natural Gamma Ray Sonde, APS = Accelerator Porosity Sonde, HLDS = Hostile Environment Litho-Density Sonde.

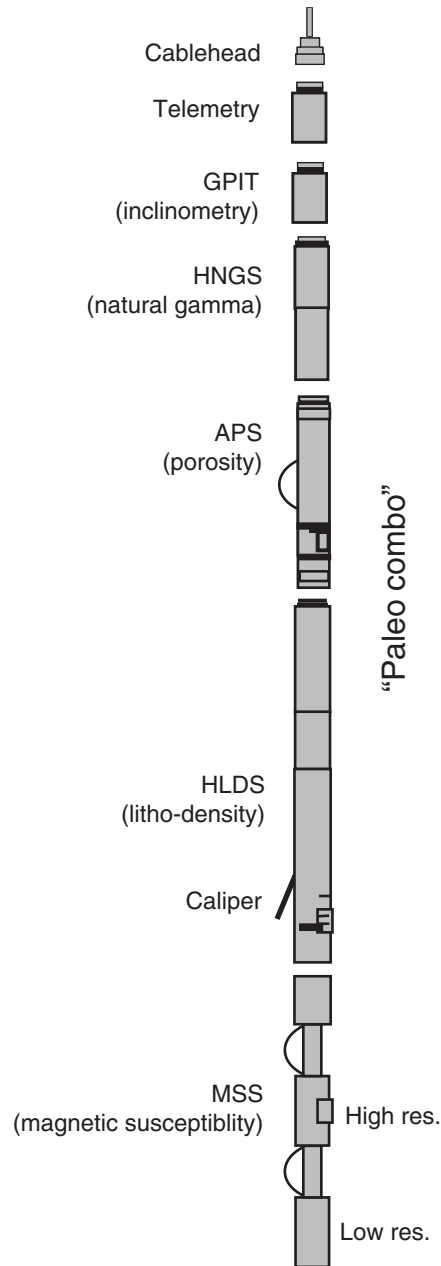


**Figure F23.** Schematic showing typical deployment of T2P and SET-P penetration probes. **A, B.** Drill string pushes probe into formation. **C.** Successful deployment in which probe stays in ground and bottom-hole assembly slides upward as drill string is raised. **D.** Unsuccessful deployment in which partial coupling occurs between drill string and Colleted Delivery System, partially pulling tool out of hole. **E.** Good penetration record characterized by abrupt increase in pressure, followed by slow dissipation of pressure while tool is left in ground. **F.** Poor penetration record characterized by sharp drop in pore pressure during pullout, resulting in subhydrostatic pressure that gradually builds back to formation pressure. **G.** Pressure and temperature response during an unsuccessful deployment. When the drill string is raised (bit depth decreases), pore pressures drop abruptly and temperature rises because the probe is being pulled out of the formation. UTC = Universal Time Coordinated.

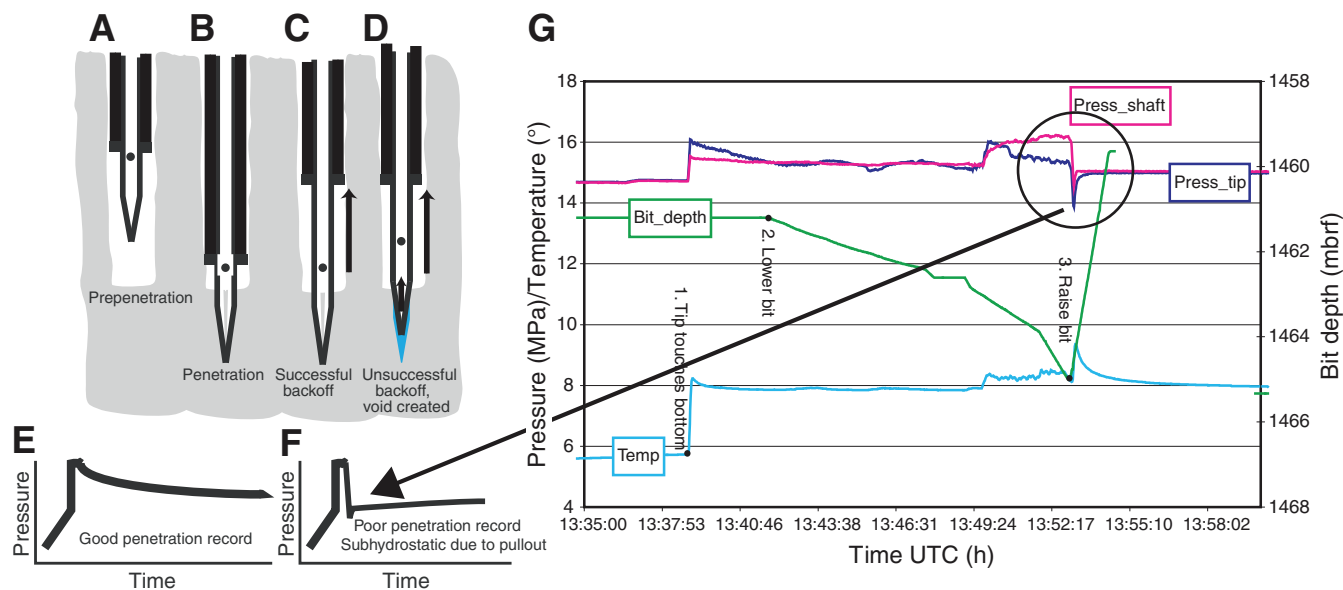


**Figure F24.** Stages of penetrometer deployment. **A.** RS overshoot released and pulled uphole. **B.** Drill string pressurized to pump penetrometer into formation. **C.** Penetrometer raised.

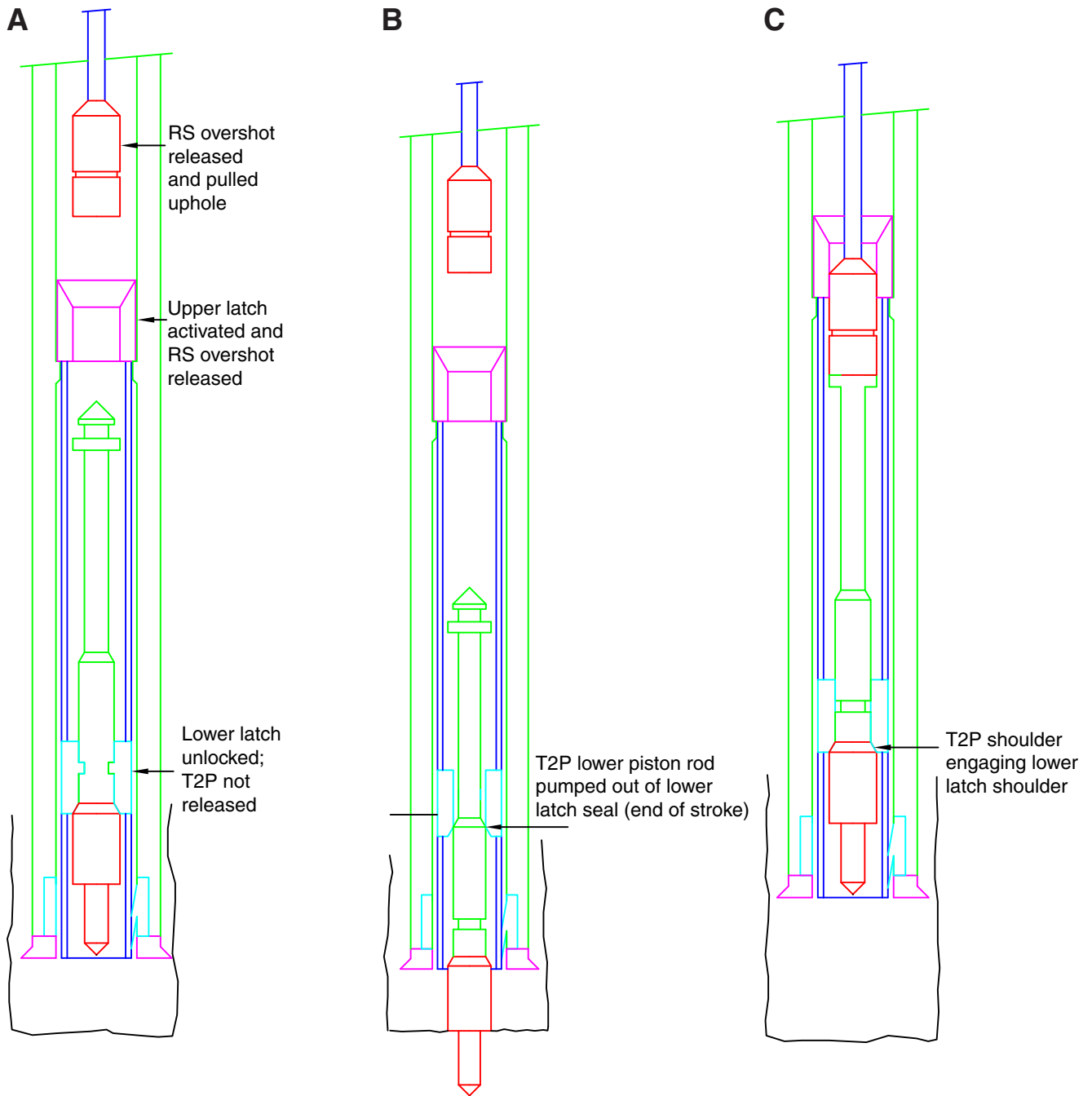


**Figure F25.** A. Bathymetric map of New Jersey continental slope (National Geophysical Data Center, [www.ngdc.noaa.gov/mgg/bathymetry/hydro.html](http://www.ngdc.noaa.gov/mgg/bathymetry/hydro.html)). ODP Leg 174A Site 1073 is located at 639 m water depth on a smooth portion of the slope (Austin, Christie-Blick, Malone, et al., 1998). B. Two-way travelt ime dip seismic Line 1002 showing regional Miocene–Pleistocene stratigraphy (Austin, Christie-Blick, Malone, et al., 1998). Black lines identify age boundaries. In the smooth zone, Pleistocene sediments completely cover Miocene strata, whereas the Miocene is exposed where canyons are present (Hampson and Robb, 1984). Modified from Dugan and Flemings (2000).

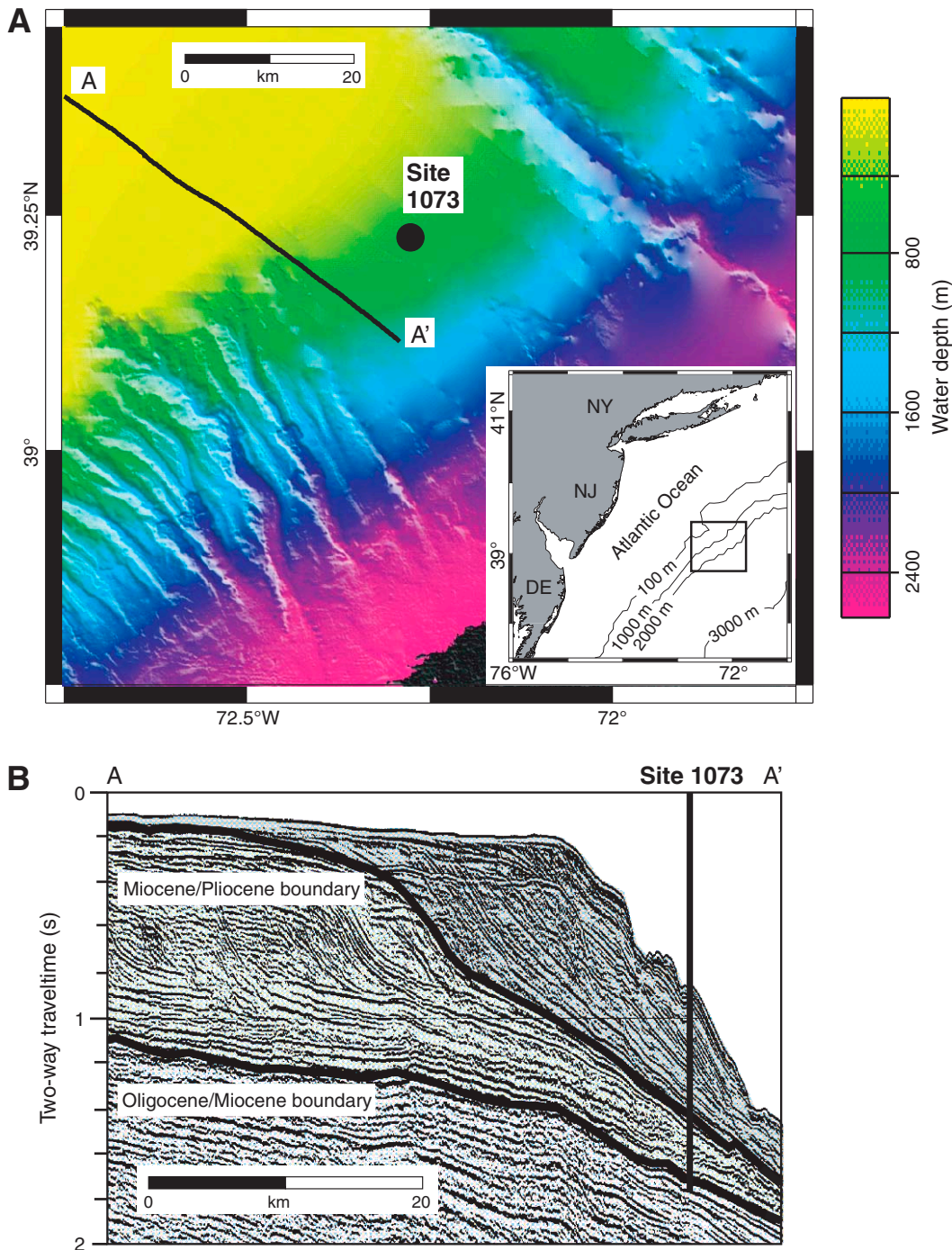
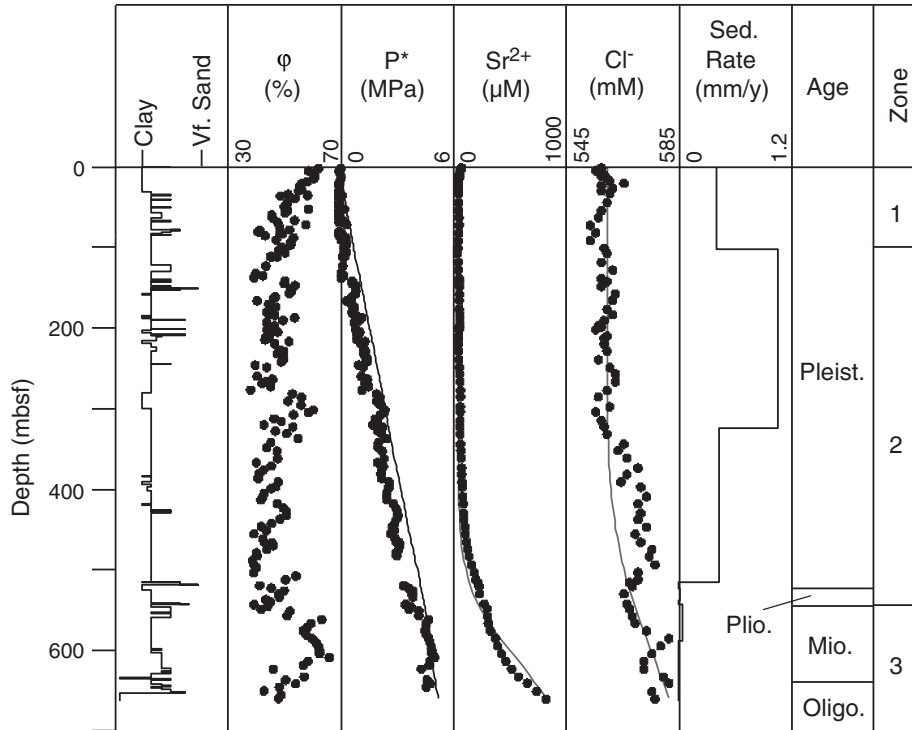


**Figure F26.** Core data from ODP Site 1073 (Fig. F23) (Austin, Christie-Blick, Malone, et al., 1998). Porosity was determined from wet and dry measurements of mass and volume of core samples. Values denoted by P\* are overpressures predicted from porosity. The solid line on the P\* plot is the reduced lithostatic stress ( $S_v - \rho_w g z$ ). Pleistocene sedimentation rates far exceed Miocene and Pliocene sedimentation rates, as inferred from biostratigraphic data. Modified from Dugan and Flemings (2002). Vf. = very fine.



## Site summaries

### ODP Site 1073

<b>Priority:</b>	Primary
<b>Position:</b>	39°13.52'N, 72°16.55'W
<b>Water depth (m):</b>	650
<b>Target drilling depth (mbsf):</b>	100
<b>Approved maximum penetration (mbsf):</b>	Request 300; pending EPSP approval
<b>Survey coverage:</b>	NA
<b>Objective:</b>	MDHDS engineering test
<b>Coring program:</b>	<ul style="list-style-type: none"><li>• NA</li><li>• Hole B: wash down to 100 mbsf and test MDHDS</li><li>• See Table <a href="#">T1</a></li></ul>
<b>Wireline logging program:</b>	NA
<b>Anticipated lithology:</b>	



## Site summaries (continued)

### Site JA-1A

<b>Priority:</b>	Primary
<b>Position:</b>	39°55.00'N, 51°47.00'W
<b>Water depth (m):</b>	4940
<b>Target drilling depth (mbsf):</b>	400
<b>Approved maximum penetration (mbsf):</b>	Request 700; pending EPSP approval
<b>Survey coverage:</b>	<ul style="list-style-type: none"> <li>• Primary line: KNR 179-1, Line 7, SP 204 0520</li> <li>• Crossing line: KNR 179-1, Line 10, SP 206 0227</li> </ul>
<b>Objective:</b>	Deep end of depth transect in shallowly buried lower Eocene to Albian drift; deepwater chemistry and history of the Deep Western Boundary Current; Paleogene hyperthermals; PETM. This site has the deepest water depth in the proposed drilling program. Below Eocene CCD.
<b>Coring program:</b>	<ul style="list-style-type: none"> <li>• Hole A: APC/XCB to 400 mbsf with orientation and APCT-3</li> <li>• Hole B: APC/XCB to 400 mbsf</li> <li>• Hole C: APC/XCB to 400 mbsf</li> <li>• See <a href="#">“Drilling strategy”</a> and Tables <a href="#">T1</a>, <a href="#">T2</a></li> </ul>
<b>Wireline logging program:</b>	<ul style="list-style-type: none"> <li>• Hole C: Wireline logging with triple combo and FMS-sonic</li> <li>• See <a href="#">“Downhole measurements strategy”</a> and Tables <a href="#">T1</a>, <a href="#">T2</a></li> </ul>
<b>Anticipated lithology:</b>	Carbonate ooze, hemipelagic clay, shallow-water carbonates

## Site summaries (continued)

### Site JA-14A

<b>Priority:</b>	Primary
<b>Position:</b>	40°3.00'N, 51°49.00'W
<b>Water depth (m):</b>	4250
<b>Target drilling depth (mbsf):</b>	250
<b>Approved maximum penetration (mbsf):</b>	Request 700; pending EPSP approval
<b>Survey coverage:</b>	<ul style="list-style-type: none"> <li>• Primary line: KNR 179-1, Line 7, SP 204 0747</li> <li>• Crossing lines: KNR 179-1, Line 14, SP 206 1345</li> </ul>
<b>Objective:</b>	Lower end of depth transect; lower to upper Eocene and possible Eocene/Oligocene boundary (entire section of Eocene strata is ~500 m thick at this site, allowing potential deeper penetration than currently proposed); early Eocene warm period; Eocene hyperthermals; middle and late Eocene impacts; transition to icehouse climate; Eocene CCD; chemistry of Eocene deep water. Just above Eocene CCD.
<b>Coring program:</b>	<ul style="list-style-type: none"> <li>• Hole A: APC/XCB to 250 mbsf with orientation and APCT-3</li> <li>• Hole B: APC/XCB to 250 mbsf</li> <li>• Hole C: APC/XCB to 250 mbsf</li> <li>• See <a href="#">“Drilling strategy”</a> and Tables <a href="#">T1</a>, <a href="#">T2</a></li> </ul>
<b>Wireline logging program:</b>	<ul style="list-style-type: none"> <li>• NA</li> <li>• See <a href="#">“Downhole measurements strategy”</a> and Tables <a href="#">T1</a>, <a href="#">T2</a></li> </ul>
<b>Anticipated lithology:</b>	Carbonate ooze, hemipelagic clay, shallow-water carbonates

## Site summaries (continued)

### Site JA-5A

<b>Priority:</b>	Primary
<b>Position:</b>	40°13.00'N, 51°40.00'W
<b>Water depth (mbrf):</b>	3900
<b>Target drilling depth (mbsf):</b>	250
<b>Approved maximum penetration (mbsf):</b>	Request 700; pending EPSP approval
<b>Survey coverage:</b>	<ul style="list-style-type: none"> <li>• Primary line: KNR 179-1, Line 5, SP 203 2037</li> <li>• Crossing lines: KNR 179-1, Line 16, SP 206 1750</li> </ul>
<b>Objective:</b>	Lower middle of depth transect; lower to upper Eocene and possible Eocene/Oligocene boundary (entire section of Eocene strata is ~700 m thick at this site, allowing potential deeper penetration than currently proposed); early Eocene warm period; Eocene hyperthermals; middle and late Eocene impacts; transition to icehouse climate; Eocene CCD; chemistry of Eocene deep water.
<b>Coring program:</b>	<ul style="list-style-type: none"> <li>• Hole A: APC/XCB to 250 mbsf with orientation and APCT-3</li> <li>• Hole B: APC/XCB to 250 mbsf</li> <li>• Hole C: APC/XCB to 250 mbsf</li> <li>• See <a href="#">"Drilling strategy"</a> and Tables <a href="#">T1</a>, <a href="#">T2</a></li> </ul>
<b>Wireline logging program:</b>	<ul style="list-style-type: none"> <li>• NA</li> <li>• See <a href="#">"Downhole measurements strategy"</a> and Tables <a href="#">T1</a>, <a href="#">T2</a></li> </ul>
<b>Anticipated lithology:</b>	Carbonate ooze, hemipelagic clay, shallow-water carbonates

## Site summaries (continued)

### Site SENR-16A

<b>Priority:</b>	Primary
<b>Position:</b>	40°14.00'N, 47°30.00'W
<b>Water depth (mbrf):</b>	4150
<b>Target drilling depth (mbsf):</b>	400
<b>Approved maximum penetration (mbsf):</b>	Request 900; pending EPSP approval
<b>Survey coverage:</b>	<ul style="list-style-type: none"> <li>• Primary line: KNR 179-1, Line 46, SP 218 2155</li> <li>• Crossing line: MCS Line RC2510 11B, SP 1600Z 3073</li> </ul>
<b>Objective:</b>	Lower Oligocene and upper Eocene with record of E/O boundary; biotic changes around the E/O and late Eocene; late Eocene impact horizons; transition to different type of drift sedimentation and associated changes in flow characteristics of the Deep Western Boundary Current; CCD evolution; middle of depth transect.
<b>Coring program:</b>	<ul style="list-style-type: none"> <li>• Hole A: APC/XCB to 300 mbsf with orientation and APCT-3</li> <li>• Hole B: APC/XCB to 300 mbsf</li> <li>• Hole C: APC/XCB to 300 mbsf</li> <li>• See <a href="#">"Drilling strategy"</a> and Tables <a href="#">T1</a>, <a href="#">T2</a></li> </ul>
<b>Wireline logging program:</b>	<ul style="list-style-type: none"> <li>• Hole C: Wireline logging with triple combo and FMS-sonic</li> <li>• See <a href="#">"Downhole measurements strategy"</a> and Tables <a href="#">T1</a>, <a href="#">T2</a></li> </ul>
<b>Anticipated lithology:</b>	Carbonate ooze, hemipelagic clay, shallow-water carbonates

## Site summaries (continued)

### Site SENR-11A

<b>Priority:</b>	Primary
<b>Position:</b>	41°37.00'N, 48°58.00'W
<b>Water depth (m):</b>	3300
<b>Target drilling depth (mbsf):</b>	300
<b>Approved maximum penetration (mbsf):</b>	Request 600; pending EPSP approval
<b>Survey coverage:</b>	<ul style="list-style-type: none"> <li>• Primary line: KNR 179-1, Line 22, SP 208 0637</li> <li>• Crossing line: KNR 179-1, Line 25, SP 210 0120</li> </ul>
<b>Objective:</b>	Upper middle of depth transect (entire section of Eocene strata is ~550 m thick at this site); early Eocene warm period; eocene hyperthermals; chemistry of Eocene deepwater. This is the shallowest highly expanded section of Eocene in the survey area, with excellent potential for very high sedimentation rates.
<b>Coring program:</b>	<ul style="list-style-type: none"> <li>• Hole A: APC/XCB to 300 mbsf with orientation and APCT-3</li> <li>• Hole B: APC/XCB to 300 mbsf</li> <li>• Hole C: APC/XCB to 300 mbsf</li> <li>• See <a href="#">"Drilling strategy"</a> and Tables <a href="#">T1</a>, <a href="#">T2</a></li> </ul>
<b>Wireline logging program:</b>	<ul style="list-style-type: none"> <li>• Hole C: Wireline logging with triple combo and FMS-sonic</li> <li>• See <a href="#">"Downhole measurements strategy"</a> and Tables <a href="#">T1</a>, <a href="#">T2</a></li> </ul>
<b>Anticipated lithology:</b>	Carbonate ooze, hemipelagic clay, shallow-water carbonates

## Site summaries (continued)

### Site SENR-19B

<b>Priority:</b>	Primary
<b>Position:</b>	41°40.00'N, 49°18.00'W
<b>Water depth (m):</b>	2470
<b>Target drilling depth (mbsf):</b>	250
<b>Approved maximum penetration (mbsf):</b>	Request 300; pending EPSP approval
<b>Survey coverage:</b>	<ul style="list-style-type: none"> <li>• Primary line: KNR 179-1, Line 27, SP 210 1637</li> <li>• Crossing line: KNR 179-1, Line 24, SP 209 2120</li> </ul>
<b>Objective:</b>	Shallow end of depth transect; lower Eocene to upper Eocene pelagic cap; record of early Eocene warm period; transition to icehouse climate; middle and late Eocene impacts; Eocene hyperthermals.
<b>Coring program:</b>	<ul style="list-style-type: none"> <li>• Hole A: APC/XCB to 250 mbsf with orientation and APCT-3</li> <li>• Hole B: APC/XCB to 250 mbsf</li> <li>• Hole C: APC/XCB to 250 mbsf</li> <li>• See <a href="#">“Drilling strategy”</a> and Tables <a href="#">T1</a>, <a href="#">T2</a></li> </ul>
<b>Wireline logging program:</b>	<ul style="list-style-type: none"> <li>• NA</li> <li>• See <a href="#">“Downhole measurements strategy”</a> and Tables <a href="#">T1</a>, <a href="#">T2</a></li> </ul>
<b>Anticipated lithology:</b>	Carbonate ooze, hemipelagic clay, shallow-water carbonates

## Site summaries (continued)

### Site JA-15A

<b>Priority:</b>	Alternate
<b>Position:</b>	40°10.00'N, 51°50.00'W
<b>Water depth (mbrf):</b>	4290
<b>Target drilling depth (mbsf):</b>	200, possibly 400
<b>Approved maximum penetration (mbsf):</b>	Request 500; pending EPSP approval
<b>Survey coverage:</b>	<ul style="list-style-type: none"> <li>• Primary line: KNR 179-1, Line 7, SP 204 0840</li> <li>• Crossing line: KNR 179-1, Line 16, SP 206 1605</li> </ul>
<b>Objective:</b>	Middle of depth transect; lower to upper Eocene and possible Eocene/Oligocene boundary. The entire section of Eocene strata is ~200 m thick at this site, and the Eocene section is probably contaminated with younger sediments because the site sits in a basin; however, this site has ~250 m of Cretaceous–Paleogene strata under ~200 m burial. These strata crop out just north of JA-4 (where there is ~300 m of Cretaceous–Paleogene sediments), but we have no crossing line.
<b>Coring program:</b>	<ul style="list-style-type: none"> <li>• Hole A: APC/XCB to 200 mbsf with orientation and APCT-3</li> <li>• Hole B: APC/XCB to 200 mbsf</li> <li>• Hole C: APC/XCB to 200 mbsf</li> <li>• See <a href="#">“Drilling strategy”</a> and Tables <a href="#">T1</a>, <a href="#">T3</a></li> </ul>
<b>Wireline logging program:</b>	<ul style="list-style-type: none"> <li>• If deeper drilling, logging with triple combo and FMS-sonic</li> <li>• See <a href="#">“Downhole measurements strategy”</a> and Tables <a href="#">T1</a>, <a href="#">T3</a></li> </ul>
<b>Anticipated lithology:</b>	Carbonate ooze, hemipelagic clay, shallow-water carbonates

## Site summaries (continued)

### Site SENR-10A

<b>Priority:</b>	Primary
<b>Position:</b>	40°4.00'N, 47°43.00'W
<b>Water depth (m):</b>	4250
<b>Target drilling depth (mbsf):</b>	200, possibly 400
<b>Approved maximum penetration (mbsf):</b>	Request 800; pending EPSP approval
<b>Survey coverage:</b>	<ul style="list-style-type: none"> <li>• Primary line: KNR 179-1, Line 46, SP 218 1915</li> <li>• Crossing lines: KNR 179-1, Line 49, SP 221 0753</li> </ul>
<b>Objective:</b>	Lower Eocene to upper Eocene/Oligocene carbonate ooze and calcareous claystone; Eocene hyperthermals; middle and late Eocene impacts; early Eocene warm period and transition to icehouse; Eocene/Oligocene boundary in an expanded drift deposit; refined cyclostratigraphic timescale and magnetic chronology; middle of depth transect.
<b>Coring program:</b>	<ul style="list-style-type: none"> <li>• Hole A: APC/XCB to 300 mbsf with orientation</li> <li>• Hole B: APC/XCB to 300 mbsf</li> <li>• Hole C: APC/XCB to 300 mbsf</li> <li>• See <a href="#">“Drilling strategy”</a> and Tables <a href="#">T1</a>, <a href="#">T3</a></li> </ul>
<b>Wireline logging program:</b>	<ul style="list-style-type: none"> <li>• If deeper drilling, logging with triple combo and FMS-sonic</li> <li>• See <a href="#">“Downhole measurements strategy”</a> and Tables <a href="#">T1</a>, <a href="#">T3</a></li> </ul>
<b>Anticipated lithology:</b>	Carbonate ooze, hemipelagic clay, shallow-water carbonates



## Site summaries (continued)

### Site SENR-1B

<b>Priority:</b>	Alternate
<b>Position:</b>	41°36.00'N, 49°18.00'W
<b>Water depth (m):</b>	2750
<b>Target drilling depth (mbsf):</b>	200
<b>Approved maximum penetration (mbsf):</b>	Request 500; pending EPSP approval
<b>Survey coverage:</b>	<ul style="list-style-type: none"> <li>• Primary line: KNR 179-1, Line 20, SP 207 1610 (alternate site: SP 207 1555, but no crossing line)</li> <li>• Crossing lines: KNR 179-1, Line 52, SP 224 0410</li> </ul>
<b>Objective:</b>	Shallow end of the depth transect; ~200 m of lower Eocene to Campanian ooze, overlying ~200 m of Albian–Coniacian pelagic sediments and reef strata; PETM; Paleocene hyperthermals.
<b>Coring program:</b>	<ul style="list-style-type: none"> <li>• Hole A: APC/XCB to 250 mbsf with orientation and APCT-3</li> <li>• Hole B: APC/XCB to 250 mbsf</li> <li>• Hole C: APC/XCB to 250 mbsf</li> <li>• See <a href="#">“Drilling strategy”</a> and Tables <a href="#">T1</a>, <a href="#">T3</a></li> </ul>
<b>Wireline logging program:</b>	<ul style="list-style-type: none"> <li>• NA</li> <li>• See <a href="#">“Downhole measurements strategy”</a> and Tables <a href="#">T1</a>, <a href="#">T3</a></li> </ul>
<b>Anticipated lithology:</b>	Carbonate ooze, hemipelagic clay, shallow-water carbonates

## Site summaries (continued)

### Site SENR-18A

<b>Priority:</b>	Alternate
<b>Position:</b>	41°04.00'N, 49°17.00'W
<b>Water depth (mbrf):</b>	3540
<b>Target drilling depth (mbsf):</b>	400
<b>Approved maximum penetration (mbsf):</b>	Request 600; pending EPSP approval
<b>Survey coverage:</b>	<ul style="list-style-type: none"> <li>• Primary line(s): KNR 179-1, Line 53, SP 224 0850</li> <li>• Crossing line: KNR 179-1, Line 31, SP 211 1451</li> </ul>
<b>Objective:</b>	Upper middle of depth transect (the entire section of Eocene strata is ~100 m thick beneath ~100 m of Pleistocene, with >350 m of Cretaceous–Paleogene below this); early Eocene warm period; Eocene hyperthermals; chemistry of Eocene and Cretaceous deep water; Cretaceous OAEs; Cretaceous climate; K/P boundary; Cretaceous CCD.
<b>Coring program:</b>	<ul style="list-style-type: none"> <li>• Hole A: APC/XCB to 400 mbsf with orientation and APCT-3</li> <li>• Hole B: APC/XCB to 400 mbsf</li> <li>• Hole C: APC/XCB to 400 mbsf</li> <li>• See <a href="#">“Drilling strategy”</a> and Tables <a href="#">T1</a>, <a href="#">T3</a></li> </ul>
<b>Wireline logging program:</b>	<ul style="list-style-type: none"> <li>• Hole C: Wireline logging with triple combo and FMS-sonic</li> <li>• See <a href="#">“Downhole measurements strategy”</a> and Tables <a href="#">T1</a>, <a href="#">T3</a></li> </ul>
<b>Anticipated lithology:</b>	Carbonate ooze, hemipelagic clay, shallow-water carbonates

## Site summaries (continued)

### Site JA-13A

<b>Priority:</b>	Alternate
<b>Position:</b>	40°0.00'N, 51°49.00'W
<b>Water depth (m):</b>	4710
<b>Target drilling depth (mbsf):</b>	250
<b>Approved maximum penetration (mbsf):</b>	Request 600; pending EPSP approval
<b>Survey coverage:</b>	<ul style="list-style-type: none"> <li>• Primary line: KNR 179-1, Line 7, SP 204 0615</li> <li>• Crossing line: KNR 179-1, Line 12, SP 206 0455</li> </ul>
<b>Objective:</b>	Lower end of depth transect; lower to upper Eocene and possible Eocene/Oligocene boundary (the entire section of Eocene strata is ~500 m thick at this site, allowing potential deeper penetration than currently proposed); early Eocene warm period; Eocene hyperthermals; middle and late Eocene impacts; transition to icehouse climate; Eocene CCD; chemistry of Eocene deep water. Just above the Eocene CCD.
<b>Coring program:</b>	<ul style="list-style-type: none"> <li>• Hole A: APC/XCB to 250 mbsf with orientation and APCT-3</li> <li>• Hole B: APC/XCB to 250 mbsf</li> <li>• Hole C: APC/XCB to 250 mbsf</li> <li>• See <a href="#">“Drilling strategy”</a> and Tables <a href="#">T1</a>, <a href="#">T3</a></li> </ul>
<b>Wireline logging program:</b>	<ul style="list-style-type: none"> <li>• NA</li> <li>• See <a href="#">“Downhole measurements strategy”</a> and Tables <a href="#">T1</a>, <a href="#">T3</a></li> </ul>
<b>Anticipated lithology:</b>	Carbonate ooze, hemipelagic clay, shallow-water carbonates

## Site summaries (continued)

### Site JA-3A

<b>Priority:</b>	Alternate
<b>Position:</b>	40°3.00'N, 51°37.00'W
<b>Water depth (mbrf):</b>	4725
<b>Target drilling depth (mbsf):</b>	250
<b>Approved maximum penetration (mbsf):</b>	Request 700; pending EPSP approval
<b>Survey coverage:</b>	<ul style="list-style-type: none"> <li>• Primary line: KNR 179-1, Line 5, SP 203 2314</li> <li>• Crossing lines: KNR 179-1, Line 12, SP 206 0645</li> </ul>
<b>Objective:</b>	Lower end of depth transect; lower to upper Eocene and possible Eocene/Oligocene boundary (the entire section of Eocene strata is ~400 m thick at this site, with another 350 m of Cretaceous–early Paleogene); early Eocene warm period; Eocene hyperthermals; middle and late Eocene impacts; transition to icehouse climate; Eocene CCD; chemistry of Eocene deep water. Thinning of Eocene section from JA-7 suggests the site is within the Eocene lysocline but still has a respectable Eocene sediment cover.
<b>Coring program:</b>	<ul style="list-style-type: none"> <li>• Hole A: APC/XCB to 250 mbsf with orientation and APCT-3</li> <li>• Hole B: APC/XCB to 250 mbsf</li> <li>• Hole C: APC/XCB to 250 mbsf</li> <li>• See <a href="#">“Drilling strategy”</a> and Tables <a href="#">T1</a>, <a href="#">T3</a></li> </ul>
<b>Wireline logging program:</b>	<ul style="list-style-type: none"> <li>• NA</li> <li>• See <a href="#">“Downhole measurements strategy”</a> and Tables <a href="#">T1</a>, <a href="#">T3</a></li> </ul>
<b>Anticipated lithology:</b>	Carbonate ooze, hemipelagic clay, shallow-water carbonates

## Site summaries (continued)

### Site JA-4A

<b>Priority:</b>	Alternate
<b>Position:</b>	40°10.00'N, 51°38.00'W
<b>Water depth (m):</b>	4250
<b>Target drilling depth (mbsf):</b>	250
<b>Approved maximum penetration (mbsf):</b>	Request 700; pending EPSP approval
<b>Survey coverage:</b>	<ul style="list-style-type: none"> <li>• Primary line: KNR 179-1, Line 5, SP 203 2145</li> <li>• Crossing lines: KNR 179-1, Line 14, SP 206 1140</li> </ul>
<b>Objective:</b>	Middle of depth transect; lower to upper Eocene and possible Eocene/Oligocene boundary (the entire section of Eocene strata is ~700 m thick at this site, allowing potential deeper penetration than currently proposed); early Eocene warm period; Eocene hyperthermals; middle and late Eocene impacts; transition to icehouse climate; Eocene CCD; chemistry of Eocene deep water.
<b>Coring program:</b>	<ul style="list-style-type: none"> <li>• Hole A: APC/XCB to 250 mbsf with orientation and APCT-3</li> <li>• Hole B: APC/XCB to 250 mbsf</li> <li>• Hole C: APC/XCB to 250 mbsf</li> <li>• See <a href="#">"Drilling strategy"</a> and Tables <a href="#">T1</a>, <a href="#">T3</a></li> </ul>
<b>Wireline logging program:</b>	<ul style="list-style-type: none"> <li>• NA</li> <li>• See <a href="#">"Downhole measurements strategy"</a> and Tables <a href="#">T1</a>, <a href="#">T3</a></li> </ul>
<b>Anticipated lithology:</b>	Carbonate ooze, hemipelagic clay, shallow-water carbonates

## Scientific participants

The current list of participants for Expedition 342 can be found at [iodp.tamu.edu/scienceops/expeditions/newfoundland\\_sediment\\_drifts.html](http://iodp.tamu.edu/scienceops/expeditions/newfoundland_sediment_drifts.html).